TESIS DE LA UNIVERSIDAD DE ZARAGOZA
2020
27

Sergio Sisó Bayona

Factores morfológicos y anatónicos que regulan el intercambio de gases en especies mediterráneas del género Quercus

Departamento
Ciencias Agrarias y del Medio Natural

Director/es
Peguero Pina, José Javier
Gil Pelegrin, Eustaquio

ISSN 2254-7606

Prensas de la Universidad
Universidad Zaragoza

ISSN 2254-7606

Universidad Zaragoza
1542

Tesis Doctoral

FACTORES MORFOLÓGICOS Y ANATÓNICOS QUE REGULAN EL INTERCAMBIO DE GASES EN ESPECIES MEDITERRÁNEAS DEL GÉNERO QUERCUS

Autor

Sergio Sisó Bayona

Director/es

Peguero Pina, José Javier
Gil Pelegrin, Eustaquio

UNIVERSIDAD DE ZARAGOZA

Ciencias Agrarias y del Medio Natural

2019

TESIS DOCTORAL
POR COMPENDIO DE PUBLICACIONES

Factores morfológicos y anatómicos que regulan el intercambio de gases en especies mediterráneas del género *Quercus*.

Autor:

Sergio Sisó Bayona

Directores:

Dr. Eustaquio Gil Pelegrín
Unidad de Recursos Forestales, Centro de Investigación y Tecnología Agroalimentaria de Aragón

Dr. José Javier Peguero Pina
Unidad de Recursos Forestales, Centro de Investigación y Tecnología Agroalimentaria de Aragón

Departamento: Ciencias Agrarias y del Medio Natural

UNIVERSIDAD DE ZARAGOZA

Agradecimientos

Deseo expresar mi más sincero agradecimiento a todas las personas que han hecho posible la elaboración de esta tesis doctoral:

En primer lugar, a la persona que me inicio en este mundo, que con su apoyo y enseñanzas pude aportar mi granito de arena y que he tenido el honor de que sea uno de mis tutores en esta tesis doctoral, el Dr. Eustaquio Gil Pelegrín. Al Dr. Jose Javier Peguero Pina, que primero fue un excelente compañero y ahora ha sido un magnifico tutor de tesis, que sin su ayuda esto no hubiera sido posible. Ellos han sabido observar, planificar y guiarme para la elaboración de este trabajo, sintiendo en todo momento su apoyo y animo. Sus orientaciones y conocimientos han sido fundamentales para su finalización.

También quisiera hacer patente mi agradecimiento a mi compañero de laboratorio, el Dr. Domingo Sancho Knapik por las valiosas aportaciones que hizo para mejorar la presente investigación y por su amistad.

En especial quiero dar mi más profunda gratitud a mi familia. Ellos son los pilares de mi vida, A mis padres, que siempre han creído en mi, que siempre me han dado las fuerzas necesarias para levantarme en los malos momentos, que me han dado todo lo necesario para poder llevar a cabo mi proyecto de vida sin restricciones, allá donde estén solo espero que se sientan muy orgullosos de mi y que estén muy felices por lo que hoy puedo conseguir. A mi mujer y a mis hijos que son mi gasolina en el día a día y que para mí lo son todo en esta vida. Que siempre me apoyan, me animan y que me ayudan a seguir adelante pase lo que pase, para lograr mis metas y mis sueños. A mis hermanos y sus familias por su apoyo constante y ánimos. Sólo espero ser capaz de devolverles algún día lo mucho que me han aportado.

A todos ellos quiero expresarles mi mayor reconocimiento y gratitud

Índice de contenido

1. TESIS COMO COMPENDIO DE TRABAJOS PREVIAMENTE PUBLICADOS

La presente tesis doctoral, de acuerdo con el informe correspondiente, autorizado por los Directores de Tesis y el Órgano Responsable del Programa de Doctorado, se presenta como un compendio de cuatro trabajos previamente publicados. Las referencias completas de los artículos que constituyen el cuerpo de la tesis son los siguientes:

Peguero-Pina JJ, Sisó S, Flexas J, Garcia-Nogales A, Niinemets Ü, Sancho-Knapik D, Saz MA, Gil-Pelegrín E. 2017. Cell-level anatomical characteristics explain high mesophyll conductance and photosynthetic capacity in sclerophyllous Mediterranean oaks. New Phytologist 214:585–596.

Peguero-Pina JJ, Sisó S, Sancho-Knapik D, Díaz-Espejo A, Flexas J, Galmés J, Gil-Pelegrín E. 2016. Leaf morphological and physiological adaptations of a deciduous oak (*Quercus faginea Lam*.) to the Mediterranean climate: a comparison with a closely related temperate species (*Quercus robur L*.). Tree Physiology 36: 287–299.

Peguero-Pina JJ, Sisó S, Flexas J, Galmés J, Niinemets Ü, Sancho-Knapik D, Gil-Pelegrín E. 2017.Coordinated modifications in mesophyll conductance, photosynthetic potentials and leaf nitrogen contribute to explain the large variation in foliage net assimilation rates across *Quercus ilex* provenances. Tree Physiology 37: 1084–1094.

Peguero-Pina JJ, Sisó S, Fernández-Marín B, Flexas J, Galmés J, García-Plazaola JI, Niinemets Ü, Sancho-Knapik D, Gil-Pelegrín E. 2016. Leaf functional plasticity decreases the water consumption without further consequences for carbon uptake in *Quercus coccifera L*. under Mediterranean conditions. Tree Physiology 36: 356–367.

1. INTRODUCCIÓN GENERAL

1.1. Características principales del clima mediterráneo

El clima mediterráneo se caracteriza por la presencia de veranos cálidos, inviernos suaves o fríos y un régimen de lluvias con un periodo de **sequía estival** (Lionello et al. 2006). La precipitación total anual media es superior a los 300 mm (Grove et al., 1977), aunque podemos encontrar localizaciones con valores alrededor de los 2000 mm, debido a la influencia de factores orográficos (Cuadrat et al., 2007). Hay que destacar que la mitad de la precipitación anual se da durante el periodo invernal (Deitch et al., 2017) y menos del 20% durante el verano. Este hecho propicia la existencia de un periodo de aridez estival, característica genuina del clima mediterráneo y que lo diferencia de otros tipos de clima (Walter 1985; Breckle 2002). La Figura 1.1. muestra un diagrama ombrotérmico típico de un clima mediterráneo, donde se aprecia la concentración de la precipitación durante el periodo invernal y la existencia de un periodo de aridez estival (zona en rosa, donde P<2T) desde mayo hasta mediados de septiembre.

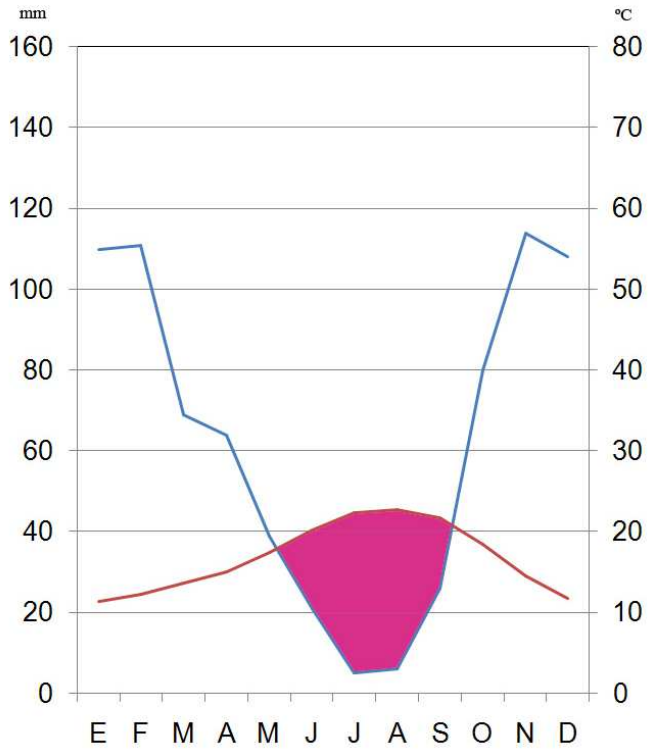

Fig. 1.1 Ombrotermograma típico de un clima tipo mediterráneo (hemisferio norte) con veranos cálidos y secos e inviernos suaves y lluviosos.

Köppen, al existir un verano seco, clasifica estos climas como Cs (Köppen, 1936), pudiéndose subdividir entre Csa y Csb según se superen o no los 22 ºC de temperatura media en el mes más cálido, si bien los Csb pueden ser considerados casi como una transición a espacios más oceánicos desde el punto de vista de la precipitación. A pesar de estas características comunes, el rango térmico y pluviométrico de los espacios clasificados dentro del clima mediterráneo es elevado. Esta gran **variabilidad** se puede constatar mediante el análisis de los datos de precipitación y temperatura *extraídos* de un conjunto de más de 2000 puntos con un clima Cs (Peel et al., 2007) a partir de la base de datos WorldClim V2.0 (Fick y Hijmans 2017). Efectivamente, este análisis evidencia la notable variabilidad térmica existente en estos espacios, pero sobre todo el amplio rango de registros que ofrecen los valores de precipitación (Figura 1.2). Con respecto a la aridez, la Figura 1.2f constata que este periodo se da durante el verano, e incluso se extiende a finales de la primavera y principios de otoño en algunos lugares. La variabilidad de la sequía atmosférica (estimada como el déficit de presión de vapor de la atmósfera, VPD) es muy importante entre localidades, con valores que van de los 2 a los 4 kPa (aproximadamente) durante los meses de verano (Figura 1.2e).

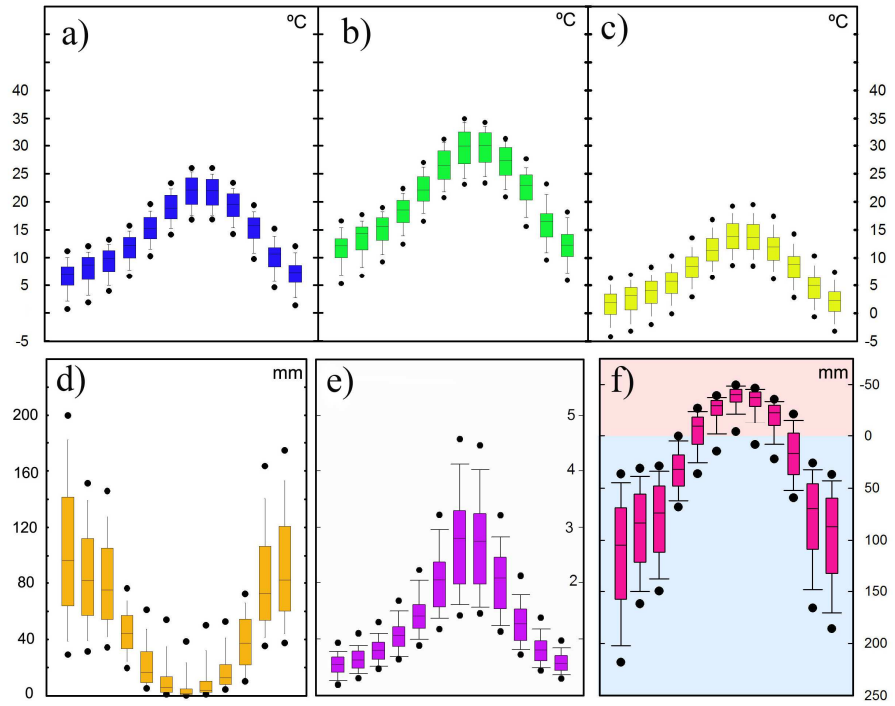

Fig. 1.2 a, b y c muestran los valores de temperatura media, máxima y mínima mensual extraídos respectivamente de un conjunto de más de 2000 puntos con clima Cs. d y e muestran la precipitación mensual y el déficit de presión de vapor (VPD) respectivamente del mismo conjunto de puntos. f muestra la diferencia entre P y 2T, indicando aridez (área rosada) según Gaussen (ver texto para más detalles). Modificado a partir de Gil-Pelegrín et al (2017)

1.2. ¿Dónde podemos encontrar el clima mediterráneo?

Las regiones que tienen características climáticas propias del clima mediterráneo están localizadas en la fachada oeste de los continentes, entre los 30º y 40º de latitud en ambos hemisferios (Lionello et al. 2006). Concretamente, se pueden encontrar en (i) regiones de Europa, África y Asia que rodean la cuenca mediterránea (excluyendo Egipto, Libia y la mayor parte de Túnez) y extendiéndose al sur de Turquía y el norte de Siria; (ii) la costa del Pacífico de América del Norte, que se extiende a través del estado de California en EE. UU. y Nueva California en México; (iii) la costa central de Chile; (iv) una gran área del oeste y sur de Australia; y (v) la región del Cabo de Sudáfrica. A continuación, vamos a profundizar y describir las características climáticas más importantes de las dos regiones del Hemisferio Norte representativas del clima mediterráneo: la Cuenca Mediterránea y costa del Pacifico en California (USA) y Baja California (Méjico).

1.2.1. La Cuenca Mediterránea

Los rasgos generales de la cuenca mediterránea son: verano seco a muy seco (p<20% total anual), temperaturas elevadas en esa estación, en especial en agosto debido a la inercia térmica que favorece la presencia del Mar Mediterráneo, e inviernos fríos o suaves, estos rasgos hacen que este clima sea único en el mundo. La precipitación anual oscila entre 400-800 mm y la temperatura anual media entre 16 y 19 º C. La Figura 1.3. muestra el diagrama ombrotérmico de tres localizaciones diferentes de la cuenca mediterránea.

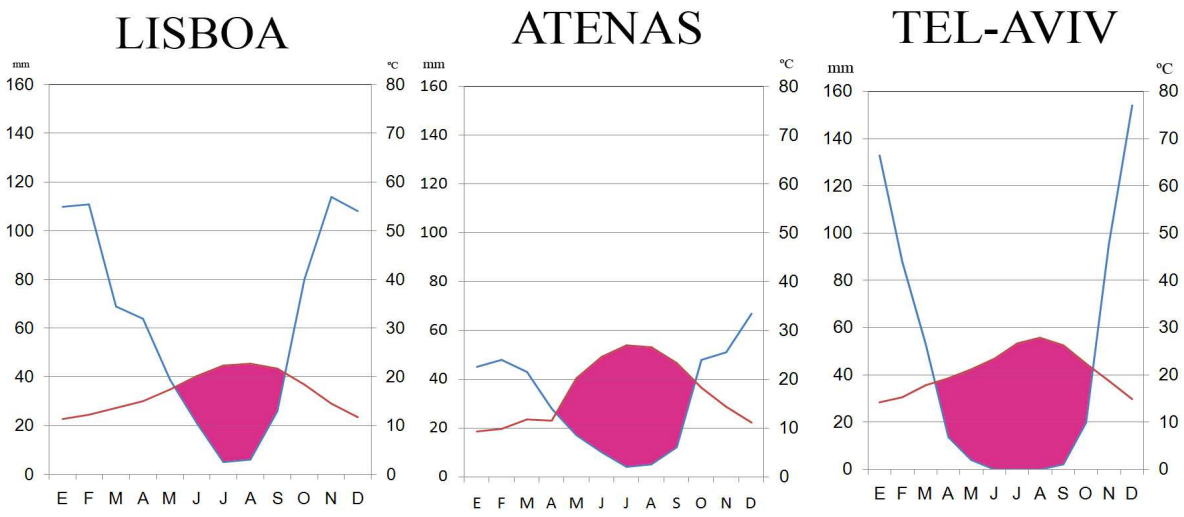

Fig. 1.3. Diagrama ombrotermico de tres localizaciones de la cuenca mediterránea

En esta zona existen una gran variedad de situaciones que le confieren un alto grado de heterogeneidad en lo referente al régimen climático. Hay varios factores geográficos relacionados con la situación latitudinal de la cuenca mediterránea que se superponen a los patrones atmosféricos: (i) las diferencias de altitud entre montañas y valles, (ii) la proximidad a las masas marinas y (iii) la exposición a los vientos del oeste. Todos estos factores inducen la existencia de un complejo mosaico climático y gradientes climáticos extremos (Castro-Díez et al., 1997). Aunque la existencia de veranos secos e inviernos lluviosos es una característica común del clima en la cuenca mediterránea, la génesis de anticiclones térmicos dentro de los continentes durante el invierno (Wallen 1970) puede reducir drásticamente la precipitación registrada durante los meses más fríos del año, produciendo un segundo mínimo de precipitación (Cuadrat et al., 2007). La influencia de las altas presiones desaparece durante la primavera con la llegada de los frentes de aire húmedo del Atlántico. Por lo tanto, esta estación es la más húmeda del año en la mayoría de las áreas de la cuenca mediterránea, especialmente en la Península Ibérica.

1.2.2. Costa Pacífica de EE. UU. Y México: California y Baja California

El clima mediterráneo en California (EE. UU.) se localiza en una franja que va desde las regiones costeras del Pacífico hasta el pie de monte de Sierra Nevada, incluida una gran parte de Central Valley, donde el clima se vuelve más cálido y seco. También hay áreas bajo clima mediterráneo en el norte de Baja California (México), con veranos cálidos y secos, inviernos suaves, alta variabilidad interanual de precipitación y alta frecuencia de sequías severas. Los gradientes climáticos en esta región están relacionados con cambios en la latitud, la proximidad al Océano Pacífico, la altitud y la continentalidad. Las condiciones climáticas están marcadas profundamente por la presencia del Pacífico y los sistemas de presión asociados, pero también por las altas y bajas térmicas que se desarrollan en el interior del continente americano. La ubicación del "*Pacific High*", una extensa área de altas presiones relacionadas con su posición latitudinal subtropical, es responsable de la sequía de verano y del gradiente de precipitación norte-sur. Su cambio gradual en invierno permite la llegada de frentes húmedos asociados con la dinámica atmosférica de la zona templada. La lluvia es más alta cuando los frentes alcanzan las estribaciones de las cordilleras costeras y Sierra Nevada (Bryson y Hare, 1974). La Figura 1.4 muestra el diagrama ombrotérmico de tres

localizaciones diferentes de California y Baja California.

Fig. 1.4. Diagrama ombrotermico de tres localizaciones de California y Baja California.

1.3. ¿Por qué es tan importante el clima mediterráneo?

Las regiones bajo el clima mediterráneo ocupan una superficie pequeña del total mundial, con un alto grado de fragmentación en diferentes territorios del hemisferio Norte y Sur. A pesar de su relativa importancia desde un punto de vista territorial, las áreas bajo climas de tipo mediterráneo mantienen una parte significativa de la biomasa terrestre, la productividad primaria neta y la biodiversidad, con casi el 20% de la diversidad de especies de plantas vasculares conocidas en la Tierra (Atjay et al., 1979; Valiente-Banuet et al. 2006), confiriendo a estas áreas una gran importancia en la actualidad. Además, las regiones bajo clima mediterráneo están caracterizadas por una intensa ocupación humana que ha modelizado la transformación del paisaje primitivo. En concreto, algunas de las sociedades más avanzadas de la historia se han desarrollado en la cuenca Mediterránea (Büntgen et al. 2011), con una enorme capacidad para influenciar y modificar el medio ambiente. Además, cambios tales como la ocupación del suelo, a través de su efecto en el albedo, pueden haber alterado la circulación atmosférica regional en el mar Mediterráneo e influenciado en última instancia algunos aspectos climáticos desde el año 4000 A.C. (Reale and Dirmeyer 2000). Sin embargo, el uso humano de la tierra también ha contribuido a aumentar la diversidad de escenarios ecológicos y como consecuencia, el actual interés en este paisaje (Lasanta et al. 2016).

La importancia del clima mediterráneo se ve reflejada en el hecho de haya merecido su propia consideración fitoclimática. Así, Schimper (1903) le dedicó un capítulo en su síntesis fitogeográfica de la vegetación de la tierra "*Plant Geography upon a Physiological Basis*", en el que identificó las áreas bajo climas de tipo mediterráneo como "las regiones con temperaturas suaves con inviernos lluviosos y sequía estival prolongada", enumerando las diversas áreas bajo clima mediterráneo ya mencionadas anteriormente en este capítulo. Después, Walter (1985) propuso el Zonobioma IV, "del Bosque esclerófilo" o "Zonobioma de las regiones áridas con inviernos lluviosos y húmedos" (Breckle 2002), mientras que Rivas-Martínez et al. (2011) propusieron la consideración de un Macrobioclima para este tipo de clima.

1.4. El género Quercus en los ecosistemas con climas de tipo mediterrráneo

El género *Quercus* L. (Fagaceae) incluye unas 400 especies de árboles y arbustos distribuidos por el Hemisferio Norte en diversos fitoclimas muy contrastados, incluyendo las áreas de Europa y Norteamérica bajo la influencia del clima mediterráneo. (Manos et al. 1999, Kremer et al. 2012).

Como se ha descrito anteriormente, a pesar de que la sequía estival es una característica común a todos ellos, los climas de tipo mediterráneo son muy diversos, con una marcada influencia en la fisonomía de la vegetación, y especialmente en lo que al género *Quercus* se refiere. Desde una perspectiva fitoclimática, y teniendo en cuenta la presencia de diferentes especies de robles, el clima de tipo mediterráneo genuino puede evolucionar hacia (i) sub-climas más cálidos y secos, en transición a los áridos (Fig. 1.5a), (ii) los más suaves y húmedos, en transición a climas templados (Fig. 1.5b) o (iii) variantes más secas y frías, más cercanas a los climas esteparios típicos (Fig. 1.5c). Estas transiciones climáticas también se pueden expresar en términos de Zonobiomas de Walter (Walter 1985; Breckle 2002) (Fig. 1.6). Según esta clasificación, el Zonobioma IV o "*Zonobiome of the Sclerophyllic Woodlands*" es considerado el Clima genuino de tipo mediterráneo, y es *Q. ilex* la especie representativa del género *Quercus*. Cuando aumenta la aridez, en una transición progresiva a Zonobiome III o "Zonobiome of Hot Deserts ", *Q. ilex* sería sustituido por *Q. coccifera*, que está presente en áreas de climas semiáridos (Vilagrosa et al. 2003a, b, 2010). La transición al Zonobioma VI o "Zonobiome of

Deciduous Forests" implicaría una reducción del período de aridez estival, un invierno más frío y una mayor precipitación. Desde un punto de vista de los robles, en la Península Ibérica se puede considerar este clima de transición, con robles caducifolios de invierno de hoja pequeña, como *Q. faginea* (Sánchez de Dios et al. 2009). La transición a condiciones secas pero más frías, hacia el Zonobiome VII o "*Zonobiome of Steppes and Cold Deserts*" debería implicar el dominio de algunas especies de robles que son capaces de soportar tales condiciones climaticas, como *Q. ilex* subsp. *rotundifolia* en la cuenca del Mediterráneo occidental y *Q. baloot* en el suroeste Asia.

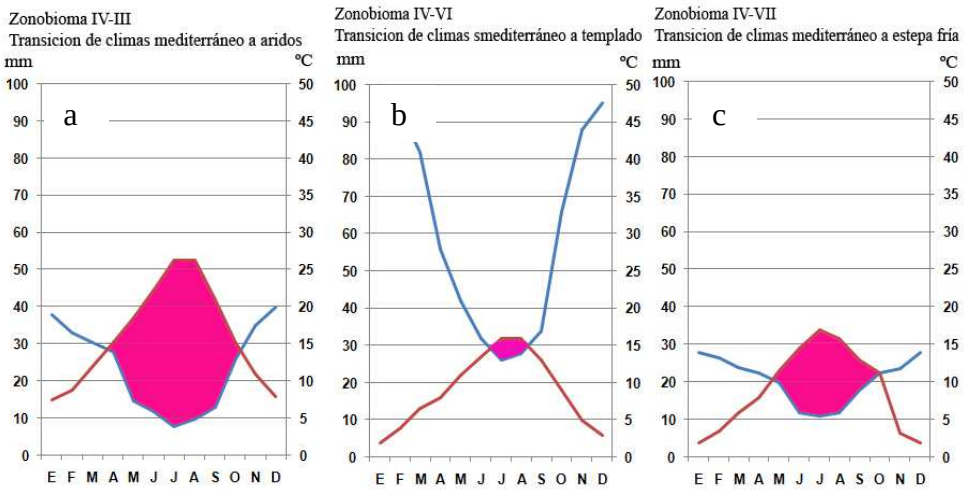

Fig. 1.5 Climogramas de zonas de transición dentro del clima mediterráneo a árido (a), templado (b) y estepa fría (c).

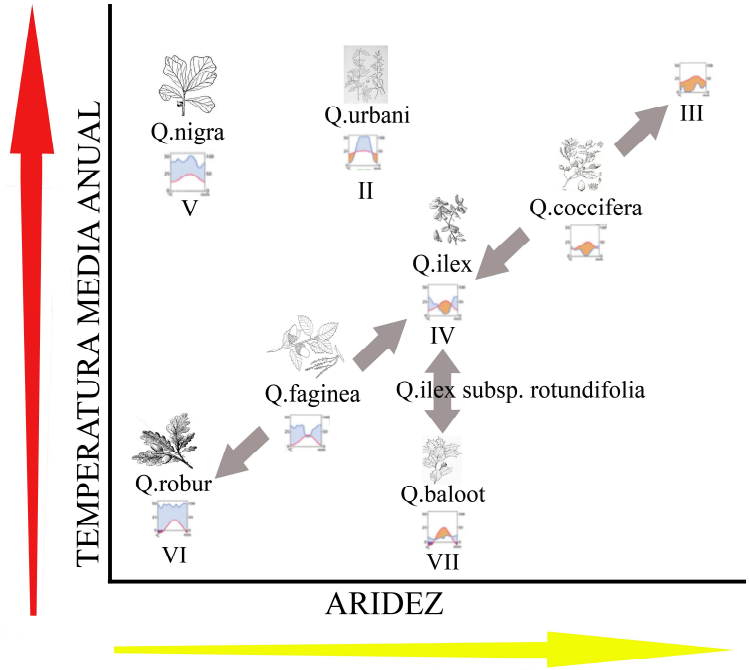

Fig. 1.6 Transición de Zonobioma IV a condiciones más áridas (III), húmedas y frías (VI) y más frías (VII) y especies de Quercus* Ilustración 1*características de estas transiciones. Zonobiomas de acuerdo con la clasificación de Walter (Breckle 2002).

Por lo tanto, la diversidad asociada a los climas de tipo mediterráneo parece expresarse en el género *Quercus* a través de la gran variabilidad fisionómica y funcional que presentan los robles que actualmente habitan en estos ecosistemas, lo que dificulta la definición de un prototipo de **roble mediterráneo** genuino. Una visión histórica de los robles en los climas mediterráneos puede ayudar a entender esta complejidad actual.

La mayoría de los autores consideran que la sequía estival que caracteriza este tipo de clima no se estableció en el hemisferio norte hasta fines del Terciario-inicio del Cuaternario (entre 7 y 2,8 millones de años dependiendo de la región) (Suc 1984; Verdú et al. 2003; Jiménez-Moreno et al. 2010; Millar 2012). Anteriormente, a comienzos del Terciario, las regiones mediterráneas actuales tenían un clima cálido y húmedo caracterizado por un régimen de precipitación distribuido a lo largo del año (Verdú et al. 2003; Valiente-Banuet et al., 2006; Ackerly 2009; Millar, 2012). Bajo estas condiciones climáticas húmedas, la vegetación en estas áreas del hemisferio norte estaba formada por abundantes bosques perennifolios de roble-laurel-madroño (Valiente-Banuet et al., 2006) donde los taxones esclerófilos eran elementos menores (Axelrod 1975, 1989), constituyendo en la mayoría de los casos, el sotobosque (Valiente-Banuet et al., 2006). Durante el Terciario temprano, los climas áridos y los ambientes secos comenzaron a desarrollarse (Millar 2012) y los bosques laurófilos tuvieron que adaptarse a estas nuevas condiciones (Axelrod 1977). Mientras que muchas especies de plantas se extinguieron, los arbustos esclerófilos de hoja perenne presentes en el sotobosque se expandieron geográficamente (Valiente-Banuet et al., 2006).

Los climas áridos y los ambientes secos continuaron desarrollándose durante el Terciario medio-tardío, modificando la composición de la flora (Millar 2012). En este momento, algunos autores señalan la presencia común de hojas esclerófilas correspondientes al tipo de robles "*ilex*" o "*suber*" en el sur de Europa (Kovar-Eder 2003) y al tipo "*chrysolepis*" en el oeste de EE. UU. (Retallack 2004). Posteriormente, al final del Terciario, con esta tendencia paleoclimática general hacia una mayor aridez, la precipitación del verano comenzó a disminuir en las áreas mediterráneas actuales (Axelrod 1973; Suc 1984). El cambio a climas de tipo mediterráneo llevó a los componentes taxonómicos supervivientes de la antigua flora a buscar refugios en las áreas mediterráneas actuales (Axelrod 1975). Además, la presencia de los taxones xerofíticos actuales del sur de Europa (tipo-*Quercus ilex*, *Phillyrea*, *Olea*, *Cistus*, *Pistacia*) fue aumentando progresivamente y parecen haber sido los más resistentes a las nuevas condiciones climáticas (Suc 1984). Una situación similar ocurrió en California, cuando la

intensificación de los climas de tipo mediterráneo derivó en un predominio de especies perennifolias de *Quercus* (Millar 2012). Es decir, el roble esclerófilo perennifolio arquetípico que vive en la actualidad en condiciones áridas en los ecosistemas mediterráneos podría tener su origen en los linajes pre-mediterráneos que existieron durante el Terciario en América del Norte y Eurasia, donde el clima era cálido y húmedo (Herrera 1992; Verdú et al., 2003; Valiente-Banuet et al., 2006).

No solo las especies de *Quercus* esclerofilas perennes como *Q. ilex* o *Q. chrysolepis* habitan actualmente en las regiones mediterráneas del hemisferio norte. Los robles de hoja caduca como *Q. faginea* o *Q. lobata* también coexisten bajo un régimen climático de tipo mediterráneo. Sin embargo, el origen de estos taxones caducifolios parece ser muy distinto del de sus congéneres perennifolios anteriormente citados. Según Mai (1991), también había una vegetación templada caducifolia de hoja ancha (la llamada Flora Arctoterciaria) que ocupaba latitudes muy septentrionales en América del Norte y Eurasia a principios del Terciario. Ancestros de los actuales robles blancos y negros (grupos Quercus y Lobatae, respectivamente, según Denk y Grimm 2009) parecen haber sido parte de esta flora (Nixon 2002, Kovar-Eder 2003). Durante el Terciario Medio y Superior, una tendencia global hacia un descenso de las temperaturas provocó un desplazamiento de esta vegetación caducifolia hacia latitudes más meridionales (Mai 1991, Kovar-Eder 2003). Esto implicó la aparición de elementos arctoteciarios en las áreas mediterráneas (Cuenca mediterránea y California) antes de la aparición de climas de tipo mediterráneo (Axelrod 1973, Kovar-Eder 2003, Ackerly 2009). La presencia actual de los tipos de roble caducifolio que viven en climas de tipo mediterráneo podría haber implicado una adaptación posterior de los antepasados del roble arctoterciario al régimen mediterráneo seco en expansión, en oposición al esclerófilo perennifolio pre-adaptado (Suc 1984, Blumler 1991; Nixon 2002; Peguero-Pina y otros, 2016a).

Por lo tanto, en la actualidad podemos encontrar dos tipos de robles que coexisten en las regiones mediterráneas del hemisferio norte: el tipo esclerófilo perennifolio más reconocido y el tipo malacófilo caducifolio invernal apenas reconocido (Barbero y otros 1992, Castro-Díez y Montserrat-Martí 1998, Damesin y otros 1998; Mediavilla y Escudero 2004). El primero se ha asociado comúnmente al arquetipo del clima de tipo mediterráneo (Walter 1985) y ha servido para desarrollar el concepto de "evolución convergente" entre las regiones mediterráneas (Mooney y Dunn 1970; Cody y Mooney 1978; Shmida 1981; Shmida y Whittaker 1984). Sin embargo, los robles esclerófilos de hoja perenne también se pueden encontrar en climas no mediterráneos (Poudyal et al., 2004; Zhang et al., 2005;

Singh et al., 2006), siendo componentes importantes de la vegetación en varias regiones (como Arizona, Norte de México, Pakistán, India, Nepal y Afganistán) que reciben su precipitación máxima en verano (Blumler 2005 y referencias en el mismo). El tipo caducifolio de invierno, a pesar de ser menos reconocido, también puede considerarse un tipo de adaptación a la sequía extrema del verano tan efectiva como el tipo perenne (Blumler 1991, Barbero y otros 1992, Scarascia-Mugnozza y otros 2000). De hecho, los robles de hoja caduca de invierno a menudo son dominantes en muchas áreas de California (Barbour 1988; Griffin1971,1973,1777; Vankat 1982) y la cuenca mediterránea (Barbero et al, 1992; Radoglou 1996). Por otra parte, también se pueden encontrar en algunos de los subtipos más áridos de los climas mediterráneos (Dufour-Dror y Ertas 2004). La coexistencia de ambos tipos de robles en condiciones mediterráneas ya fue reportada por Schimper (1903) y posteriormente por otros autores (Tognetti et al., 1998, Nardini et al., 1999, Manes et al., 2006, Montserrat-Martí, et al., 2009). Esta coincidencia ha sido señalada como una de las características distintivas del Bioma mediterráneo (Givnish 2002; Baldocchi et al., 2010; Noce et al.2016).

A pesar de que no existe una explicación general para la coexistencia de los robles mediterráneos perennifolios y caducifolios, se puede asumir que tal co-ocurrencia es una cuestión de variaciones locales en el clima o en las características del suelo. Así, los robles caducifolios mediterráneos podrían dominar aquellos sitios caracterizados por una precipitación relativamente más alta y una temperatura de invierno más baja (Chabot y Hicks 1982) y/o aquellas zonas con suelos más pesados y fértiles que pueden mantener altos niveles de contenido de agua (Salleo et al. 2002; Moreno et al. 2011). Por el contrario, los robles perennifolios podrían estar restringidos por la competencia o predominar en los lugares más secos y/o con sustratos gruesos, rocosos o infértiles que promueven bajos contenidos de agua en el suelo (Blumler 1991; Gasith y Resh 1999; Manes et al 2006; Di Paola et al. al. 2017). En este sentido, *Q. ilex*, como un roble perennifolio genuino, que puede crecer en una gran variedad de climas y sustratos en su área de distribución occidental en la cuenca mediterránea (Barbero et al., 1992), no compite con éxito con especies caducifolias de *Quercus* coexistentes, como *Q. faginea*, excepto en condiciones de desarrollo deficiente del suelo (Peguero-Pina et al., 2015). De acuerdo con esta idea, la coexistencia de ambos tipos de robles mediterráneos sería posible en un ambiente heterogéneo, mientras que la homogeneidad debería implicar el dominio de un solo tipo de roble en el paisaje.

Como consecuencia de la importancia primordial del agua del suelo en la coexistencia de estas especies en áreas bajo climas de tipo mediterráneo, la acción humana a lo largo de los siglos constituye un factor crucial que explica la mayoría de los patrones de distribución presentes (Dufour-Dror y Ertas 2004). Los registros de la influencia humana en la distribución de las especies de *Quercus* ya se encuentran desde 6000 AC, donde los bosques de robles caducifolios comenzaron a ser reemplazados por árboles de hoja perenne en la cuenca mediterránea occidental (Follieri et al., 1988; Reille y Pons 1992; Riera-Mora y Esteban-Amat 1994). Estos reemplazos pueden deberse a la erosión y degradación del suelo, que perjudica a las especies caducifolias en beneficio de las perennifolias. Por el contrario, la distribución de un roble también puede verse favorecida por la actividad humana si dicha especie es utilizable por los humanos. Este es el caso de *Q. suber*, cuyo nicho en la Cuenca del Mediterráneo occidental se ha ampliado a expensas de *Q. canariensis* (Urbieta et al., 2008). Es decir, la actividad humana puede influir en el patrón de distribución a escala local o regional. Además, Sánchez de Dios et al. (2009) predijeron que los cambios climáticos y ambientales, acelerados por la actividad humana, podrían reducir la presencia en la Península Ibérica de los robles caducifolios mediterráneos *Q. pubescens*, *Q. pyrenaica* y *Q. faginea*.

1.5. Respuestas de los robles a las limitaciones impuestas por el clima mediterráneo

Tal y como se ha descrito anteriormente, las dos características principales del clima mediterráneo son i/ la existencia de un periodo de aridez estival (genuina de este tipo de climas) y ii/ los inviernos fríos (común a otros tipos de climas). Estas dos situaciones limitan el funcionamiento de la vegetación, produciendo una fragmentación del periodo vegetativo ("*splitting*") que es considerado como la verdadera esencia del clima mediterráneo con respecto a la ecofisiología de la vegetación leñosa (Mitrakos 1980, Castro-Díez y Montserrat-Martí 1998, Montserrat-Martí et al., 2009). Este hecho hace que las plantas tengan dos estaciones favorables para desarrollar su actividad (primavera y otoño) y una situación de estrés en el resto de estaciones. Durante estos periodos las plantas están sometidas a unas condiciones menos favorables, con un acortamiento del periodo de crecimiento y una disminución de su actividad fotosintética (García-Plazaola et al., 1999; Corcuera et al., 2005a, b). La coexistencia de especies de *Quercus* de hoja perenne y hoja caduca de invierno ofrece la oportunidad de estudiar el papel de estos dos patrones fenológicos desde una perspectiva funcional (Kikuzawa 1991), especialmente

bajo las restricciones ambientales impuestas por el clima de tipo mediterráneo (Montserrat-Martí et al. al. 2009).

El hábito caducifolio invernal es el predominante en áreas de clima templado con inviernos fríos (Walter 1985; Breckle 2002), ya que el desprendimiento de hojas antes de la llegada del frio invernal ha sido reconocido como un mecanismo para evadir la sequía fisiológica causada por las bajas temperaturas (Schimper 1903). La ausencia de hojas durante los meses de invierno restringe la actividad fotosintética al período cálido, que se espera sea lo suficientemente favorable para un roble de hoja caduca de invierno en términos de ganancia de carbono. Peguero-Pina et al. (2016a) describe las condiciones ambientales típicas impuestas por el clima templado utilizando *Q. robur* como referencia. Bajo las condiciones de verano que caracterizan su hábitat genuino (temperaturas moderadas, alta disponibilidad de agua y bajos valores máximos de VPD), *Q. robur* puede soportar una gran superficie foliar, tanto en términos del tamaño de la hoja como de la cantidad de hojas por brote. Este hecho permite a esta especie lograr un balance de carbono muy favorable durante el período vegetativo. A medida que la sequía atmosférica y edáfica aumenta en la transición a las zonas bajo clima de tipo mediterráneo en latitudes más bajas, estas especies templadas genuinas son sustituidas por los llamados robles "sub-mediterráneos" (Himrane et al., 2004; Sánchez de Dios et al., 2009). En la Península Ibérica, la existencia de cierta aridez estival y valores máximos de VPD cercanos a 3 kPa se consideran de suma importancia para explicar la sustitución de *Q. robur* por *Q. faginea*, con valores mucho más bajos superficie foliar transpirante (Peguero-Pina et al., 2016a). Sin embargo, a pesar de los excelentes beneficios para reducir la transpiración en climas más secos, un área foliar reducida también disminuye el potencial fotosintético de esta especie. Efectivamente, la reducción severa en el área foliar transpirante, junto con la poca disponibilidad de agua durante el período vegetativo en las áreas sub-mediterráneas (Corcuera et al., 2004a, b; Pasho et al., 2011; Peguero-Pina et al., 2015), causa una disminución general de la asimilación neta de carbono durante este período (Peguero-Pina et al., 2016a). Así, el período vegetativo puede reducirse a unas pocas semanas en primavera y otoño (Montserrat-Martí et al., 2009), cuando las condiciones ambientales no limitan la actividad fotosintética (Abadía et al., 1996; Mediavilla y Escudero, 2003). La reducción en la fotosíntesis durante los días más secos del verano ha sido reportada en varias especies de *Quercus* mediterráneos caducifolios de Europa o Norteamérica (Damesin y Rambal 1995; Xu y Baldocchi 2003; Poyatos et al. al. 2008; Siam et al., 2009). El acceso a aguas profundas en suelos bien desarrollados ha sido propuesto como el

mecanismo ecológico que explica la supervivencia de los robles de hoja caduca en zonas con cierta aridez veraniega (Esteso-Martínez et al., 2006; Urbieta et al., 2008; Moreno et al. 2011). Por lo tanto, un aumento adicional en la aridez veraniega debido a factores climáticos (González-Rebollar et al., 1995; del Río y Penas 2006) o a una escasez de agua debido a la degradación del suelo (Blondel y Aronson 1995; Salleo et al., 2002; Corcuera et al. al. 2005a; Peguero-Pina et al., 2014) podría asociarse a la sustitución de robles caducifolios por perennifolios en áreas bajo climas de tipo mediterráneo.

Sin embargo, bajo tales circunstancias, incluso los árboles de hoja perenne no siempre son capaces de mantener una actividad fotosintética máxima durante todo el período vegetativo (Faria et al., 1998; Limousin et al., 2010a; Vaz et al., 2010). En este contexto, el acortamiento del periodo de crecimiento debido a la sequía estival se ve acentuado por las bajas temperaturas invernales, que también limitan la asimilación neta de carbono en los perennifolios mediterráneos (García-Plazaola et al., 1999; Corcuera et al., 2005a, b). Este "splitting" del periodo vegetativo (en el sentido dado por Kikuzawa 1991) puede conferir una ventaja funcional a perennifolios como *Q. ilex*, ya que las hojas del año anterior pueden comenzar a contribuir positivamente a la asimilación neta de carbono de la planta tan pronto como la temperatura aumenta en la primavera (Corcuera et al., 2005b), mucho antes de la fecha de brotación media reportada en esta especie (Castro-Díez y Montserrat-Martí 1998; Ogaya y Peñuelas 2003).

1.6. La esclerofilia en los robles mediterranéos: implicaciones funcionales

En las anteriores secciones se ha explicado de manera detallada la coexistencia de dos tipos de robles en las regiones mediterráneas del hemisferio norte, con características foliares contrastadas (hábito foliar, grado de esclerofilia) y diferentes estrategias para enfrentarse a las limitaciones impuestas por el clima mediterráneo.

La existencia de diferencias en el grado de esclerofilia entre los dos tipos de robles mediterráneos ha sido puesta de manifiesto a través de la cuantificación de la relación entre el peso seco y el área foliar ("*leaf dry mass per unit area*", en adelante LMA) (ver Gil-Pelegrín et al. 2017 y referencias incluidas). Así, Corcuera et al. (2002) demostraron que los robles mediterráneos perennifolios (*Q. agrifolia*, *Q. chrysolepis*, *Q. coccifera*, *Q. ilex ssp. ilex*, *Q. ilex* ssp. *ballota* = *Q.ilex* ssp. *rotundifolia*, *Q. suber*) presentan un valor promedio de LMA (150 g m^{-2}) significativamente más alto que los robles mediterráneos

caducifolios (*Q. cerris*, *Q. faginea Q. frainetto*, *Q. pyrenaica*) (80 g m^{-2}), siendo los robles nemorales (*Q. alba*, *Q. laurifolia*, *Q. nigra*, *Q. petraea*, *Q. robur*, *Q. rubra*, *Q. velutina*) los que muestran un valor medio de LMA sensiblemente más bajo (< 70 g m^{-2}). Villar y Merino (2001) también reportaron valores de LMA para robles de hoja perenne mediterráneos (*Q. agrifolia*, *Q. coccifera*, *Q. rotundifolia* = *Q. ilex* ssp. *rotundifolia*, *Q. suber*) (160 g m^{-2}) mucho más altos que para robles mediterráneos de hoja caduca (*Q. douglasii*, *Q. faginea*, *Q. keloggii*, *Q. lobat*a, *Q. pyrenaica*) (112 g m^{-2}). Por lo tanto, LMA es uno de los parámetros funcionales más importantes que separan de manera más clara los dos tipos de robles mediterráneos entre sí y con los robles nemorales.

Existe un consenso general acerca de que valores altos de LMA pueden afectar negativamente a la fotosíntesis expresada con base en peso seco de hoja (Wright et al. 2004, 2005), lo que se ha asociado a una mayor inversión en tejidos no fotosintéticos y/o a una menor eficiencia del mesófilo fotosintéticamente activo (Niinemets et al. 2009a, b; Hassiotou et al. 2010). Sin embargo, desde un punto de vista global, la relación entre LMA y la fotosíntesis expresada con base en área foliar (A_N) es menos evidente y puede estar modulada por otro tipo de factores. En este sentido, numerosos estudios publicados durante los últimos años han puesto de manifiesto que A_N está muy influenciada por la difusión del CO_2 desde las cavidades sub-estomáticas hasta los sitios de carboxilación dentro del cloroplasto (denominada **conductancia del mesófilo**, g_m) (ver Flexas et al. 2012 y referencias incluidas). La ruta a través del mesófilo comprende una serie de "barreras físicas" a la difusión del CO_2, incluyendo los espacios aéreos intercelulares, las paredes celulares, las membranas lipídicas, el citoplasma y el estroma del cloroplasto. Estas "barreras físicas" difieren en su tamaño y naturaleza, lo que constituye una fuente de variabilidad potencial en los valores de g_m. Flexas et al. (2008) pusieron de manifiesto que g_m presenta un alto grado de variabilidad interespecífica y que está influenciada negativamente por altos valores de LMA.

El hecho de que g_m esté limitada por valores altos de LMA (que se puede explicar por incrementos en el espesor y/o densidad de la hoja, Niinemets, 2001) ha sido relacionado con i/ un incremento en la resistencia la difusión del CO_2 a través de los espacios aéreos intercelulares asociado con mayores espesores y densidades foliares (Niinemets et al. 2009, Hassiotou et al., 2010, Tosens et al., 2012a, Tomás et al., 2013), y ii/ la existencia de paredes celulares más gruesas en especies con alta densidad foliar, lo que limita mucho la difusión de CO_2 (Peguero-Pina et al., 2012; Tosens et al., 2012a; Tomás et al., 2013). Por lo tanto, teniendo en cuenta que g_m es principal factor limitante

para A_N en muchas especies mediterráneas esclerófilas (Roupsard et al., 1996; Piel, 2002; Flexas et al., 2014; Galmés et al., 2014; Niinemets & Keenan, 2014), sería esperable una relación negativa entre A_N y LMA, al menos para este grupo de especies. De acuerdo con este postulado, Hassiotou et al. (2009) encontraron que A_N y g_m tendían a disminuir a medida que LMA se incrementaba en siete especies esclerófilas del género *Banksia* con un amplio rango de valores de LMA.

Sin embargo, contrariamente a lo esperado, Flexas et al. (2014) evidenciaron que las especies mediterráneas presentaban valores medios de A_N similares las plantas de otros biomas a pesar de tener valores de LMA significativamente más altos. Así, Peguero-Pina et al. (2009) muestran valores de A_N para tres robles mediterráneos perennifolios - *Q. coccifera*, *Q. ilex* y *Q. suber* - muy similares a aquellos descritos en diversas especies de robles de climas templados con LMA más bajos, como *Q. robur*, *Q. petraea*, *Q. cerris*, *Q. rubra* o *Q. prinus* (Epron et al., 1992, 1993; Valentini et al., 1995; Turnbull et al., 2002; Cano et al., 2013; Steinbrecher et al., 2013). Flexas et al. (2014) propusieron una posible explicación para este fenómeno, hipotetizando que los altos valores de LMA en las especies mediterráneas son también responsables de una mayor capacidad de carboxilación por área foliar ($V_{c,max}$) debido a un incremento de la concentración de la enzima Rubisco por área en hojas más gruesas con un mayor número de capas celulares.

Diversos estudios demuestran que la principal fuente de variación del LMA en los robles mediterráneos es el cambio en el espesor de la hoja (Niinemets 2015, González-Zurdo et al. 2016, Sancho-Knapik et al. 2019). Además del LMA y el espesor foliar, otros caracteres estructurales y anatómicos que determinan cuantitativamente la variabilidad en g_m y A_N son: el grado de empaquetamiento de unas células del mesófilo con respecto a otras, el grosor de la pared celular, el volumen de espacios aéreos intercelulares (ya mencionado anteriormente), el empaquetamiento de las células del mesófilo con respecto a la distancia y posición de los estomas, el área de mesófilo y cloroplastos expuesta a espacios aéreos intercelulares por unidad de área foliar (S_m/S y S_c/S, respectivamente) y el tamaño de los cloroplastos (Terashima et al. 2011, Tosens et al. 2012b, Tomás et al. 2013). Variaciones en estos caracteres foliares o celulares podrían tener una influencia positiva en g_m y, en consecuencia, en A_N en especies con altos valores de LMA. En concreto, algunos estudios ya indican que las hojas con mesófilos más gruesos presentan valores mayores de S_m/S y S_c/S, con un incremento concomitante en g_m (Hanba et al., 1999, 2002; Terashima et al., 2006), lo que se puede interpretar como un medio para mejorar la fotosíntesis en especies con altos valores de LMA. Sin embargo, otros estudios

ponen en cuestión la generalidad de este mecanismo, ya que no encuentran una correlación positiva entre espesor foliar y S_m/S (Slaton & Smith 2002) o S_c/S (Tosens et al. 2012a).

Los robles mediterráneos perennifolios y caducifolios constituyen un excelente marco teórico para elucidar la existencia de estas adaptaciones anatómicas y/o bioquímicas que podrían mejorar la conductancia del mesófilo y/o la capacidad de carboxilación por área, compensando las restricciones impuestas por el LMA en la asimilación neta de CO_2 por área. Este contexto constituye la base de los cuatro trabajos presentados en la tesis.

El **primer artículo** presentado se ha centrado en la comparación de los parámetros anatómicos, morfológicos y fotosintéticos en 7 especies perennifolias mediterráneas de *Quercus* de Europa (*Q. coccifera*, *Q. ilex* subp. *rotundifolia*, *Q. ilex* subsp. *ilex* y *Q. suber*) y Norteamérica (*Q. agrifolia*, *Q. chrysolepis* y *Q. wislizeni*) con valores contrastados de LMA. En este trabajo se demuestra que la variación interespecífica encontrada en los valores de A_N es consecuencia de las diferencias encontradas en g_m, el factor más limitante para la asimilación de carbono en estas especies. La existencia de adaptaciones anatómicas a nivel celular (las especies con valores más altos de A_N también presentan mayores valores de S_c/S) explica que algunas de estas especies tengan tasas de fotosíntesis similares a sus congéneres caducifolios a pesar de sus altos valores de LMA.

El **segundo artículo** presentado también indaga en la posible existencia de estos mecanismos compensatorios anatómicos y/o bioquímicos en *Q. robur* y *Q. faginea*, dos especies caducifolias de origen arctoterciario y muy próximas filogenéticamente. Este trabajo demuestra que *Q. faginea* puede ser considerado como un ejemplo de adaptación de un roble caducifolio a los climas de tipo mediterráneo con aridez estival, principalmente por una disminución del área foliar transpirante con respecto a *Q. robur*. El efecto negativo de este hecho sobre el balance de carbono de *Q. faginea* se ve parcialmente atenuado por la mayor capacidad fotosintética de esta especie, como consecuencia de una mayor conductancia estomática, conductancia del mesófilo y velocidad de carboxilación.

El **tercer artículo** se centra en la encina, la especie de roble perennifolio más representativa de la vegetación mediterránea y que además presenta un mayor grado de variación intra-específica en diversos caracteres funcionales. En concreto, en este capítulo se realiza un estudio comparado de los parámetros anatómicos, morfológicos y fotosintéticos en 4 procedencias de *Q. ilex* subsp. *ilex* (Gerona, Veneto, Lazio y Sardinia) y 3 de *Q. ilex* subsp. *rotundifolia* (Cazorla, Extremadura y Soria) para determinar el grado

de variabilidad intra-específica de estos parámetros. Los resultados obtenidos evidencian que la variablidad intra-específica encontrada en g_m se puede atribuir a cambios en el grosor de la pared celular, grosor de los cloroplastos y S_c/S. Además, también se encuentra una relación positiva de g_m y A_N con la velocidad de carboxilación, asociada con un incremento de nitrógeno por área en las procedencias con valores más altos de LMA.

Por último, el **cuarto artículo** de la tesis analiza el grado de plasticidad fenotípica en el roble mediterráneo perennifolio *Q. coccifera* creciendo bajo condiciones mediterráneas (Zaragoza) y oceánicas (Gipuzkoa). Este trabajo demuestra que, a pesar de la fuerte reducción de la conductancia estomática encontrada en Zaragoza, no existen diferencias significativas en A_N entre ambas condiciones, ya que los valores de g_m (el principal factor limitante a la fotosíntesis en esta especie) son iguales en ambos sitios. Este hecho tiene importantes consecuencias respecto a la eficiencia en el uso de los principales recursos (agua y nitrógeno) bajo diferentes condiciones climáticas, lo que también se discute en este capítulo.

2. COPIA DE LOS TRABAJOS PUBLICADOS

New Phytologist

Research

Cell-level anatomical characteristics explain high mesophyll conductance and photosynthetic capacity in sclerophyllous Mediterranean oaks

José Javier Peguero-Pina[1,2]*, Sergio Sisó[1]*, Jaume Flexas[3], Jeroni Galmés[3], Ana García-Nogales[4], Ülo Niinemets[5], Domingo Sancho-Knapik[1,2], Miguel Ángel Saz[6] and Eustaquio Gil-Pelegrín[1,2]

[1]Unidad de Recursos Forestales, Centro de Investigación y Tecnología Agroalimentaria de Aragón, Gobierno de Aragón, Avda. Montañana 930, 50059 Zaragoza, Spain; [2]Instituto Agroalimentario de Aragón -IA2- (CITA-Universidad de Zaragoza), 50013 Zaragoza, Spain; [3]Research Group on Plant Biology under Mediterranean Conditions, Departament de Biologia, Universitat de les Illes Balears, Carretera de Valldemossa km 7.5, 07122 Palma de Mallorca, Spain; [4]Department of Physical, Chemical and Natural Systems, University Pablo Olavide, Carretera de Utrera km 1, 41013 Sevilla, Spain; [5]Institute of Agricultural and Environmental Sciences, Estonian University of Life Sciences, Kreutzwaldi 1, Tartu 51014, Estonia; [6]Departamento de Geografía y Ordenación del Territorio, Universidad de Zaragoza, 50009 Zaragoza, Spain

Author for correspondence:
Eustaquio Gil-Pelegrín
Tel: +34 976 716394
Email: egilp@aragon.es

Received: *20 September 2016*
Accepted: *22 November 2016*

New Phytologist (2017)
doi: 10.1111/nph.14406

Key words: anatomical adaptations, leaf mass per area (LMA), Mediterranean-type climate, mesophyll conductance (g_m), photosynthesis, *Quercus*, sclerophylly.

Summary

- Leaf mass per area (LMA) has been suggested to negatively affect the mesophyll conductance to CO_2 (g_m), which is the most limiting factor for area-based photosynthesis (A_N) in many Mediterranean sclerophyll species. However, despite their high LMA, these species have similar A_N to plants from other biomes. Variations in other leaf anatomical traits, such as mesophyll and chloroplast surface area exposed to intercellular air space (S_m/S and S_c/S), may offset the restrictions imposed by high LMA in g_m and A_N in these species.
- Seven sclerophyllous Mediterranean oaks from Europe/North Africa and North America with contrasting LMA were compared in terms of morphological, anatomical and photosynthetic traits.
- Mediterranean oaks showed specific differences in A_N that go beyond the common morphological leaf traits reported for these species (reduced leaf area and thick leaves). These variations resulted mainly from the differences in g_m, the most limiting factor for carbon assimilation in these species.
- Species with higher A_N showed increased S_c/S, which implies increased g_m without changes in stomatal conductance. The occurrence of this anatomical adaptation at the cell level allowed evergreen oaks to reach A_N values comparable to congeneric deciduous species despite their higher LMA.

Introduction

Mediterranean-type ecosystems are characterized by the presence of woody evergreen sclerophyllous species that exhibit high leaf dry mass per unit area (LMA) (Kummerow, 1973; Galmés *et al.*, 2005, 2012), with small and thickened leaves (Traiser *et al.*, 2005). This vegetation type includes several species of the genus *Quercus* (Fagaceae), the so-called Mediterranean oaks, that can be found in Mediterranean-type evergreen woodlands of Europe and North America (Manos *et al.*, 1999; Kremer *et al.*, 2012). These species belong to different infrageneric groups (Denk & Grimm, 2009), but share common convergent leaf morphological and functional traits including high LMA (Corcuera *et al.*, 2002).

LMA is considered a key structural trait that has the potential to negatively affect the mass-based photosynthetic performance of the plant (Wright *et al.*, 2004, 2005), which has been associated with a higher investment in nonphotosynthetic tissue and/or a lower efficiency of the photosynthetically active mesophyll (Niinemets *et al.*, 2009; Hassiotou *et al.*, 2010). When considered globally, the relationship between LMA and area-based net CO_2 assimilation (A_N) is less clear. However, an essential component of A_N, the mesophyll conductance to CO_2 (g_m), has been shown to be negatively related to LMA (Flexas *et al.*, 2008). Hence, as g_m is the most limiting factor for A_N in many Mediterranean sclerophyll species (Roupsard *et al.*, 1996; Piel, 2002; Flexas *et al.*, 2014; Galmés *et al.*, 2014; Niinemets & Keenan, 2014; Peguero-Pina *et al.*, 2016a), a negative relationship between A_N and LMA is expected, at least within this group of species. Accordingly, Hassiotou *et al.* (2009) found that A_N tended to be lower as LMA increased for seven species of the Australian sclerophyllous genus *Banksia* covering a wide range of high LMA. These authors also found that high-LMA species

*These authors contributed equally to this work.

showed a significantly lower CO_2 diffusion conductance from substomatal cavities to the chloroplasts (i.e. g_m).

The fact that g_m is constrained by large LMA (which can be explained by increases in leaf thickness and/or leaf density) has been mostly related to: (1) an increase in the resistance of the CO_2 gas-phase conductance associated with greater leaf thickness and density (Niinemets *et al.*, 2009; Hassiotou *et al.*, 2010; Tosens *et al.*, 2012a; Tomás *et al.*, 2013), and (2) the thicker cell walls observed in species with high leaf density, significantly limiting CO_2 diffusion in the leaf liquid phase (Peguero-Pina *et al.*, 2012; Tosens *et al.*, 2012a; Tomás *et al.*, 2013). Therefore, Mediterranean plants with high LMA – including Mediterranean oaks – would be expected to present lower photosynthetic capacities than species from other biomes with lower LMA. However, contrary to expectations, Flexas *et al.* (2014) found that despite having higher average LMA, Mediterranean species, on average, have similar photosynthetic capacity on an area basis as plants from any other biomes. In fact, Peguero-Pina *et al.* (2009) reported values of net CO_2 assimilation rate for Mediterranean oaks *Quercus coccifera*, *Quercus ilex* and *Quercus suber* that were very similar to those found in other temperate oak species with lower LMA, such as *Quercus robur*, *Quercus petraea*, *Quercus cerris*, *Quercus rubra* or *Quercus prinus* (Epron *et al.*, 1992, 1993; Valentini *et al.*, 1995; Turnbull *et al.*, 2002; Cano *et al.*, 2013; Steinbrecher *et al.*, 2013; Peguero-Pina *et al.*, 2016b). A possible explanation for these contradictory findings was provided by Flexas *et al.* (2014), who hypothesized that high LMA in Mediterranean species is also responsible for the enhanced capacity of carboxylation per area ($V_{c,max}$) due to increased Rubisco content per area in thicker leaves with more cell layers.

Variation in LMA in Mediterranean oaks is primarily driven by variations in leaf thickness and to a lesser degree in the other component of LMA, leaf density (Niinemets, 2015; González-Zurdo *et al.*, 2016). Besides LMA and leaf thickness, there are other leaf structural and anatomical traits, including packing of mesophyll cells relative to each other, thickness of mesophyll cell walls, leaf airspace volume (the aforementioned traits are the primary determinants of leaf density), packing of mesophyll cells relative to the distance and position of stomata, mesophyll and chloroplast surface area exposed to intercellular air space per unit of leaf area (S_m/S and S_c/S, respectively) and chloroplast size, that quantitatively determine the variability in g_m and photosynthetic capacity among species (Tomás *et al.*, 2013; Peguero-Pina *et al.*, 2016b) or even within the same species growing under contrasting environmental conditions (Terashima *et al.*, 2011; Tosens *et al.*, 2012b; Peguero-Pina *et al.*, 2016a,c). Variations in such cellular or whole leaf traits could positively influence g_m and, consequently, net CO_2 assimilation in evergreen sclerophyllous species with large LMA values. Several studies have indicated that leaves with thicker mesophyll have larger S_m/S and/or S_c/S, implying a greater g_m in thicker leaves (Hanba *et al.*, 1999, 2002; Terashima *et al.*, 2006; Peguero-Pina *et al.*, 2016b). This could be interpreted as a way for improving photosynthesis in species with high LMA. However, other studies call into question the generality of such a mechanism, because they did not find a correlation between leaf thickness and S_m/S (Slaton & Smith, 2002) or S_c/S (Tosens *et al.*, 2012a).

The Mediterranean oaks constitute an excellent framework to elucidate the existence of anatomical and/or biochemical adaptations that may offset the restrictions imposed by high LMA in g_m and A_N. Furthermore, regardless of the convergence in overall leaf appearance, Corcuera *et al.* (2002) pointed out that Mediterranean oaks showed a high dispersion in their LMA values despite their 'sclerophyllous condition', contrary to the patterns in deciduous temperate and warm temperate Mediterranean oak species. Therefore, we hypothesize that: (1) these differences in LMA among the Mediterranean oaks would also be expressed in terms of specific differences in photosynthetic activity on an area basis (A_N); and (2) the presence of anatomical adaptations (e.g. increased S_m/S or S_c/S) would allow these evergreen oaks to reach A_N values comparable to congeneric deciduous species despite their higher LMA (Corcuera *et al.*, 2002) and lower stomatal conductance (Peguero-Pina *et al.*, 2009), two factors that could limit the photosynthetic activity in the Mediterranean oaks. To test these hypotheses, in this study we compared the morphological, anatomical and photosynthetic traits and the share of different photosynthetic limitations of seven Mediterranean oaks from Europe/North Africa and North America in a common garden.

Materials and Methods

Plant material and experimental conditions

Seven representative evergreen sclerophyllous Mediterranean oak species from Europe/North Africa and North America belonging to different infrageneric groups (Denk & Grimm, 2009) were studied: *Ilex* group (*Q. coccifera* L., *Q. ilex* subsp. *rotundifolia* Lam. and *Q. ilex* subsp. *ilex* L.), *Cerris* group (*Q. suber* L.), *Lobatae* group (*Quercus agrifolia* Née. and *Quercus wislizeni* A. DC.) and *Protobalanus* group (*Quercus chrysolepis* Liebm.) (Table 1). The seeds of the seven species were collected from one population per species (see Table 1 for details), sown in 2009 and cultivated in 0.5 l containers inside a glasshouse under the same conditions with a mixture of 80% compost (Neuhaus Humin Substrat N6; Klasman-Deilmann GmbH, Geeste, Germany) and 20% perlite. After the first growth cycle, the seedlings were transplanted to 25 l containers filled with the same mixture of compost and perlite and cultivated outdoors at CITA de Aragón (41°39′N, 0°52′W, Zaragoza, Spain) under Mediterranean conditions (mean annual temperature 15.4°C, total annual precipitation 298 mm). Nutrients were supplied as slow-release fertilizer (Osmocote Plus, Sierra Chemical, Milpitas, CA, USA). The fertilizer (3 g l^{-1} growth substrate) was applied to the top 10 cm layer of substrate. All plants were grown under the same environmental conditions and drip-irrigated every 2 d. Each potted plant was located in the centre of a plastic pallet of 1 m^2, which ensured a minimum distance among plants. We used 10 4-yr-old plants per species of similar size (*c.* 65 cm height and 20 mm in basal diameter), so the area of the experimental field was 70 m^2. The position of each plant was randomized within the experimental field. The measurements were carried out in summer 2012 using

Table 1 Geographical origin, infrageneric classification, exact location and mean climatic characteristics where seeds were collected for the seven studied *Quercus* species

Species	Origin	Group	Latitude	Longitude	T (°C)	T_s (°C)	P (mm)	P_s (mm)	MAI	Gaussen index
Q. chrysolepis	North America	Protobalanus	39°27′N	123°05′W	12.5	19.4	1114	14	49	5
Q. agrifolia	North America	Lobatae	39°18′N	123°45′W	14.3	19.1	954	15	39	5
Q. wislizeni	North America	Lobatae	34°16′N	118°04′W	15.4	23.4	851	13	34	5
Q. coccifera	Europe/North Africa	Ilex	41°47′N	00°30′W	12.4	20.8	440	79	20	3
Q. ilex subsp. *ilex*	Europe	Ilex	41°13′N	13°03′E	15.5	22.4	940	83	34	3
Q. ilex subsp. *rotundifolia*	Europe/North Africa	Ilex	41°46′N	02°29′W	10.9	19.2	514	104	25	2
Q. suber	Europe/North Africa	Cerris	40°10′N	06°14′W	15.0	23.8	469	37	19	4

T and T_s, mean annual and summer temperature; P and P_s, total annual and summer precipitation; MAI, Martonne's aridity index.

current-year fully developed leaves and just before irrigation (at field capacity), when predawn water potential was below −0.1 MPa (data not shown).

Although the distribution ranges of the studied species (Supporting Information Fig. S1) are typically Mediterranean with summer drought, there are slight differences among species in the climate at origins (Table 1; Figs S2, S3). Climatic information was obtained for the studied species from the WorldClim database (http://www.worldclim.org/) using geographical points throughout the distribution range of each species (Fig. S1). To quantify aridity, we calculated Martonne's aridity index (MAI = P/(T+ 10)) and Gaussen index (the number of months in which P < 2T, where P is monthly precipitation in mm and T is monthly mean temperature in °C). Moreover, the maximum daily vapour pressure deficit (VPD_{max}, kPa) (Fig. S3) was calculated using data obtained from the WeatherSpark database (http://weatherspark.com/).

Leaf gas exchange and chlorophyll fluorescence measurements

Leaf gas exchange and chlorophyll fluorescence parameters were measured simultaneously using an open gas exchange system (CIRAS-2; PP-Systems, Amesbury, MA, USA) fitted with an automatic universal leaf cuvette (PLC6-U; PP-Systems) and an FMS II portable pulse amplitude modulated fluorometer (Hansatech Instruments Ltd, King's Lynn, UK). Six CO_2 response curves were measured per species using light-adapted mature leaves. The photosynthesis measurements started at a CO_2 concentration surrounding the leaf (C_a) of 400 μmol mol^{-1}, and a saturating photosynthetic photon flux density (PPFD) of 1500 μmol m^{-2} s^{-1}. Leaf temperature and VPD were maintained at 25°C and 1.25 kPa, respectively, during all measurements. Once the steady state gas exchange rate was reached under these conditions (usually in 30 min after clamping the leaf), net assimilation rate (A_N), stomatal conductance (g_s) and the effective quantum yield of photosystem II (PSII; Φ_{PSII}) were estimated. Thereafter, C_a was decreased stepwise down to 50 μmol mol^{-1}. Upon completion of the measurements at low C_a, C_a was increased again to 400 μmol mol^{-1} to restore the original value of A_N. C_a was further increased stepwise to 1800 μmol mol^{-1} and all the steady-state photosynthetic characteristics were recorded at each C_a. Leakage of CO_2 in and out of the cuvette was determined for the same range of CO_2 concentrations with a photosynthetically inactive leaf enclosed (obtained by heating the leaf until no variable chlorophyll fluorescence was observed), and used to correct for measured leaf fluxes (Flexas *et al.*, 2007a).

For Φ_{PSII}, the steady-state fluorescence (F_S) and the maximum fluorescence during a light-saturating pulse of *c.* 8000 μmol m^{-2} s^{-1} (F'_M) were estimated, and Φ_{PSII} was calculated as $(F'_M - F_S)/F'_M$ (Genty *et al.*, 1989). Photosynthetic electron transport rate (J_F) was then calculated according to Krall & Edwards (1992), multiplying Φ_{PSII} by PPFD and by α (a term which includes the product of leaf absorptance and the partitioning of absorbed quanta between PSI and II). The term α was previously determined as the slope of the relationship between Φ_{PSII} and Φ_{CO2} (i.e. the quantum efficiency of CO_2 fixation) obtained by varying light intensity under nonphotorespiratory conditions in an atmosphere containing <1% O_2 (Valentini *et al.*, 1995). Five photosynthesis vs PPFD response curves were measured per species to determine α.

Estimation of mesophyll conductance, g_m, by gas exchange and chlorophyll fluorescence

Mesophyll conductance (g_m) was estimated according to the method of Harley *et al.* (1992), as follows:

$$g_m = \frac{A_N}{\frac{C_i - \Gamma^*(J_F + 8(A_N + R_L))}{J_F - 4(A_N + R_L)}} \quad \text{Eqn 1}$$

where A_N and the substomatal CO_2 concentration (C_i) were taken from the gas exchange measurements at saturating light, whereas Γ* (the chloroplastic CO_2 compensation point in the absence of mitochondrial respiration) and R_L (the respiration rate in the light) were estimated for each species following the method described by Flexas *et al.* (2007b). The values of g_m obtained were used to convert A_N–C_i responses into A_N–C_c responses (where C_c is the chloroplastic CO_2 concentration) using the equation $C_c = C_i - A_N/g_m$. The maximum ribulose-1,5-bisphosphate carboxylation ($V_{c,max}$) and photosynthetic electron transport (J_{max}) capacities were calculated from the A_N–C_c curves, using

the Rubisco kinetic constants and their temperature dependencies described by Bernacchi *et al.* (2002). The model of Farquhar *et al.* (1980) was fitted to the data by applying iterative curve-fitting (minimum least-square difference) using the Solver tool of Microsoft Excel.

Morphological and anatomical measurements

After the gas exchange measurements, sections of 1 × 1 mm were cut between the main veins for anatomical measurements from the same leaves used for gas exchange (one leaf per plant from six plants per species). Leaf material was quickly fixed under vacuum with 2% *p*-formaldehyde (2%) and glutaraldehyde (4%) in 0.1 M phosphate buffer solution (pH 7.2) and post-fixed for 1 h in 1% osmium tetroxide. Samples were dehydrated in: (1) a graded ethanol series and (2) propylene oxide and subsequently embedded in Embed-812 embedding medium (EMS, Hatfield, PA, USA). Semi-thin (0.8 µm) and ultrathin (90 nm) cross-sections were cut with an ultramicrotome (Reichert & Jung model Ultracut E). Semi-thin cross-sections were stained with 1% toluidine blue and viewed under a light microscope (Optika B-600TiFL, Optika Microscopes, Ponteranica, Italy). Ultrathin cross-sections were contrasted with uranyl acetate and lead citrate and viewed under a transmission electron microscope (H600, Hitachi, Tokyo, Japan). ImageJ software (http://rsb.info.nih.gov/nih-image/) was further used to measure leaf anatomical characteristics from the micrographs. Light microscopy images were used to determine leaf thickness, mesophyll thickness between the two epidermal layers, number of palisade layers and the fraction of the mesophyll tissue occupied by the intercellular air spaces (f_{ias}) (Syvertsen *et al.*, 1995; Tomás *et al.*, 2013). S_m/S and S_c/S were calculated from light and electron micrographs following the method of Syvertsen *et al.* (1995). Thus, S_m/S is given as:

$$S_{mes}/S = \frac{L_{mes}}{W}\gamma \qquad \text{Eqn 2}$$

where W is the width of the section measured, and L_{mes} is the total length of mesophyll cells facing the intercellular airspace. The curvature correction factor (γ), which depends on the shape of the cells (Evans *et al.*, 1994), was measured and calculated for each species according to Thain (1983) for palisade and spongy cells by measuring their width and height and calculating an average width/height ratio. Analogously, S_c/S was calculated as:

$$S_c/S = \frac{L_c}{L_{mes}} S_{mes}/S \qquad \text{Eqn 3}$$

where L_c is the total length of chloroplast surface area facing the intercellular airspace in the section. Electron micrographs were used to determine cell wall thickness (T_{cw}), cytoplasm thickness (T_{cyt}), chloroplast length (i.e. the major axis length of the chloroplast parallel to the cell wall, L_{chl}) and chloroplast thickness (i.e. the minor axis length of the chloroplast perpendicular to the cell wall, T_{chl}) (Tomás *et al.*, 2013). Three different sections and four to six different fields of view per leaf were used for measurements of each anatomical characteristic.

LMA was measured in 30 mature leaves sampled from 10 individuals per species (i.e. three leaves were randomly taken and the average LMA was calculated from each individual). Leaf area was measured after scanning the leaves with the ImageJ software. Leaves were then oven dried at 70°C for 3 d to determine their dry mass. LMA was calculated as the ratio of foliage dry mass to foliage area.

Mesophyll conductance modelled on the basis of anatomical characteristics

Leaf anatomical characteristics were used to estimate mesophyll conductance (g_m) as a composite conductance for within-leaf gas and liquid diffusion pathways, according to the one-dimensional gas diffusion model of Niinemets & Reichstein (2003) as applied by Tosens *et al.* (2012b):

$$g_m = \frac{1}{\frac{1}{g_{ias}} + \frac{R \cdot T_k}{H \cdot g_{liq}}} \qquad \text{Eqn 4}$$

where g_{ias} is the gas phase conductance inside the leaf from substomatal cavities to the outer surface of cell walls, g_{liq} is the conductance in the leaf liquid and lipid phases from the outer surface of cell walls to chloroplasts, R is the gas constant (Pa m^3 K^{-1} mol^{-1}), T_k is absolute temperature (K) and H is Henry's law constant for CO_2 (Pa m^3 mol^{-1}). g_m is defined as a gas-phase conductance, and thus $H/(RT_k)$, the dimensionless form of Henry's law constant, is needed to convert g_{liq} to corresponding gas-phase equivalent conductance (Niinemets & Reichstein, 2003).

The intercellular gas-phase conductance (and the reciprocal term, r_{ias}) was obtained according to Niinemets & Reichstein (2003) as:

$$g_{ias} = \frac{1}{r_{ias}} = \frac{D_A \cdot f_{ias}}{\Delta L_{ias} \cdot \tau} \qquad \text{Eqn 5}$$

where ΔL_{ias} (m) is the average gas-phase thickness, τ is the diffusion path tortuosity (1.57 m m^{-1}, Syvertsen *et al.*, 1995), D_A is the diffusivity of CO_2 in air (1.51 × 10^{-5} m^2 s^{-1} at 25°C) and f_{ias} is the fraction of intercellular air spaces. ΔL_{ias} was taken as half the mesophyll thickness. Total liquid phase conductance (g_{liq}) from the outer surface of cell walls to the carboxylation sites in the chloroplasts is the sum of serial resistances of the cell wall (r_{cw}), the plasmalemma (r_{pl}) and inside the cell ($r_{cel,tot}$) (Tomás *et al.*, 2013):

$$g_{liq} = \frac{S_m}{(r_{cw} + r_{pl} + r_{cel,tot}) \cdot S} \qquad \text{Eqn 6}$$

The conductance of the cell wall was calculated as previously described by Peguero-Pina *et al.* (2012). For conductance of the plasma membrane we used an estimate of 0.0035 m s^{-1} as previously suggested (Tosens *et al.*, 2012b). The conductance inside the cell was calculated following the methodology described by Tomás *et al.* (2013), considering two different pathways of CO_2 inside the cell: one for cell wall parts lined with chloroplasts and the other for interchloroplastial areas (Tholen *et al.*, 2012).

Analysis of quantitative limitations of A_N

To separate the relative controls on A_N resulting from limited stomatal conductance (l_s), mesophyll diffusion (l_m) and biochemical capacity (l_b), we used the quantitative limitation analysis of Grassi & Magnani (2005) as applied by Tomás *et al.* (2013). Different fractional limitations, l_s, l_m and l_b ($l_s + l_m + l_b = 1$), were calculated as:

$$l_s = \frac{g_{tot}/g_s \cdot \partial A_N/\partial C_c}{g_{tot} + \partial A_N/\partial C_c} \quad \text{Eqn 7}$$

$$l_m = \frac{g_{tot}/g_m \cdot \partial A_N/\partial C_c}{g_{tot} + \partial A_N/\partial C_c} \quad \text{Eqn 8}$$

$$l_b = \frac{g_{tot}}{g_{tot} + \partial A_N/\partial C_c} \quad \text{Eqn 9}$$

where g_s is the stomatal conductance to CO_2, g_m is the mesophyll conductance according to Harley *et al.* (1992; Eqn 1) and g_{tot} is the total conductance to CO_2 from ambient air to chloroplasts (sum of the inverse CO_2 serial conductances g_s and g_m). $\partial A_N/\partial C_c$ was calculated as the slope of $A_N - C_c$ response curves over a C_c range of 50–100 μmol mol^{-1}. Quantitative limitations of photosynthesis were estimated for at least five different leaves for each species, and average estimates of the component photosynthetic limitations were calculated.

Quantitative analysis of partial limitations of g_m

The determinants of g_m were divided between the component parts of the diffusion pathway (Eqns 4–6) as in Tomás *et al.* (2013). The proportion of g_m determined by limited gas-phase conductance (l_{ias}) was calculated as:

$$l_{ias} = \frac{g_m}{g_{ias}} \quad \text{Eqn 10}$$

The share of g_m by different components of the cellular phase conductances (l_i) was determined as:

$$l_i = \frac{g_m}{g_i \frac{S_m}{S}} \quad \text{Eqn 11}$$

where l_i is the component limitation in the cell walls, the plasmalemma and inside the cells, and g_i refers to the component diffusion conductances of the corresponding diffusion pathways.

Statistical analyses

Data are expressed as means ± standard error. One-way ANOVAs were performed to identify the species effect on photosynthetic, morphological and anatomical traits (see ANOVA outputs in Table S1). Traits among species were compared by post-hoc Tukey's Honest Significant Difference test. Regarding LMA and leaf area, ANOVAs were performed using the mean values per plant as individual values. Regarding the remaining morphological and anatomical traits, ANOVAs was performed using the mean values per leaf as individual values. The effect of S_c/S_m on the linear relationship between A_N (the dependent variable) and S_m/S (the independent variable) was analysed by analysis of the variance–covariance using the GLM procedure (Dunn & Clark, 1987). The terms included in the model were: S_c/S_m (allowing for different intercepts for each group of species), S_m/S (included as a covariate) and their interaction (allowing for different slopes for each group of species), which were considered as fixed effects. If the interaction between S_c/S_m and S_m/S is not significant, a common slope can be assumed. All statistical analyses were carried out using SAS version 8.0 (SAS, Cary, NC, USA).

Results

Variation in photosynthetic capacities and mesophyll conductance among Mediterranean evergreen oaks

The correlation between LMA and A_N for the seven studied *Quercus* species was not statistically significant at $P < 0.05$ ($r^2 = 0.43$, $P = 0.10$; Fig. 1). The values of A_N and g_m showed statistically significant differences ($P < 0.05$) between the studied species, ranging from 7.6 ± 0.2 μmol CO_2 m^{-2} s^{-1} and 0.029 ± 0.002 mol CO_2 m^{-2} s^{-1} for *Q. agrifolia* to 15.6 ± 0.5 μmol CO_2 m^{-2} s^{-1} and 0.093 ± 0.006 mol CO_2 m^{-2} s^{-1} for *Q. suber* (Table 2). By contrast, no differences at $P < 0.05$ were detected in g_s and intrinsic water use efficiency (iWUE = A_N/g_s) among the studied species (Table 2). Parameters of the Farquhar *et al.* (1980) model of photosynthesis, $V_{c,max}$ and J_{max}, were not statistically different among species ($P > 0.05$), except for *Q. ilex* subsp. *rotundifolia* (Table 2). Thus, species differences in A_N were primarily driven by g_m and the correlation between g_m and A_N ($r^2 = 0.87$, $F = 258.8$, $P < 0.0001$; Fig. 2b) was stronger than that found between g_s and A_N ($r^2 = 0.32$, $F = 18.6$, $P = 0.0001$; Fig. 2a). Furthermore, the correlations between $V_{c,max}$ and A_N

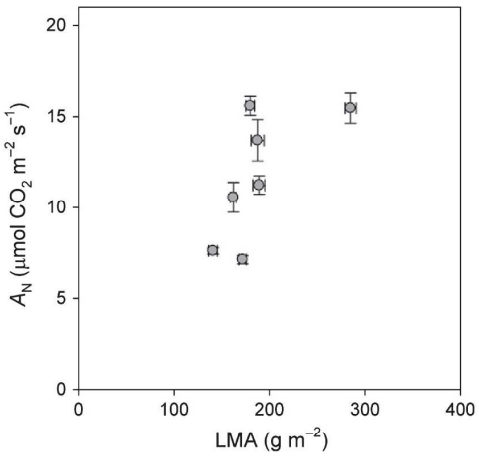

Fig. 1 Relationship between leaf mass area (LMA) and net photosynthesis (A_N) for the seven studied *Quercus* species. Data are mean ± SE.

New Phytologist

Table 2 Photosynthetic characteristics for the seven studied *Quercus* species

Species	A_N (μmol CO_2 m^{-2} s^{-1})	g_s (mol CO_2 m^{-2} s^{-1})	iWUE (μmol mol^{-1})	g_m (mol CO_2 m^{-2} s^{-1})	V_{c,max_Cc} (μmol m^{-2} s^{-1})	J_{max_Cc} (μmol m^{-2} s^{-1})
Q. chrysolepis	13.7 ± 0.8^{de}	0.180 ± 0.020^{a}	56.1 ± 4.3^{a}	0.074 ± 0.005^{cde}	191 ± 9^{a}	240 ± 18^{ab}
Q. agrifolia	7.6 ± 0.2^{ab}	0.135 ± 0.017^{a}	38.6 ± 6.0^{a}	0.029 ± 0.002^{a}	169 ± 16^{a}	202 ± 12^{a}
Q. wislizeni	10.6 ± 1.1^{bc}	0.162 ± 0.035^{a}	43.1 ± 10.5^{a}	0.048 ± 0.009^{abc}	168 ± 9^{a}	206 ± 17^{a}
Q. coccifera	11.2 ± 0.5^{cd}	0.157 ± 0.012^{a}	47.1 ± 6.6^{a}	0.057 ± 0.006^{bcd}	188 ± 14^{a}	253 ± 25^{ab}
Q. ilex subsp. *ilex*	7.12 ± 0.2^{a}	0.095 ± 0.007^{a}	47.8 ± 2.9^{a}	0.033 ± 0.001^{ab}	195 ± 21^{a}	207 ± 13^{a}
Q. ilex subsp. *rotundifolia*	15.5 ± 0.8^{e}	0.167 ± 0.023^{a}	61.1 ± 5.5^{a}	0.080 ± 0.008^{de}	311 ± 12^{b}	301 ± 7^{b}
Q. suber	15.6 ± 0.5^{e}	0.170 ± 0.009^{a}	58.0 ± 3.4^{a}	0.093 ± 0.006^{e}	167 ± 9^{a}	224 ± 6^{a}

A_N, net photosynthesis; g_s, stomatal conductance; iWUE, intrinsic water use efficiency; g_m, mesophyll conductance to CO_2; $V_{c,max}$ and J_{max}, maximum velocity of carboxylation and maximum capacity for electron transport, respectively. Data are mean ± SE. Different letters indicate significant differences among species (Tukey's test, $P < 0.05$).

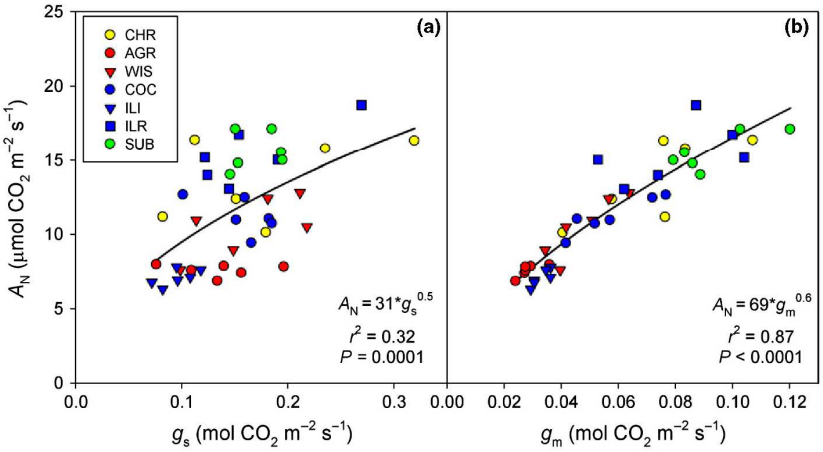

Fig. 2 Relationships between (a) stomatal conductance (g_s) and net photosynthesis (A_N) and between (b) mesophyll conductance (g_m) and net photosynthesis (A_N) for the seven studied *Quercus* species. Species abbreviations: AGR, *Q. agrifolia*; CHR, *Q. chrysolepis*; COC, *Q. coccifera*; ILI, *Q. ilex* subsp. *ilex*; ILR, *Q. ilex* subsp. *rotundifolia*; SUB, *Q. suber*; WIS, *Q. wislizeni*.

and between J_{max} and A_N were not statistically significant (data not shown). Analysis of the partitioning of photosynthetic limitations revealed that A_N was mainly limited by diffusional processes for all the studied species (Table 3).

Species differences in anatomical traits

The studied species displayed contrasting values of key leaf and cellular anatomical traits (Tables 4, 5). Using these traits to estimate mesophyll conductance (see the Materials and Methods section for details), a tight positive linear relationship was found between modelled and measured g_m values ($r^2 = 0.90$, $F = 43.2$, $P < 0.01$; Fig. 3), and it was clear that changes in g_m were primarily associated with specific changes in g_{liq} (Fig. 3). Measured g_m showed a tight positive linear relationship with S_c/S ($r^2 = 0.93$, $F = 84.1$, $P < 0.01$; Fig. 4a), but no correlation was detected between T_{cw} and T_{chl} and measured g_m (Fig. 4b and c, respectively). The values of T_{cw} found here are high compared to most species, and of a magnitude where their effect on $g_m/(S_c/S)$ is small (Fig. 5), pointing out that the small cell wall conductance exerts an important control on mesophyll conductance without differential effects among the studied species. The detailed analysis of individual limitations of g_m confirmed that the cell wall was the main limiting factor in all species, except *Q. ilex* subsp. *rotundifolia* (see Table S2). The strong influence of S_c/S in determining the specific differences in g_m also has a direct influence on net photosynthesis, as reflected in the linear relationship between S_c/S and A_N ($r^2 = 0.89$, $F = 41.9$, $P < 0.01$; Fig. 6). On the other hand, although the relationship between S_m/S and A_N for the seven studied *Quercus* species was statistically significant ($r^2 = 0.51$, $P < 0.05$; data not shown), separation of the species among two groups as a function of S_c/S_m ratio (Table 5) yielded two

Table 3 Relative stomatal (l_s), mesophyll (l_m) and biochemical (l_b) photosynthesis limitations for the seven studied *Quercus* species

Species	l_s (%)	l_m (%)	l_b (%)
Q. chrysolepis	26.6 ± 4.8^{a}	58.0 ± 4.9^{ab}	15.4 ± 1.3^{c}
Q. agrifolia	17.2 ± 2.6^{a}	74.9 ± 2.7^{c}	7.8 ± 0.2^{ab}
Q. wislizeni	20.1 ± 2.0^{a}	65.3 ± 2.2^{bc}	14.6 ± 1.1^{c}
Q. coccifera	22.8 ± 2.9^{a}	61.2 ± 3.4^{ab}	15.9 ± 0.8^{c}
Q. ilex subsp. *ilex*	24.4 ± 1.0^{a}	69.4 ± 0.9^{bc}	6.2 ± 0.3^{a}
Q. ilex subsp. *rotundifolia*	29.8 ± 3.4^{a}	60.1 ± 3.6^{ab}	10.1 ± 0.7^{b}
Q. suber	26.7 ± 1.6^{a}	48.6 ± 2.0^{a}	24.7 ± 0.7^{d}

Data are mean ± SE. Different letters indicate significant differences among species (Tukey's test, $P < 0.05$).

Table 4 Leaf area, leaf mass area (LMA), leaf thickness, total mesophyll thickness, spongy and palisade mesophyll thickness and number of palisade layers for the seven studied *Quercus* species

Species	Leaf area (cm^2)	LMA ($g\ m^{-2}$)	Leaf thickness (μm)	Mesophyll thickness (μm)	Spongy thickness (μm)	Palisade thickness (μm)	No. of palisade layers
Q. chrysolepis	3.50 ± 0.17^{b}	187.6 ± 6.8^{c}	281 ± 6^{c}	242 ± 9^{c}	124 ± 8^{ab}	118 ± 4^{bc}	2
Q. agrifolia	1.67 ± 0.21^{a}	141.0 ± 4.7^{a}	197 ± 5^{a}	171 ± 5^{a}	97 ± 4^{a}	74 ± 4^{a}	2
Q. wislizeni	5.13 ± 0.29^{c}	162.2 ± 3.2^{ab}	239 ± 9^{b}	201 ± 8^{ab}	112 ± 3^{a}	90 ± 6^{a}	2
Q. coccifera	1.58 ± 0.13^{a}	189.3 ± 6.4^{c}	315 ± 8^{cd}	278 ± 7^{d}	143 ± 5^{b}	135 ± 3^{d}	3
Q. ilex subsp. *ilex*	10.24 ± 0.58^{d}	172.0 ± 4.0^{bc}	278 ± 7^{c}	240 ± 6^{c}	122 ± 8^{ab}	118 ± 7^{bc}	2
Q. ilex subsp. *rotundifolia*	3.78 ± 0.33^{bc}	284.9 ± 5.8^{d}	348 ± 10^{d}	291 ± 16^{cd}	156 ± 10^{b}	136 ± 6^{cd}	3
Q. suber	3.69 ± 0.34^{bc}	179.9 ± 4.6^{bc}	228 ± 7^{ab}	200 ± 8^{ab}	104 ± 10^{a}	96 ± 6^{ab}	2

Data are mean ± SE. Different letters indicate significant differences among species (Tukey's test, $P < 0.05$).

Table 5 Fraction of the mesophyll tissue occupied by the intercellular air spaces (f_{ias}), mesophyll surface area exposed to intercellular air spaces (S_m/S), chloroplast surface area exposed to intercellular airspace (S_c/S), the ratio S_c/S_m, cell wall thickness (T_{cw}), cytoplasm thickness (T_{cyt}), chloroplast length (L_{chl}) and chloroplast thickness (T_{chl}) for the seven studied *Quercus* species

Species	f_{ias}	S_m/S ($m^2\ m^{-2}$)	S_c/S ($m^2\ m^{-2}$)	S_c/S_m	T_{cw} (μm)	T_{cyt} (μm)	L_{chl} (μm)	T_{chl} (μm)
Q. chrysolepis	0.19 ± 0.01^{b}	14.2 ± 0.6^{bc}	12.5 ± 0.9^{b}	0.87 ± 0.03^{b}	0.411 ± 0.016^{cd}	0.098 ± 0.038^{a}	6.28 ± 0.24^{c}	3.53 ± 0.16^{d}
Q. agrifolia	0.27 ± 0.02^{c}	6.3 ± 0.3^{a}	4.9 ± 0.4^{a}	0.78 ± 0.03^{b}	0.266 ± 0.013^{a}	0.259 ± 0.032^{b}	3.88 ± 0.23^{a}	1.69 ± 0.10^{ab}
Q. wislizeni	0.07 ± 0.01^{a}	8.9 ± 1.8^{ab}	7.8 ± 1.6^{ab}	0.88 ± 0.02^{b}	0.344 ± 0.015^{bc}	0.045 ± 0.013^{a}	4.48 ± 0.19^{ab}	1.74 ± 0.08^{b}
Q. coccifera	0.08 ± 0.01^{a}	17.3 ± 1.8^{cd}	9.9 ± 1.6^{ab}	0.57 ± 0.02^{a}	0.454 ± 0.026^{de}	0.063 ± 0.027^{a}	5.13 ± 0.23^{b}	2.43 ± 0.13^{c}
Q. ilex subsp. *ilex*	0.11 ± 0.01^{a}	12.0 ± 0.9^{ab}	6.5 ± 0.7^{ab}	0.54 ± 0.03^{a}	0.484 ± 0.014^{e}	0.143 ± 0.023^{ab}	5.07 ± 0.16^{b}	1.80 ± 0.14^{ab}
Q. ilex subsp. *rotundifolia*	0.07 ± 0.01^{a}	21.1 ± 0.6^{d}	11.5 ± 0.9^{b}	0.56 ± 0.03^{a}	0.362 ± 0.08^{bc}	0.085 ± 0.023^{a}	4.10 ± 0.21^{ab}	1.17 ± 0.10^{a}
Q. suber	0.10 ± 0.01^{a}	16.6 ± 0.4^{cd}	13.1 ± 1.0^{b}	0.79 ± 0.07^{b}	0.298 ± 0.012^{ab}	0.101 ± 0.034^{a}	4.59 ± 0.21^{ab}	1.80 ± 0.08^{b}

Data are mean ± SE. Different letters indicate significant differences among species (Tukey's test, $P < 0.05$).

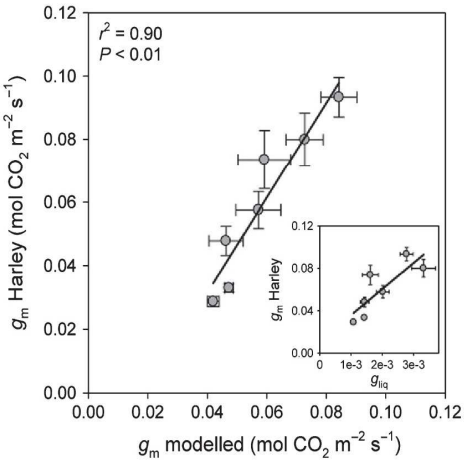

Fig. 3 Relationship between mesophyll conductance (g_m) modelled with anatomical traits and g_m measured with the Harley *et al.* (1992) method for the seven studied *Quercus* species. The inset shows the relationship between the conductance in liquid and lipid phases (g_{liq}) and g_m measured with the Harley *et al.* method ($r^2 = 0.68$, $P = 0.0228$). Data are mean ± SE.

tighter correlations (Fig. 7). The variance–covariance analysis indicated that the interaction between S_c/S_m and S_m/S was not significant, indicating that the slopes of both relationships were not statistically different at $P < 0.05$.

Discussion

This work confirms the existence of a convergence in several morphological traits among Mediterranean oaks with a diverse phylogenetic background. Such morphological leaf traits have been interpreted as adaptations to withstand summer drought (Morrow & Mooney, 1974; Poole & Miller, 1975; Baldocchi & Xu, 2007; Galmés *et al.*, 2012), given that water is the main limiting resource for plant growth in Mediterranean-type climates (Di Castri, 1981; Rhizopoulou & Mitrakos, 1990; Mediavilla & Escudero, 2003, 2004; Corcuera *et al.*, 2004). Thus, all the studied species show a reduced leaf area and thick leaves (Table 4), resulting in high LMA values when compared with other oak species from temperate climates (Corcuera *et al.*, 2002; Esteso-Martínez *et al.*, 2006). Furthermore, such convergence is common in the evergreen sclerophyllous vegetation typical for Mediterranean-type climates. Moreover, we found high values of cell wall thickness for all the studied species (Table 5; Fig. 5), similar to other evergreen tree species but higher than some deciduous trees (Tomás *et al.*, 2013). Specifically, the studied species showed T_{cw} values on average between 266 ± 13 and 484 ± 14 nm (Table 5), which were in the range reported by Hassiotou *et al.* (2010) for 18 *Banksia* species with high LMA values and by Tosens *et al.* (2012a) for 32 Australian sclerophyllous species. Besides morphological traits, the studied species shared low g_s and high iWUE values (Table 2; Fig. 2a). A reduced

New Phytologist

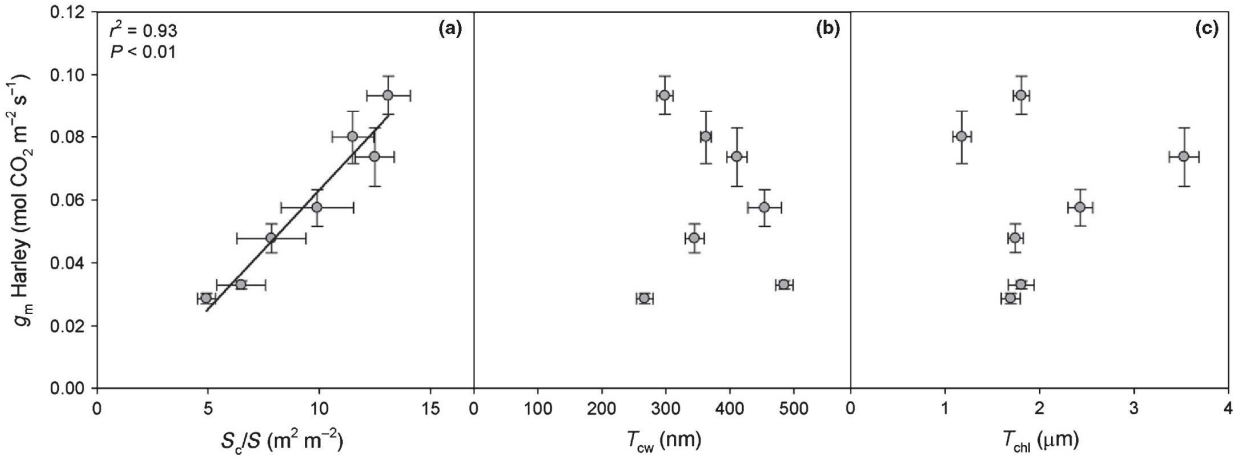

Fig. 4 Relationships between mesophyll conductance (g_m) measured with the Harley *et al.* (1992) method and (a) chloroplast surface area exposed to intercellular airspace (S_c/S), (b) cell wall thickness (T_{cw}) and (c) chloroplast thickness (T_{chl}) for the seven studied *Quercus* species. Data are mean ± SE. The relationships between g_m and T_{cw}, and between g_m and T_{chl}, were not statistically significant at $P < 0.05$.

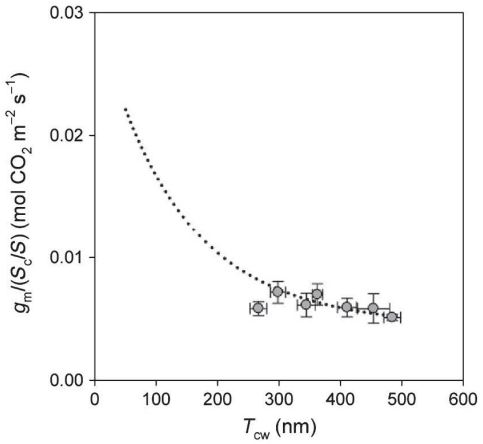

Fig. 5 Relationship between cell wall thickness (T_{cw}) and mesophyll conductance measured with the Harley *et al.* (1992) method per chloroplast surface area exposed to intercellular airspace ($g_m/(S_c/S)$) for the seven studied *Quercus* species. Data are mean ± SE. Dotted line shows the relationship found between T_{cw} and ($g_m/(S_c/S)$) by Terashima *et al.* (2011).

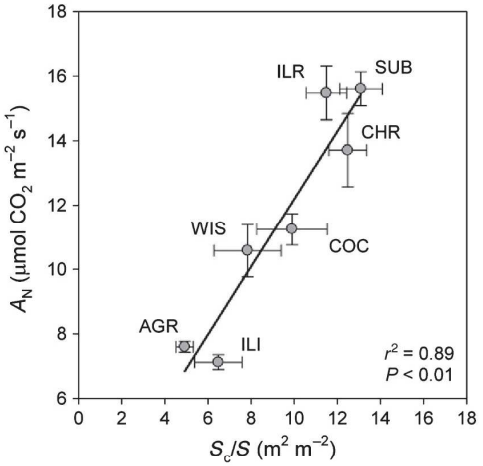

Fig. 6 Relationship between chloroplast surface area exposed to intercellular airspace (S_c/S) and net photosynthesis (A_N) for the seven studied *Quercus* species. Data are mean ± SE. Species abbreviations: AGR, *Q. agrifolia*; CHR, *Q. chrysolepis*; COC, *Q. coccifera*; ILI, *Q. ilex* subsp. *ilex*; ILR, *Q. ilex* subsp. *rotundifolia*; SUB, *Q. suber*; WIS, *Q. wislizeni*.

stomatal conductance, which is not necessarily a common feature in Mediterranean woody plants (Vilagrosa *et al.*, 2003; Peguero-Pina *et al.*, 2016b), can be interpreted in the sclerophyllous Mediterranean oaks studied here as a conservative strategy in terms of water consumption (Mediavilla & Escudero, 2003; Valladares *et al.*, 2005; Ozturk *et al.*, 2010). Moreover, the increased iWUE when compared with species from other biomes (Gulías *et al.*, 2003) has been described as an adaptive trait and a response to water scarcity in Mediterranean-type climates (Medrano *et al.*, 2009). However, despite these similarities, the present study reports the existence of differences in the photosynthetic activity among these Mediterranean evergreen oaks, which goes beyond the typical suites of morphological leaf traits reported for evergreen sclerophyllous species. Variations in the inherent photosynthetic capacity among the studied species were not related to variations in LMA (Fig. 1) and resulted mainly from the differences in g_m (Fig. 2b), which arise from the fact that mesophyll conductance was the most limiting factor for carbon assimilation in Mediterranean oaks (Table 3), regardless of the genetic background of the studied species.

In the present study, g_m estimates modelled based on leaf anatomical properties were very similar to those estimated using the conventional method for the seven studied species (Fig. 3). In previous studies, a good correspondence was generally found between estimated g_m using both methods when largely different species are pooled in the comparison (Tosens *et al.*, 2012a, 2016;

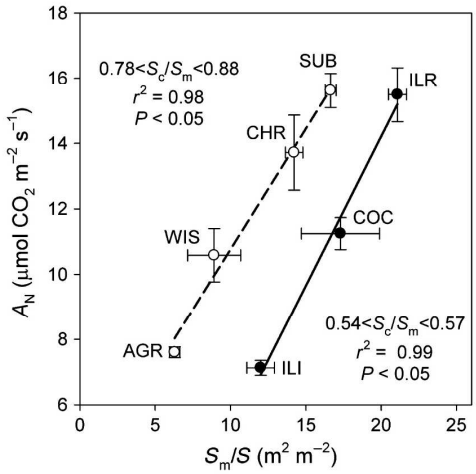

Fig. 7 Relationships between mesophyll surface area exposed to intercellular airspace (S_m/S) and net photosynthesis (A_N) for species with values for the ratio between chloroplast and mesophyll surface area exposed to intercellular airspace (S_c/S_m) between 0.78 and 0.88 (open symbols) and between 0.54 and 0.57 (closed symbols) (see Table 5). Data are mean ± SE. Species abbreviations: AGR, *Q. agrifolia*; CHR, *Q. chrysolepis*; COC, *Q. coccifera*; ILI, *Q. ilex* subsp. *ilex*; ILR, *Q. ilex* subsp. *rotundifolia*; SUB, *Q. suber*; WIS, *Q. wislizeni*.

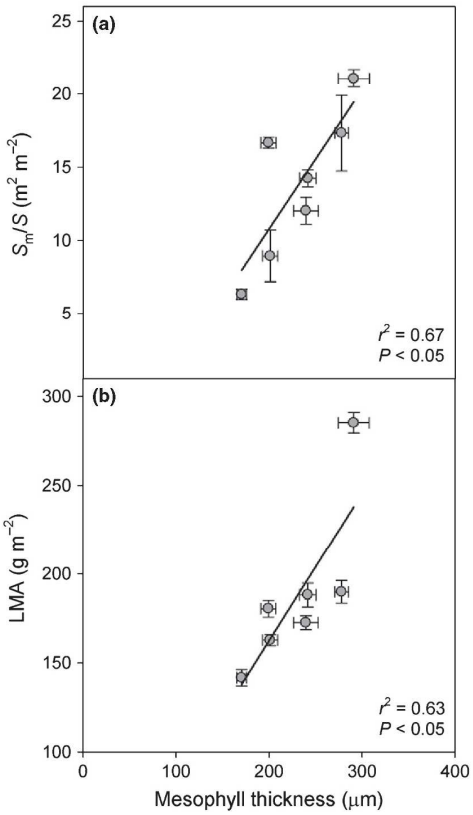

Fig. 8 Relationships between (a) mesophyll thickness and mesophyll surface area exposed to intercellular airspace (S_m/S), and between (b) mesophyll thickness and leaf mass area (LMA) for the seven studied *Quercus* species. Data are mean ± SE.

Tomás *et al.*, 2013; Carriquí *et al.*, 2015). However, such a correspondence was usually lost when comparing genotypes within a single species, especially under drought conditions (Tomás *et al.*, 2014). In this regard, Flexas *et al.* (2012) stated that g_m responds to different environmental factors (i.e. soil water availability, growth irradiance and temperature), which indicates that other additional mechanisms besides leaf anatomical traits regulate mesophyll conductance and photosynthetic activity under changing conditions. Here we have shown that the correlation between *in vivo* g_m and anatomical traits still holds under an intermediate situation when congeneric species were compared. The good correspondence between measured and simulated g_m estimates largely supports a predominant role of structural characteristics in determining photosynthetic differences among Mediterranean oaks. However, the key issue is that the contribution of different ultracellular and cellular components can vary strongly and, as our study demonstrates, the species differentiation in g_m is not necessarily determined by the most limiting component (cell walls in our study), but by components that exert a relatively minor control over total g_m. In particular, differences in g_m between the studied species can be partly attributed to the variation in leaf anatomical traits, mainly through the changes in S_c/S (Table 5; Fig. 4a) which is a key trait dominating variations in g_{liq}. In our study, species with higher photosynthetic ability have increased S_c/S and, consequently, higher g_m values with only slight changes in g_s (Fig. 2a).

From an anatomical perspective, S_c/S is determined by the combination of two independent factors, namely S_c/S_m and S_m/S. However, despite the strong lineal relationship found between S_c/S and A_N (Fig. 6), the correlations between S_c/S_m and A_N and between S_m/S and A_N were not statistically significant at $P<0.05$ for the seven studied *Quercus* species (data not shown). Regarding S_c/S_m, in this study we have found a clear segregation in two groups among the studied species. Thus, species from the *Ilex* group showed S_c/S_m values much lower than the remaining studied species (Table 5). With respect to the second factor, S_m/S, we have found two different lineal relationships between this parameter and A_N for each group of species classified according to the two different S_c/S_m values (Fig. 7). Thus, species from the *Ilex* group required higher S_m/S values to reach net CO_2 assimilation rates similar to those showed by the other species, in order to compensate for the lower S_c/S_m ratio (Figs 7, S4), which is an anatomical factor that exerts a strong influence on g_m. This mechanism – the increase of S_m/S – must be reached at the expense of an increase in mesophyll thickness (Fig. 8).

Our results suggest that the increased S_c/S found in Mediterranean oaks can improve g_m and, consequently, net CO_2 assimilation through anatomical adaptations at the cell level. These results agree with those previously reported in several studies (Hanba *et al.*, 1999, 2002; Terashima *et al.*, 2006; Peguero-Pina *et al.*, 2016b). By contrast, Tosens *et al.* (2012a) did not find a positive correlation between S_c/S and mesophyll thickness in several Australian sclerophyllous species. Previous studies have

shown other changes in the liquid-phase component of the diffusion conductance, including modifications in cell wall thickness (Peguero-Pina *et al.*, 2012) or chloroplast thickness (Peguero-Pina *et al.*, 2016c). Again such anatomical modifications reflect the circumstance that, in most cases, g_{liq} is the strongest limitation for photosynthesis because the CO_2 diffusion coefficient in the liquid phase is four orders of magnitude smaller than that in air (Niinemets & Reichstein, 2003).

Our study was carried out in a common garden, so the specific differences in the photosynthetic performance of the Mediterranean oaks could be related to the climatic characteristics of the natural distribution ranges of each studied species. Although a prolonged summer drought period is characteristic for all these species, its severity varies somewhat across the species ranges (Table 1; Figs S2, S3). Other climatic traits also vary within and among species ranges, and such site-specific differences in the climatic characteristics could be reflected in the functional performance of the Mediterranean oaks. Indeed, species living under more continental conditions, such as *Q. chrysolepis* and *Q. ilex* subsp. *rotundifolia*, had A_N and LMA values much higher than those occurring in mild coastal areas (i.e. *Q. agrifolia* and *Q. ilex* subsp. *ilex*). In this regard, a negative linear relationship was found between the length of the vegetation period (estimated here roughly as the number of months with mean monthly temperatures above 7.5°C; Montero de Burgos & González-Rebollar, 1974) and A_N for the studied species ($r^2 = 0.67$, $P < 0.05$; Fig. S5). Therefore, the increased instantaneous photosynthetic potential found in these two species may compensate for the shortening of their vegetation period due to a combination of a negative carbon balance during winter and the drought-induced limitations of photosynthesis during summer, as previously reported by Corcuera *et al.* (2005) for *Q. ilex* subsp. *rotundifolia*. By contrast, other authors have found that Mediterranean oak species occurring at sites with milder conditions showed a positive carbon balance during winter; for example, García-Plazaola *et al.* (1999) found that *Q. ilex* subsp. *ilex* maintained photosynthetic rates during winter that were very similar to those reported in the present study in summer.

Conclusions

To the best of our knowledge, this is the first interspecific comparison of photosynthetic characteristics and underlying leaf anatomical traits among Mediterranean oaks from Europe/North Africa and North America. Despite their morphological similarity, we observed strong differences in the functional performance of individual species. We conclude that g_m is the main factor determining carbon assimilation in Mediterranean evergreen oak species. Differentiation in g_m among these species is not necessarily determined by the most limiting component (the cell wall), but by components that exert a relatively minor control over total g_m. Thus, species with higher A_N showed increased S_c/S values, which imply increased g_m values without significant changes in stomatal conductance and, therefore, water losses. The occurrence of this anatomical adaptation at the cell level allowed evergreen oaks to reach A_N values comparable to congeneric deciduous species despite their higher LMA.

Acknowledgements

Financial support from Gobierno de Aragón (H38 research group) is acknowledged. The work of D.S-K. is supported by a DOC INIA contract co-funded by the Spanish National Institute for Agriculture and Food Research and Technology (INIA) and the European Social Fund (ESF).

Author contributions

J.J.P-P., S.S., D.S-K. and E.G-P. planned and designed the research; S.S. and A.G-N. performed the experiments; J.J.P-P., D.S-K., J.F., J.G., U.N., M.A.S. and E.G-P. analysed the data; J.J.P-P., J.F., A.G-N., U.N. and E.G-P. wrote the manuscript.

References

Baldocchi DD, Xu L. 2007. What limits evaporation from Mediterranean oak woodlands – the supply of moisture in the soil, physiological control by plants or the demand by the atmosphere? *Advances in Water Resources* **30**: 2113–2122.

Bernacchi CJ, Portis AR, Nakano H, von Caemmerer S, Long SP. 2002. Temperature response of mesophyll conductance. Implications for the determination of Rubisco enzyme kinetics and for limitations to photosynthesis in vivo. *Plant Physiology* **130**: 1992–1998.

Cano FJ, Sánchez-Gómez D, Rodríguez-Calcerrada J, Warren CR, Gil L, Aranda I. 2013. Effects of drought on mesophyll conductance and photosynthetic limitations at different tree canopy layers. *Plant, Cell & Environment* **36**: 1961–1980.

Carriquí M, Cabrera HM, Conesa MÀ, Coopman RE, Douthe C, Gago J, Gallé A, Galmés J, Ribas-Carbó M, Tomás M *et al.* 2015. Diffusional limitations explain the lower photosynthetic capacity of ferns as compared with angiosperms in a common garden study. *Plant, Cell & Environment* **38**: 448–460.

Corcuera L, Camarero JJ, Gil-Pelegrín E. 2002. Functional groups in *Quercus* species derived from the analysis of pressure–volume curves. *Trees – Structure and Function* **16**: 465–472.

Corcuera L, Camarero JJ, Gil-Pelegrín E. 2004. Effects of a severe drought on *Quercus ilex* radial growth and xylem anatomy. *Trees – Structure and Function* **18**: 83–92.

Corcuera L, Morales F, Abadía A, Gil-Pelegrín E. 2005. Seasonal changes in photosynthesis and photoprotection in a *Quercus ilex* subsp. *ballota* woodland located in its upper altitudinal extreme in the Iberian Peninsula. *Tree Physiology* **25**: 599–608.

Denk T, Grimm GW. 2009. Significance of pollen characteristics for infrageneric classification and phylogeny in *Quercus* (Fagaceae). *International Journal of Plant Science* **170**: 926–940.

Di Castri F. 1981. Mediterranean-type shrublands of the world. In: Di Castri F, Goodall DW, Specht RL, eds. *Mediterranean-type shrublands*. Amsterdam, the Netherlands: Elsevier, 1–52.

Dunn OJ, Clark VA. 1987. *Applied statistics. Analysis of variance and regression.* New York, NY, USA: John Wiley & Sons Inc.

Epron D, Dreyer E, Aussenac G. 1993. A comparison of photosynthetic responses to water stress in seedlings from 3 oak species: *Quercus petraea* (Matt.) Liebl., *Q. rubra* L. and *Q. cerris* L. *Annales des Sciences Forestières* **50** (Suppl 1): 48–60.

Epron D, Dreyer E, Breda N. 1992. Photosynthesis of oak trees [*Quercus petraea* (Matt.) Liebl.] during drought under field conditions: diurnal course of net CO_2 assimilation and photochemical efficiency of photosystem II. *Plant, Cell & Environment* **15**: 809–820.

Esteso-Martínez J, Valladares F, Camarero JJ, Gil-Pelegrín E. 2006. Crown architecture and leaf habit are associated with intrinsically different light-harvesting efficiencies in *Quercus* seedlings from contrasting environments. *Annals of Forest Science* **63**: 511–518.

Evans JR, von Caemmerer S, Setchell BA, Hudson GS. 1994. The relationship between CO_2 transfer conductance and leaf anatomy in transgenic tobacco with a reduced content of Rubisco. *Australian Journal of Plant Physiology* **21**: 475–495.

Farquhar GD, von Caemmerer S, Berry JA. 1980. A biochemical model of photosynthetic CO_2 assimilation in leaves of C_3 species. *Planta* **149**: 78–90.

Flexas J, Barbour MM, Brendel O, Cabrera HM, Carriquí M, Díaz-Espejo A, Douthe C, Dreyer E, Ferrio JP, Gago J *et al.* 2012. Mesophyll diffusion conductance to CO_2: an unappreciated central player in photosynthesis. *Plant Science* **193–194**: 70–84.

Flexas J, Díaz-Espejo A, Berry JA, Galmés J, Cifre J, Kaldenhoff R, Medrano H, Ribas-Carbó M. 2007a. Analysis of leakage in IRGA's leaf chambers of open gas exchange systems: quantification and its effects in photosynthesis parameterization. *Journal of Experimental Botany* **58**: 1533–1543.

Flexas J, Díaz-Espejo A, Gago J, Gallé A, Galmés J, Gulías J, Medrano H. 2014. Photosynthetic limitations in Mediterranean plants: a review. *Environmental and Experimental Botany* **103**: 12–23.

Flexas J, Ortuño MF, Ribas-Carbó M, Díaz-Espejo A, Flórez-Sarasa ID, Medrano H. 2007b. Mesophyll conductance to CO_2 in *Arabidopsis thaliana*. *New Phytologist* **175**: 501–511.

Flexas J, Ribas-Carbó M, Díaz-Espejo A, Galmés J, Medrano H. 2008. Mesophyll conductance to CO_2: current knowledge and future prospects. *Plant, Cell & Environment* **31**: 601–621.

Galmés J, Andralojc PJ, Kapralov MV, Flexas J, Keys J, Molins A, Parry MAJ, Conesa MÀ. 2014. Environmentally driven evolution of Rubisco and improved photosynthesis and growth within the C_3 genus *Limonium* (Plumbaginaceae). *New Phytologist* **203**: 989–999.

Galmés J, Cifre J, Medrano H, Flexas J. 2005. Modulation of relative growth rate and its components by water stress in Mediterranean species with different growth forms. *Oecologia* **145**: 21–31.

Galmés J, Flexas J, Medrano H, Niinemets Ü, Valladares F. 2012. Ecophysiology of photosynthesis in semi-arid environments. In: Flexas J, Loreto F, Medrano H, eds. *Terrestrial photosynthesis in a changing environment. A molecular, physiological and ecological approach*. Cambridge, UK: Cambridge University Press, 448–464.

García-Plazaola JI, Artetxe U, Becerril JM. 1999. Diurnal changes in antioxidant and carotenoid composition in the Mediterranean schlerophyll tree *Quercus ilex* L. during winter. *Plant Science* **143**: 125–133.

Genty B, Briantais JM, Baker NR. 1989. The relationship between the quantum yield of photosynthetic electron transport and quenching of chlorophyll fluorescence. *Biochimica et Biophysica Acta* **990**: 87–92.

González-Zurdo P, Escudero A, Babiano J, García-Ciudad A, Mediavilla S. 2016. Costs of leaf reinforcement in response to winter cold in evergreen species. *Tree Physiology* **36**: 273–286.

Grassi G, Magnani F. 2005. Stomatal, mesophyll conductance and biochemical limitations to photosynthesis as affected by drought and leaf ontogeny in ash and oak trees. *Plant, Cell & Environment* **28**: 834–849.

Gulías J, Flexas J, Mus M, Cifre J, Lefi E, Medrano H. 2003. Relationship between maximum leaf photosynthesis, nitrogen content and specific leaf area in Balearic endemic and non-endemic Mediterranean species. *Annals of Botany* **92**: 215–222.

Hanba YT, Kogami H, Terashima I. 2002. The effect of growth irradiance on leaf anatomy and photosynthesis in *Acer* species differing in light demand. *Plant, Cell & Environment* **25**: 1021–1030.

Hanba YT, Miyazawa SI, Terashima I. 1999. The influence of leaf thickness on the CO_2 transfer conductance and leaf stable carbon isotope ratio for some evergreen tree species in Japanese warm temperate forests. *Functional Ecology* **13**: 632–639.

Harley PC, Loreto F, Di Marco G, Sharkey TD. 1992. Theoretical considerations when estimating the mesophyll conductance to CO_2 flux by the analysis of the response of photosynthesis to CO_2. *Plant Physiology* **98**: 1429–1436.

Hassiotou F, Ludwig M, Renton M, Veneklaas EJ, Evans JR. 2009. Influence of leaf dry mass per area, CO_2 and irradiance on mesophyll conductance in sclerophylls. *Journal of Experimental Botany* **60**: 2303–2314.

Hassiotou F, Renton M, Ludwig M, Evans JR, Veneklaas EJ. 2010. Photosynthesis at an extreme end of the leaf trait spectrum: how does it relate to high leaf dry mass per area and associated structural parameters? *Journal of Experimental Botany* **61**: 3015–3028.

Krall JP, Edwards GE. 1992. Relationship between photosystem II activity and CO_2 fixation in leaves. *Physiologia Plantarum* **86**: 80–187.

Kremer A, Abbott AG, Carlson JE, Manos PS, Plomion C, Sisco P, Staton ME, Ueno S, Vendramin GG. 2012. Genomics of Fagaceae. *Tree Genetics & Genomes* **8**: 583–610.

Kummerow J. 1973. Comparative anatomy of sclerophylls of Mediterranean climatic areas. In: Di Castri F, Mooney HA, eds. *Mediterranean-type ecosystems: origin and structure*. Berlin, Germany: Springer, 213–224.

Manos PS, Doyle JJ, Nixon KC. 1999. Phylogeny, biogeography and processes of molecular differentiation in *Quercus* subgenus *Quercus* (Fagaceae). *Molecular Phylogenetics and Evolution* **12**: 333–349.

Mediavilla S, Escudero A. 2003. Stomatal responses to drought at a Mediterranean site: a comparative study of co-occurring woody species differing in leaf longevity. *Tree Physiology* **23**: 987–996.

Mediavilla S, Escudero A. 2004. Stomatal responses to drought of mature trees and seedlings of two co-occurring Mediterranean oaks. *Forest Ecology and Management* **187**: 281–294.

Medrano H, Flexas J, Galmés J. 2009. Variability in water use efficiency at the leaf level among Mediterranean plants with different growth forms. *Plant and Soil* **317**: 17–29.

Montero de Burgos J, González-Rebollar J. 1974. *Diagramas Bioclimáticos*. Madrid, Spain: ICONA.

Morrow PA, Mooney HA. 1974. Drought adaptations in two Californian evergreen sclerophylls. *Oecologia* **15**: 205–222.

Niinemets Ü. 2015. Is there a species spectrum within the world-wide leaf economics spectrum? Major variations in leaf functional traits in the Mediterranean sclerophyll *Quercus ilex*. *New Phytologist* **205**: 79–96.

Niinemets Ü, Keenan TF. 2014. Photosynthetic responses to stress in Mediterranean evergreens: mechanisms and models. *Environmental and Experimental Botany* **103**: 24–41.

Niinemets Ü, Reichstein M. 2003. Controls on the emission of plant volatiles through stomata: a sensitivity analysis. *Journal of Geophysical Research* **108**: 4211.

Niinemets Ü, Wright IJ, Evans JR. 2009. Leaf mesophyll diffusion conductance in 35 Australian sclerophylls covering a broad range of foliage structural and physiological variation. *Journal of Experimental Botany* **60**: 2433–2449.

Ozturk M, Dogan Y, Sakcali MS, Doulis A, Karam F. 2010. Ecophysiological responses of some maquis (*Ceratonia siliqua* L., *Olea oleaster* Hoffm. & Link, *Pistacia lentiscus* and *Quercus coccifera* L.) plant species to drought in the east Mediterranean ecosystem. *Journal of Environmental Biology* **31**: 233–245.

Peguero-Pina JJ, Flexas J, Galmés J, Niinemets Ü, Sancho-Knapik D, Barredo G, Villarroya D, Gil-Pelegrín E. 2012. Leaf anatomical properties in relation to differences in mesophyll conductance to CO_2 and photosynthesis in two related Mediterranean *Abies* species. *Plant, Cell & Environment* **35**: 2121–2129.

Peguero-Pina JJ, Sancho-Knapik D, Flexas J, Galmés J, Niinemets Ü, Gil-Pelegrín E. 2016c. Light acclimation of photosynthesis in two closely related firs (*Abies pinsapo* Boiss. and *Abies alba* Mill.): the role of leaf anatomy and mesophyll conductance to CO_2. *Tree Physiology* **36**: 300–310.

Peguero-Pina JJ, Sancho-Knapik D, Morales F, Flexas J, Gil-Pelegrín E. 2009. Differential photosynthetic performance and photoprotection mechanisms of three Mediterranean evergreen oaks under severe drought stress. *Functional Plant Biology* **36**: 453–462.

Peguero-Pina JJ, Sisó S, Fernández-Marín B, Flexas J, Galmés J, García-Plazaola JI, Niinemets Ü, Sancho-Knapik D, Gil-Pelegrín E. 2016a. Leaf functional plasticity decreases the water consumption without further consequences for carbon uptake in *Quercus coccifera* L. under Mediterranean conditions. *Tree Physiology* **36**: 356–367.

Peguero-Pina JJ, Sisó S, Sancho-Knapik D, Díaz-Espejo A, Flexas J, Galmés J, Gil-Pelegrín E. 2016b. Leaf morphological and physiological adaptations of a deciduous oak (*Quercus faginea* Lam.) to the Mediterranean climate: a

comparison with a closely related temperate species (*Quercus robur* L.). *Tree Physiology* **36**: 287–299.

Piel C. 2002. *Diffusion du CO_2 dans le mésophylle des plantes à métabolisme C_3.* PhD thesis, Paris, France: Université Paris XI Orsay.

Poole DK, Miller PC. 1975. Water relations of selected species of chaparral and coastal communities. *Ecology* **56**: 1118–1128.

Rhizopoulou S, Mitrakos K. 1990. Water relations of evergreen sclerophylls. I. Seasonal changes in the water relations of eleven species from the same environment. *Annals of Botany* **65**: 171–178.

Roupsard O, Gross P, Dreyer E. 1996. Limitation of photosynthetic activity by CO_2 availability in the chloroplasts of oak leaves from different species and during drought. *Annales des Sciences Forestières* **53**: 243–254.

Slaton MR, Smith WK. 2002. Mesophyll architecture and cell exposure to intercellular air space in alpine, desert, and forest species. *International Journal of Plant Sciences* **163**: 937–948.

Steinbrecher R, Contran N, Gugerli F, Schnitzler JP, Zimmer I, Menard T, Günthardt-Goerg MS. 2013. Inter- and intra-specific variability in isoprene production and photosynthesis of Central European oak species. *Plant Biology* **15**(Suppl. 1): 148–156.

Syvertsen JP, Lloyd J, McConchie C, Kriedemann PE, Farquhar GD. 1995. On the relationship between leaf anatomy and CO_2 diffusion through the mesophyll of hypostomatous leaves. *Plant, Cell & Environment* **18**: 149–157.

Terashima I, Hanba YT, Tazoe Y, Vyas P, Yano S. 2006. Irradiance and phenotype: comparative eco-development of sun and shade leaves in relation to photosynthetic CO_2 diffusion. *Journal of Experimental Botany* **57**: 343–354.

Terashima I, Hanba YT, Tholen D, Niinemets Ü. 2011. Leaf functional anatomy in relation to photosynthesis. *Plant Physiology* **155**: 108–116.

Thain JF. 1983. Curvature correlation factors in the measurements of cell surface areas in plant tissues. *Journal of Experimental Botany* **34**: 87–94.

Tholen D, Ethier G, Genty B, Pepin S, Zhu X. 2012. Variable mesophyll conductance revisited: theoretical background and experimental implications. *Plant, Cell & Environment* **35**: 2087–2103.

Tomás M, Flexas J, Copolovici L, Galmés J, Hallik L, Medrano H, Ribas-Carbó M, Tosens T, Vislap V, Niinemets Ü. 2013. Importance of leaf anatomy in determining mesophyll diffusion conductance to CO_2 across species: quantitative limitations and scaling up by models. *Journal of Experimental Botany* **64**: 2269–2281.

Tomás M, Medrano H, Brugnoli E, Escalona JM, Martorell S, Pou A, Ribas-Carbó M, Flexas J. 2014. Variability of mesophyll conductance in grapevine cultivars under water stress conditions in relation to leaf anatomy and water use efficiency. *Australian Journal of Grape and Wine Research* **20**: 272–280.

Tosens T, Niinemets Ü, Vislap V, Eichelmann H, Castro-Díez P. 2012b. Developmental changes in mesophyll diffusion conductance and photosynthetic capacity under different light and water availabilities in *Populus tremula*: how structure constrains function. *Plant, Cell & Environment* **35**: 839–856.

Tosens T, Niinemets Ü, Westoby M, Wright IJ. 2012a. Anatomical basis of variation in mesophyll resistance in eastern Australian sclerophylls: news of a long and winding path. *Journal of Experimental Botany* **63**: 5105–5119.

Tosens T, Nishida K, Gago J, Coopman RE, Cabrera HM, Carriquí M, Laanisto L, Morales L, Nadal M, Rojas R *et al.* 2016. The photosynthetic capacity in 35 ferns and fern allies: mesophyll CO_2 diffusion as a key trait. *New Phytologist* **209**: 1576–1590.

Traiser C, Klotz S, Uhl D, Mosbrugger V. 2005. Environmental signals from leaves – a physiognomic analysis of European vegetation. *New Phytologist* **166**: 465–484.

Turnbull MH, Whitehead D, Tissue DT, Schuster WSF, Brown KJ, Engel VC, Griffin KL. 2002. Photosynthetic characteristics in canopies of *Quercus rubra*, *Quercus prinus* and *Acer rubrum* differ in response to soil water availability. *Oecologia* **130**: 515–524.

Valentini R, Epron D, De Angelis P, Matteucci G, Dreyer E. 1995. In situ estimation of net CO_2 assimilation, photosynthetic electron flow and photorespiration in Turkey oak (*Quercus cerris* L.) leaves: diurnal cycles under different levels of water supply. *Plant, Cell & Environment* **18**: 631–640.

Valladares F, Dobarro I, Sánchez-Gómez D, Pearcy RW. 2005. Photoinhibition and drought in Mediterranean woody saplings: scaling effects and interactions in sun and shade phenotypes. *Journal of Experimental Botany* **56**: 483–494.

Vilagrosa A, Bellot J, Vallejo VR, Gil-Pelegrín E. 2003. Cavitation, stomatal conductance, and leaf dieback in seedlings of two co-occurring Mediterranean shrubs during an intense drought. *Journal of Experimental Botany* **54**: 2015–2024.

Wright IJ, Reich PB, Cornelissen JHC, Falster DS, Groom PK, Hikosaka K, Lee W, Lusk CH, Niinemets Ü, Oleksyn J *et al.* 2005. Modulation of leaf economic traits and trait relationships by climate. *Global Ecology and Biogeography* **14**: 411–421.

Wright IJ, Reich PB, Westoby M, Ackerly DD, Baruch Z, Bongers F, Cavender-Bares J, Chapin T, Cornelissen JHC, Diemer M *et al.* 2004. The world-wide leaf economics spectrum. *Nature* **428**: 821–827.

Supporting Information

Additional Supporting Information may be found online in the Supporting Information tab for this article:

Fig. S1 Geographical locations used to obtain the climatic information for the seven studied *Quercus* species throughout their distribution ranges.

Fig. S2 Ombrothermic diagrams for the distribution ranges of the seven studied *Quercus* species.

Fig. S3 Maximum daily vapour pressure deficit (VPD_{max}) for the distribution ranges of the seven studied *Quercus* species.

Fig. S4 Schematic representation of the relationships between S_m/S and A_N for species with high and low S_c/S_m values.

Fig. S5 Relationship between the length of the vegetation period and A_N for the seven studied *Quercus* species.

Table S1 Outputs of the one-way ANOVAs performed to identify the species effect on photosynthetic, morphological and anatomical traits

Table S2 Quantitative limitations of mesophyll conductance to CO_2 (g_m) in the seven studied *Quercus* species

Please note: Wiley Blackwell are not responsible for the content or functionality of any Supporting Information supplied by the authors. Any queries (other than missing material) should be directed to the *New Phytologist* Central Office.

Tree Physiology 36, 287–299
doi:10.1093/treephys/tpv107

Research paper

Leaf morphological and physiological adaptations of a deciduous oak (*Quercus faginea* Lam.) to the Mediterranean climate: a comparison with a closely related temperate species (*Quercus robur* L.)

José Javier Peguero-Pina[1,†], Sergio Sisó[1,†], Domingo Sancho-Knapik[1], Antonio Díaz-Espejo[2], Jaume Flexas[3], Jeroni Galmés[3] and Eustaquio Gil-Pelegrín[1,4]

[1]Unidad de Recursos Forestales, Centro de Investigación y Tecnología Agroalimentaria, Gobierno de Aragón, Avenida Montañana 930, 50059 Zaragoza, Spain; [2]Irrigation and Crop Ecophysiology Group, Instituto de Recursos Naturales y Agrobiología de Sevilla (IRNAS, CSIC), Avenida Reina Mercedes 10, 41012 Sevilla, Spain; [3]Research Group on Plant Biology under Mediterranean Conditions, Departament de Biologia, Universitat de les Illes Balears, Carretera de Valldemossa, 07071 Palma de Mallorca, Spain; [4]Corresponding author (egilp@aragon.es)

Received June 12, 2015; accepted September 4, 2015; published online October 23, 2015; handling Editor Roberto Tognetti

'White oaks'—one of the main groups of the genus *Quercus* L.—are represented in western Eurasia by the 'roburoid oaks', a deciduous and closely related genetic group that should have an Arcto-Tertiary origin under temperate-nemoral climates. Nowadays, roburoid oak species such as *Quercus robur* L. are still present in these temperate climates in Europe, but others are also present in southern Europe under Mediterranean-type climates, such as *Quercus faginea* Lam. We hypothesize the existence of a coordinated functional response at the whole-shoot scale in *Q. faginea* under Mediterranean conditions to adapt to more xeric habitats. The results reveal a clear morphological and physiological segregation between *Q. robur* and *Q. faginea*, which constitute two very contrasting functional types in response to climate dryness. The most outstanding divergence between the two species is the reduction in transpiring area in *Q. faginea*, which is the main trait imposed by the water deficit in Mediterranean-type climates. The reduction in leaf area ratio in *Q. faginea* should have a negative effect on carbon gain that is partially counteracted by a higher inherent photosynthetic ability of *Q. faginea* when compared with *Q. robur*, as a consequence of higher mesophyll conductance, higher maximum velocity of carboxylation and much higher stomatal conductance (g_s). The extremely high g_s of *Q. faginea* counteracts the expected reduction in g_s imposed by the stomatal sensitivity to vapor pressure deficit, allowing this species to diminish water losses maintaining high net CO_2 assimilation values along the vegetative period under nonlimiting soil water potential values. In conclusion, the present study demonstrates that *Q. faginea* can be regarded as an example of adaptation of a deciduous oak to Mediterranean-type climates.

Keywords: leaf area, roburoid oaks, stomatal conductance, vapor pressure deficit.

Introduction

The genus *Quercus* L. (Fagaceae) comprises ~400 tree and shrub species distributed among contrasting phytoclimates in the Northern Hemisphere, from temperate and subtropical deciduous forests to Mediterranean evergreen woodlands (Manos et al. 1999, Kremer et al. 2012). Although the successive infrageneric classifications of *Quercus* have undergone changes, all of them recognized the same major groups (see

†These authors contributed equally to this study.

Denk and Grimm 2010 and references therein). One of the main groups is the so-called 'Group *Quercus*' or 'white oaks' (Denk and Grimm 2009), which is represented in western Eurasia by the so-called 'roburoid oaks' (Denk and Grimm 2010). The roburoid oaks that should have their origin in Arcto-Tertiary lineages during the Early Tertiary (Axelrod 1983, Kovar-Eder et al. 1996) are a quite coherent group of species with a high degree of genetic similarity (Olalde et al. 2002, Denk and Grimm 2010). Nowadays, one of the greatest representative roburoid oak species widely distributed along a temperate-nemoral climate is *Quercus robur* L., which is considered a meso-hygrophilous species (Piedallu et al. 2013) distributed in Europe from Spain to southern Scandinavia and from Ireland to eastern Europe (Ducousso and Bordacs 2004).

Nevertheless, the roburoid oaks are not exclusive of the temperate climates, but they are also present in southern Europe under Mediterranean-type climates (Corcuera et al. 2004, Himrane et al. 2004, Sánchez de Dios et al. 2009), which evidences the ability to survive in more xeric habitats (Kvacek and Walther 1989, Barrón et al. 2010). This may be the case of *Quercus faginea* Lam., for which the first fossil records, found in the south of France, coincide with the development of the Mediterranean seasonality during the Pliocene (Roiron 1983, Barrón et al. 2010).

Quercus faginea is the most abundant and widely distributed white oak in the Iberian Peninsula (Olalde et al. 2002). Some previous studies that have dealt with the resistance to drought of this species are mainly based on the comparison with other Mediterranean oak species, such as the evergreen *Quercus ilex* (Corcuera et al. 2002, Mediavilla and Escudero 2003). This comparison makes sense in terms of forest composition and vegetation dynamic in most continental Mediterranean areas of the Iberian Peninsula (Mediavilla and Escudero 2004), where *Q. faginea* and *Q. ilex* co-occur. These congeneric species constitute two examples of contrasting leaf habit, which itself represents quite different functional strategies (Kikuzawa 1995). In this sense, it has been proposed that the evergreen condition of *Q. ilex* would allow this species to assimilate carbon throughout a longer time period (Acherar and Rambal 1992, Ogaya and Peñuelas 2007, van Ommen Kloeke et al. 2012), which was empirically confirmed in cold Mediterranean areas (Corcuera et al. 2005*a*). On the contrary, the leaf life span of the deciduous *Q. faginea* limits the photosynthetic activity to a shorter period, implying the need for higher rates of carbon gain under favorable conditions (van Ommen Kloeke et al. 2012).

However, the importance in the Mediterranean forest landscape of the Iberian Peninsula and north of Africa of such deciduous Mediterranean oaks, such as *Q. faginea* and other congeneric species (Olalde et al. 2002, Benito Garzón et al. 2007, Sánchez de Dios et al. 2009), indicates that this leaf habit performs adequately under the limiting climatic conditions of Mediterranean areas. Therefore, some roburoid oaks, such as *Q. faginea*, must have developed functional strategies to adapt to the summer drought conditions, withstanding both edaphic and atmospheric water stresses.

In order to evaluate the physiological traits that *Q. faginea* shows for coping with the Mediterranean aridity, we established an interspecific comparison with *Q. robur*, other roburoid deciduous oak from temperate-nemoral climates. We hypothesize the existence of a coordinated functional response at the whole-shoot scale in *Q. faginea* under Mediterranean conditions. In this sense, the specific objectives of this study are (i) to analyze the morphological, anatomical, hydraulic, photosynthetic and biochemical traits of *Q. faginea* and (ii) to compare them with those from *Q. robur*, a temperate white oak genetically closely related but occurring under contrasting ecological and climatic conditions (Olalde et al. 2002, Himrane et al. 2004).

Materials and methods

Plant material and experimental conditions

Seeds from *Q. robur* L. ('Galicia' provenance, 42°34′N, 8°33′W, 300 m above sea level, Spain) and *Q. faginea* Lam. ('Alcarria-Serranía de Cuenca' provenance, 40°19′N, 2°15′W, 950 m above sea level, Spain) were sown and cultivated in 2009 under the same conditions (mixture of 80% substrate and 20% perlite in 500 ml containers) inside a transparent greenhouse of alveolar polycarbonate (CITA de Aragón, Zaragoza, Spain) that allowed passing 90% of photosynthetic photon flux density (PPFD; ~1500 mmol photons m^2 s^{-1} at midday, during the experiments) and was equipped with an evaporative cooling system, set for keeping the air temperature inside the greenhouse below 30 °C, while air vapor pressure deficit (VPD) was ~1 kPa through the experiments. Such environmental conditions are close to those recorded during the early growing season (May–June) for both species (Figure 1). Periodical surveys (twice a week) yielded no differences in the time of leaf unfolding between both species when cultivated under the same conditions (data not shown). Jato et al. (2002) also reported the same date for leaf unfolding in co-occurring populations of both species in northwestern Spain. After the first growth cycle, the seedlings were transplanted to containers of 25 l. All plants were irrigated every 2 days. Measurements were performed at the end of June 2012 in fully matured leaves of 4-year-old seedlings for both species.

The distribution ranges of each species have contrasting climatic conditions. *Quercus robur* occurs in sites where annual and summer precipitation (P and P_s, respectively) are higher than in the sites where *Q. faginea* occurs (Table 1). The mean annual and summer temperatures (T and T_s, respectively) are higher for the sites where *Q. faginea* occurs (Table 1). As a consequence, the Martonne aridity index [$MAI = P/(T + 10)$] and the Gaussen index (the number of months in which $P < 2T$, where P is the

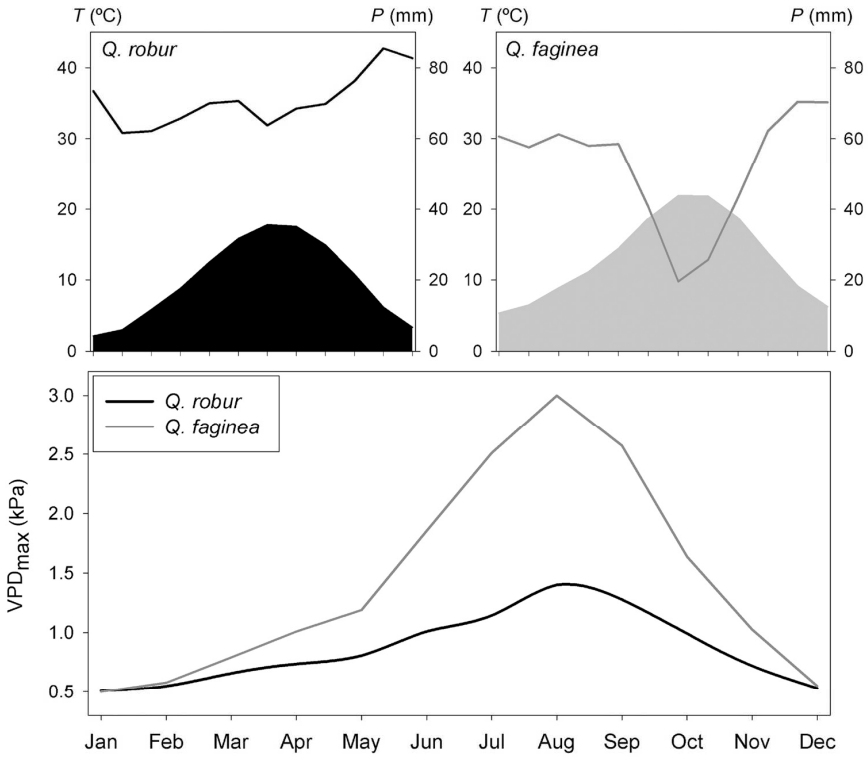

Figure 1. Ombrothermic diagrams showing temperature (T, filled areas) and precipitation (P, lines) (upper panels) and VPD_{max} (lower panel) for the distribution ranges of *Q. robur* and *Q. faginea*.

Table 1. Mean climatic characteristics for the distribution ranges of *Q. robur* and *Q. faginea*: mean annual and summer temperature (T and T_s), total annual and summer precipitation (P and P_s), MAI and Gaussen index. Data are mean ± SE. Different letters indicate statistically significant differences ($P < 0.05$).

Species	T (°C)	T_s (°C)	P (mm)	P_s (mm)	MAI	Gaussen index
Q. robur	9.9 ± 0.3a	17.0 ± 0.2a	850 ± 27a	206 ± 9a	43 ± 2a	0 ± 0a
Q. faginea	13.0 ± 0.3b	20.8 ± 0.3b	628 ± 15b	86 ± 6b	28 ± 1b	2.6 ± 0.2b

monthly precipitation in mm and T is the monthly mean temperature in °C) are also higher for the sites where *Q. faginea* occurs (Table 1, Figure 1). Climatic information was obtained from the WorldClim database (http://www.worldclim.org/) using 70 geographic points throughout the distribution range of *Q. robur* and *Q. faginea*, respectively. Moreover, VPD (kPa) was calculated using the data obtained from WeatherSpark database (http://weatherspark.com/) for six locations of *Q. robur* and *Q. faginea*, respectively. The maximum daily VPD (VPD_{max}, kPa) is much higher for the sites where *Q. faginea* occurs, especially during summer (Figure 1).

Morphological variables

Leaf area and leaf mass area (LMA) were measured in 30 mature leaves sampled from 10 individuals per species (i.e., three leaves were randomly taken from each individual). Leaf area was measured by digitalizing the leaves and using the ImageJ image analysis software (http://rsb.info.nih.gov/nih-image/). Leaves were then oven-dried at 70 °C for 3 days to determine their dry weight. The LMA was calculated as the ratio of the foliage dry weight to foliage area and was used as an estimator of sclerophylly (Corcuera et al. 2002). Major vein density (MVD) was determined in another set of 10 mature leaves per species following the method described in Scoffoni et al. (2011) with some modifications. Leaves were chemically cleared with 5% NaOH in aqueous solution, washed with bleach solution, dehydrated in an ethanol dilution series (70, 90, 95 and 100%) and stained with safranin. Then, leaves were scanned at 1200 d.p.i. resolution, and the leaf area and lengths of first-, second- and third-order veins were measured using the ImageJ software. Vein densities for each order were calculated as the vein length/leaf area ratio (LAR). The MVD was then obtained as the sum of the first-, second- and third-order vein densities. Finally, the LAR was calculated in 10 current-year shoots per species by dividing the total leaf area per shoot (measured as described above) by the dry weight of the shoot.

Stem hydraulic conductivity

The hydraulic conductivity (K_h, kg m s^{-1} MPa^{-1}) was determined in current-year stem segments of *Q. robur* and *Q. faginea*. Three stem segments (3–5 cm long and >1 mm in diameter) per branch were cut under water from 10 south-exposed branches per species. The measurement pressure was set to 4 kPa. The flow rate was determined with a PC-connected balance (Sartorius BP221S, 0.1 mg precision, Sartorius AG, Göttingen, Germany) by recording the change in weight every 10 s and fitting linear regressions over 200-s intervals. The conductivity measurements were carried out with distilled, filtered (0.22 µm) and degassed water containing 0.005% (volume/volume) Micropur (Katadyn Products, Wallisellen, Switzerland) to prevent microbial growth (Mayr et al. 2006). No native embolism was detected in the segments, as reflected by the comparison of the flow rates before and after applying short perfusions at 0.15 MPa for 60–90 s. The same stem segments were measured in length, diameter without bark and total leaf surface area supplied, to compute the main hydraulic architecture parameters, namely specific conductivity (K_s, kg m^{-1} s^{-1} MPa^{-1}) as the hydraulic conductivity on a sapwood area basis, and leaf-specific conductivity (LSC, kg m^{-1} s^{-1} MPa^{-1}) as hydraulic conductivity on a leaf area basis.

Leaf hydraulic conductance

Leaf hydraulic conductance (K_{leaf}, mmol m^{-2} s^{-1} MPa^{-1}) for *Q. robur* and *Q. faginea* was calculated following the methodology described by Brodribb et al. (2005). Six sun-exposed branches from six plants per species were collected at 07:00–08:00 h (solar time), minimizing the possibility for midday K_{leaf} depression (Brodribb and Holbrook 2004). The branches were enclosed in sealed plastic bags to prevent water loss and stored in the dark for a period of at least 1 h until stomatal closure so that all leaves from the same branch could reach the same water potential. It is assumed that this is the water potential of the leaves prior to rehydration (Ψ_0). Once this value was obtained, one leaf per branch was cut under water to prevent air entry and allowed to take up water for 30–60 s. The water potential after rehydration was subsequently obtained (Ψ_f). The K_{leaf} was calculated according to the following equation:

$$K_{leaf} = \frac{C_l \cdot \ln(\Psi_0/\Psi_f)}{t} \quad (1)$$

where C_l (mol MPa^{-1} m^{-2}) is the leaf capacitance for each species. C_l was calculated as the initial slope of the pressure–volume relationships, normalized by the leaf area (Brodribb et al. 2005). Pressure–volume relationships for *Q. robur* and *Q. faginea* were determined in six leaves per species, following the free-transpiration method described in previous studies (Vilagrosa et al. 2003).

Leaf gas exchange and chlorophyll fluorescence measurements

Leaf gas exchange parameters were determined simultaneously with measurements of chlorophyll fluorescence using an open gas exchange system (CIRAS-2, PP-Systems, Amesbury, MA, USA) fitted with an automatic universal leaf cuvette (PLC6-U, PP-Systems) with an FMS II portable pulse amplitude modulated fluorometer (Hansatech Instruments Ltd, Norfolk, UK). Six CO_2 response curves were obtained from *Q. robur* and *Q. faginea*. In light-adapted mature leaves, photosynthesis measurements started at a CO_2 concentration surrounding the shoot (C_a) of 400 µmol mol^{-1} and a saturating PPFD of 1500 µmol m^{-2} s^{-1}. Leaf temperature and VPD were maintained at 25 °C and 1.25 kPa, respectively, during measurements. Once a steady-state gas exchange rate was reached under these conditions (usually 30 min after clamping the leaf), net assimilation rate (A_N), transpiration (E), stomatal conductance (g_s) and the effective quantum yield of PSII were estimated. Thereafter, C_a was decreased stepwise down to 50 µmol mol^{-1}. Upon completion of measurements at low C_a, C_a was increased again to 400 µmol mol^{-1} to restore the original value of A_N. Then, C_a was increased stepwise to 1800 µmol mol^{-1}. Leakage of CO_2 in and out of the cuvette was determined for the same range of CO_2 concentrations with a photosynthetically inactive leaf enclosed (obtained by heating the leaf until no variable chlorophyll fluorescence was observed) and used to correct measured leaf fluxes (Flexas et al. 2007*a*).

The effective photochemical efficiency of photosystem II (Φ_{PSII}) was measured simultaneously with A_N and g_s. For Φ_{PSII}, the steady-state fluorescence (F_S) and the maximum fluorescence during a light-saturating pulse of ~8000 µmol m^{-2} s^{-1} (F'_M) were estimated, and Φ_{PSII} was calculated as $(F'_M - F_S)/F'_M$, following the procedures of Genty et al. (1989). The photosynthetic electron transport rate (J_{flu}) was then calculated according to Krall and Edwards (1992), multiplying Φ_{PSII} by PPFD and by α (a term that includes the product of leaf absorptance and the partitioning of absorbed quanta between photosystems I and II). α was previously determined for each species as the slope of the relationship between Φ_{PSII} and Φ_{CO_2} (i.e., the quantum efficiency of CO_2 fixation) obtained by varying light intensity under nonphotorespiratory conditions in an atmosphere containing <1% O_2 (Valentini et al. 1995). Five light curves from *Q. robur* and *Q. faginea* were measured to determine α.

Estimation of mesophyll conductance by gas exchange and chlorophyll fluorescence

Mesophyll conductance (g_m) was estimated according to the method of Harley et al. (1992), as follows:

$$g_m = \frac{A_N}{C_i - [\Gamma^* (J_F + 8(A_N + R_L))/J_F - 4(A_N + R_L)]} \quad (2)$$

where A_N and the substomatal CO_2 concentration (C_i) were taken from gas exchange measurements at saturating light, whereas Γ^* (the chloroplastic CO_2 photocompensation point in the absence of mitochondrial respiration) and R_L (the respiration rate in the light) were estimated for each species according to the Laisk (1977) method, following the methodology

described in Flexas et al. (2007*b*). The values of g_m obtained were used to convert A_N–C_i into A_N–C_c curves (where C_c is the chloroplastic CO_2 concentration) using the equation $C_c = C_i - A_N/g_m$. The maximum carboxylation and J_{flu} capacities ($V_{c,max}$ and J_{max}, respectively) were calculated from the A_N–C_c curves, using the Rubisco kinetic constants and their temperature dependence described by Bernacchi et al. (2002). The Farquhar model was fitted to the data by applying iterative curve fitting (minimum least-square difference) using the Solver tool of Microsoft Excel.

Anatomical measurements

After the gas exchange measurements, transverse slices of 1 × 1 mm were cut between the main veins from the same leaves for anatomical measurements. Leaf material was quickly fixed under vacuum with 2% *p*-formaldehyde (2%) and glutaraldehyde (4%) in 0.1 M phosphate buffer solution (pH 7.2) and postfixed 1 h in 1% osmium tetroxide. Samples were dehydrated in (i) a graded ethanol series and (ii) propylene oxide and subsequently embedded in Embed-812 embedding medium (EMS, Hatfield, PA, USA). Semi-thin (0.8 µm) and ultrathin (90 nm) cross sections were cut with an ultramicrotome (Reichert & Jung model Ultracut E). Semi-thin cross sections were stained with 1% toluidine blue and viewed under a light microscopy (Optika B-600TiFL, Optika Microscopes, Ponteranica, Italy). Ultrathin cross sections were contrasted with uranyl acetate and lead citrate and viewed under a transmission electron microscope (TEM H600, Hitachi, Tokyo, Japan). Anatomical characteristics were derived from the micrographs with ImageJ software (http://rsb.info.nih.gov/nih-image/). Light microscopy images were used to determine the mesophyll thickness between the two epidermal layers (t_{mes}, µm), the fraction of the mesophyll tissue occupied by the intercellular air spaces (f_{ias}) (Patakas et al. 2003), and the mesophyll (S_m/S) and chloroplast (S_c/S) surface area facing intercellular air spaces per leaf area (Evans et al. 1994, Syvertsen et al. 1995, Tomás et al. 2013). All parameters were analyzed at least in four different fields of view and at three different sections. Electron microscopy images were used to determine the cell wall thickness (T_{cw}), cytoplasm thickness (T_{cyt}), chloroplast length (L_{chl}) and chloroplast thickness (T_{chl}) (Tomás et al. 2013). Three different sections and four to six different fields of view were used for measurements of each anatomical characteristic.

Mesophyll conductance modeled on the basis of anatomical characteristics

Leaf anatomical characteristics were used to estimate the g_m as a composite conductance for within-leaf gas and liquid components, according to the 1D gas diffusion model of Niinemets and Reichstein (2003) as applied by Tosens et al. (2012*a*):

$$g_m = \frac{1}{1/g_{ias} + (R \cdot T_k/H \cdot g_{liq})} \quad (3)$$

where g_{ias} is the gas-phase conductance inside the leaf from substomatal cavities to outer surface of cell walls, g_{liq} is the conductance in liquid and lipid phases from outer surface of cell walls to chloroplasts, R is the gas constant (Pa m^3 K^{-1} mol^{-1}), T_k is the absolute temperature (K) and H is the Henry's law constant for CO_2 (Pa m^3 mol^{-1}). g_m is defined as a gas-phase conductance, and thus, $H/(RT_k)$, the dimensionless form of the Henry's law constant, is needed to convert g_{liq} to corresponding gas-phase equivalent conductance (Niinemets and Reichstein 2003).

The intercellular gas-phase conductance (and the reciprocal term, r_{ias}) was obtained according to Niinemets and Reichstein (2003) as:

$$g_{ias} = \frac{1}{r_{ias}} = \frac{D_A \cdot f_{ias}}{\Delta L_{ias} \cdot \tau} \quad (4)$$

where ΔL_{ias} (m) is the average gas-phase thickness, τ is the diffusion path tortuosity (1.57 m m^{-1}, Syvertsen et al. 1995), D_A is the diffusivity of the CO_2 in the air (1.51 × 10^{-5} m^2 s^{-1} at 25 °C) and f_{ias} is the fraction of intercellular air spaces. ΔL_{ias} was taken as the half of the mesophyll thickness. Total liquid-phase conductance (g_{liq}) from the outer surface of cell walls to the carboxylation sites in the chloroplasts is the sum of serial conductances in the cell wall (r_{cw}), plasmalemma (r_{pl}) and inside the cell ($r_{cel,tot}$) (Tomás et al. 2013):

$$g_{liq} = \frac{S_m}{(r_{cw} + r_{pl} + r_{cel,tot}) \cdot S} \quad (5)$$

The conductance of the cell wall was calculated as previously described in Peguero-Pina et al. (2012). For the conductance of plasma membrane, we used an estimate of 0.0035 m s^{-1} as previously suggested (Tosens et al. 2012*a*). The conductance inside the cell was calculated following the methodology described in Tomás et al. (2013), considering two different pathways of CO_2 inside the cell: one for cell wall parts lined with chloroplasts and the other for interchloroplastial areas (Tholen et al. 2012).

Analysis of partitioning changes in photosynthetic rate

The contribution analysis proposed by Buckley and Díaz-Espejo (2015) was used to partition changes in photosynthesis into contributions from the underlying variables. This new approach uses numerical integration having the advantage of avoiding the bias caused by discrete approximations like the widely used limitation analysis proposed by Grassi and Magnani (2005), and avoiding the need to compute partial derivatives for each variable. The method by Buckley and Díaz-Espejo (2015) relies instead on variable substitution in the photosynthesis model. This approach is easily extended to encompass effects of changes in any photosynthetic variable, under any conditions. Therefore, not only the contributions to photosynthesis in the Rubisco-limiting

region are represented now, but also those in the RuBP regeneration region.

Two analyses were performed. First, we compared *Q. robur* with *Q. faginea* to determine the main factor responsible for the lower A_N in the former species. Values in Table 4 were used to apply the contribution analysis. Second, we analyzed the effect of reduction in g_s (i.e., simulating a response to VPD or soil water deficit) in the % of contribution to A_N limitation. We assumed that, as g_s was reduced, g_m and $V_{c,max}$ were maintained constant.

Determination of total soluble protein, Rubisco and leaf nitrogen contents

Leaves from *Q. robur* and *Q. faginea* were ground in 500 µl of ice-cold extraction buffer containing 50 mM Bicine–NaOH (pH 8.0), 1 mM ethylenediaminetetracetic acid, 5% polyvinyl pyrrolidone, 6% polyethylene glycol (PEG_{4000}), 50 mM β-mercaptoethanol, 10 mM dithiothreitol and 1% protease-inhibitor cocktail (Sigma-Aldrich Co. LLC., USA). The extracts were centrifuged at 14,000*g* for 1 min at 4 °C and the total soluble protein (TSP) concentration in supernatant was quantified by the method of Bradford (1976). The concentration of Rubisco was determined with the gel electrophoresis method (Suárez et al. 2011, Bermúdez et al. 2012) using known concentrations of purified Rubisco from wheat as a standard for calibration.

Total leaf nitrogen (N) concentration was determined in dried leaves of *Q. robur* and *Q. faginea* using an Organic Elemental Analyzer (Flash EA 112, Thermo Fisher Scientific Inc., Waltham, MA, USA).

rbcL sequencing

Total genomic DNA from *Q. robur* and *Q. faginea* was isolated and purified using the DNeasy Plant Minikit (Qiagen, Hilden, Germany) following the manufacturer's instructions. The primers used for amplification and sequencing of the *rbc*L, the gene encoding the Rubisco large subunit, were esp2F (5′-ATGAGTT GTAGGGAGGGAC-3′) and 1494R (5′-GATTGGGCCGAGTTTA ATTTAC-3′) (Chen et al. 1998). Primers 414R (5′-CAAATCCTC CAGACGTAGAGC-3′) and 991R (5′-CGGTACCAGCGTGAATAT GAT-3′) (Chen et al. 1998) were also used only for sequencing.

Polymerase chain reactions (PCRs) were performed in 50 µl using BioMix Red reagent mix (Bioline Ltd, London, UK). Polymerase chain reaction program for amplifications comprised initial cycle at 94 °C for 2 min, 55 °C for 30 s, 72 °C for 4 min, followed by 30 cycles of 94 °C for 30 s, 56 °C for 45 s and 72 °C for 1 min, and a final elongation at 72 °C for 5 min. The PCR products were separated on 2% agarose gels and purified using Roche High Pure PCR Product Purification Kit (Roche Diagnostics, Barcelona, Spain). The amplified PCR products were sequenced with an ABI 3100 Genetic analyzer using the ABI BigDye™ Terminator Cycle Sequencing Ready Reaction Kit (Applied Biosystems, Foster City, CA, USA).

Sequence chromatograms were checked and manually corrected and the contigs were assembled and aligned using MEGA 5.0 (Tamura et al. 2011).

Statistical analysis

Data are expressed as means ± standard error. Student's *t*-tests were used to compare the trait values between *Q. robur* and *Q. faginea*. All statistical analyses were carried out using SAS version 8.0 (SAS, Cary, NC, USA).

Results

The study of the morphological variables revealed an outstanding lower transpiring area in *Q. faginea* when compared with *Q. robur*, in terms of single leaf area, number of leaves, total leaf area per shoot and LAR (Table 2). In contrast, MVD and LMA were higher in *Q. faginea* (Table 2).

The hydraulic parameters of current-year twigs showed a sevenfold higher K_h in *Q. robur* when compared with *Q. faginea*. However, this difference in K_h between both species was buffered when expressed on a sapwood area basis (K_s) (Table 3), indicative of the production of conductive tissues with a similar efficiency in both species, or on a leaf area basis (LSC) (Table 3), explained by the higher investment in leaf area of *Q. robur*.

At ambient CO_2 concentration, 1.25 kPa of VPD and light-saturating intensity, A_N, E and g_s were higher in *Q. faginea* (19.6 µmol CO_2 m^{-2} s^{-1}, 6.5 mol H_2O m^{-2} s^{-1} and 0.652 mol H_2O m^{-2} s^{-1}, respectively) than in *Q. robur* (12.9 µmol CO_2 m^{-2} s^{-1}, 2.5 mol H_2O m^{-2} s^{-1} and 0.252 mol H_2O m^{-2} s^{-1}, respectively) (Table 4). Both the intrinsic (iWUE = A_N/g_s) and the instantaneous (WUE = A_N/E) water use efficiency were lower in *Q. faginea* (Table 4). The values of K_{leaf} for both species showed trends consistent with those described above for leaf gas exchange parameters: the value for *Q. faginea* (27.7 ± 1.5 mmol m^{-2} s^{-1} MPa^{-1}) was higher than that for *Q. robur* (17.9 ± 1.3 mmol m^{-2} s^{-1} MPa^{-1}) (Table 3). The differences in A_N were partly associated with the greater LMA in *Q. faginea* when compared with *Q. robur* (Table 2). In fact, when the net photosynthetic rate was expressed per unit dry mass, no statistically significant differences

Table 2. Leaf area, LMA, MVD, number of leaves per shoot, total leaf area per shoot and LAR for *Q. robur* and *Q. faginea*. Data are mean ± SE. Different letters indicate statistically significant differences ($P < 0.05$) between *Q. robur* and *Q. faginea*.

	Q. robur	*Q. faginea*
Leaf area (cm^2)	15.2 ± 1.4a	3.8 ± 0.2b
LMA (mg cm^{-2})	8.94 ± 1.30a	13.65 ± 0.65b
MVD (mm mm^{-2})	0.53 ± 0.02a	1.32 ± 0.03b
Number of leaves per shoot	11.2 ± 0.9a	7.5 ± 0.7b
Total leaf area per shoot (cm^2)	180 ± 26a	31 ± 4b
LAR (m^2 kg^{-1})	7.8 ± 0.2a	5.4 ± 0.1b

Table 3. K_h, K_s, LSC and K_{leaf} for *Q. robur* and *Q. faginea*. Data are mean ± SE. Different letters indicate statistically significant differences ($P < 0.05$) between *Q. robur* and *Q. faginea*.

	Q. robur	*Q. faginea*
K_h (kg m s^{-1} MPa^{-1})	$24.2 \times 10^{-7} \pm 7.2 \times 10^{-7}$a	$3.4 \times 10^{-7} \pm 0.9 \times 10^{-7}$b
K_s (kg m^{-1} s^{-1} MPa^{-1})	1.32 ± 0.28a	0.75 ± 0.14a
LSC (kg m^{-1} s^{-1} MPa^{-1})	$2.0 \times 10^{-4} \pm 3.2 \times 10^{-5}$a	$1.5 \times 10^{-4} \pm 4.0 \times 10^{-5}$a
K_{leaf} (mmol m^{-2} s^{-1} MPa^{-1})	17.9 ± 1.3a	27.7 ± 1.5b

Table 4. Mean values for the photosynthetic parameters analyzed at PPFD = 1500 µmol photons m^{-2} s^{-1}, T_{leaf} = 25 °C and VPD = 1.25 kPa. Data are mean ± SE. Different letters indicate statistically significant differences ($P < 0.05$) between *Q. robur* and *Q. faginea*. A_N, net photosynthesis; g_s, stomatal conductance; E, transpiration; iWUE = A_N/g_S, intrinsic water use efficiency; WUE = A_N/E, instantaneous water use efficiency; g_m, mesophyll conductance to CO_2; C_i, substomatal CO_2 concentration; C_c, chloroplastic CO_2 concentration; $V_{c,max}$ and J_{max}, maximum velocity of carboxylation and maximum capacity for electron transport; J_{flu}, electron transport rate estimated by chlorophyll fluorescence.

	Q. robur	*Q. faginea*
A_N (µmol CO_2 m^{-2} s^{-1})	12.9 ± 0.5a	19.6 ± 1.1b
g_s (mol H_2O m^{-2} s^{-1})	0.252 ± 0.013a	0.652 ± 0.078b
E (mol H_2O m^{-2} s^{-1})	2.5 ± 0.02a	6.5 ± 0.8b
iWUE (µmol mol^{-1})	51.2 ± 1.8a	31.7 ± 3.1b
WUE (µmol mol^{-1})	5.1 ± 0.3a	3.0 ± 0.2b
g_m (mol H_2O m^{-2} s^{-1})	0.060 ± 0.005a	0.098 ± 0.07b
C_i (µmmol CO_2 mol^{-1} air)	288 ± 7a	293 ± 4a
C_c (µmmol CO_2 mol^{-1} air)	80 ± 2a	95 ± 4b
$V_{c,max}$ (µmol m^{-2} s^{-1})	206 ± 6a	250 ± 4b
J_{max} (µmol m^{-2} s^{-1})	248 ± 10a	292 ± 14b
J_{flu} (µmol m^{-2} s^{-1})	266 ± 8a	306 ± 13b
$J_{max} : V_{c,max}$	1.21 ± 0.03a	1.19 ± 0.04a

($P < 0.05$) were found between *Q. robur* and *Q. faginea* (data not shown).

The mesophyll conductance to CO_2 (g_m) and the chloroplastic CO_2 concentration (C_c) were higher in *Q. faginea* (Table 4). Parameterization of the Farquhar et al. (1980) model of photosynthesis yielded higher values for $V_{c,max}$ and J_{max} in *Q. faginea*, although the ratio $J_{max} : V_{c,max}$ did not show differences between the two species (Table 4).

The analysis of the partitioning changes in photosynthesis revealed that A_N in *Q. robur* and *Q. faginea* was mainly limited by diffusional processes. Stomatal and, especially, mesophyll conductance limitations were responsible for the lower A_N measured in *Q. robur* in comparison with *Q. faginea* (Figure 2). *Quercus faginea* exhibited a large range of g_s, achieving values up to three times higher than *Q. robur*. As a consequence, a 50% reduction of g_s represents a A_N limitation of only 15% in *Q. faginea*; meanwhile, it means 35% for *Q. robur* (Figure 3). However, when comparing identical absolute values of g_s in both species, the A_N limitation due to stomata is always higher in *Q. faginea* than in *Q. robur* (Figure 3), greatly due to the higher $V_{c,max}$ in *Q. faginea* (Table 4).

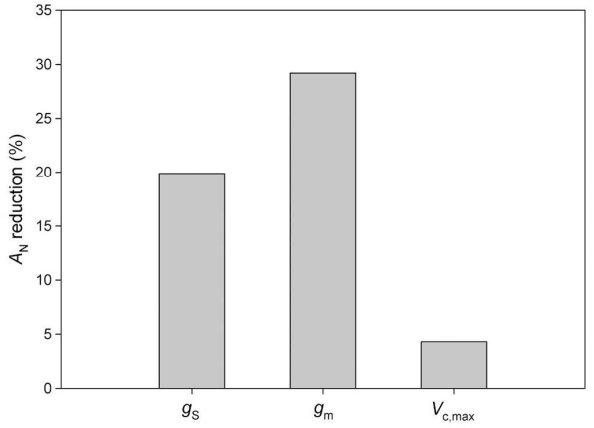

Figure 2. Contributions of individual variables (g_s, stomatal conductance; g_m, mesophyll conductance to CO_2; $V_{c,max}$, maximum velocity of carboxylation) to the reduction in net CO_2 assimilation rate (A_N) shown by *Q. robur* using the values of *Q. faginea* as reference.

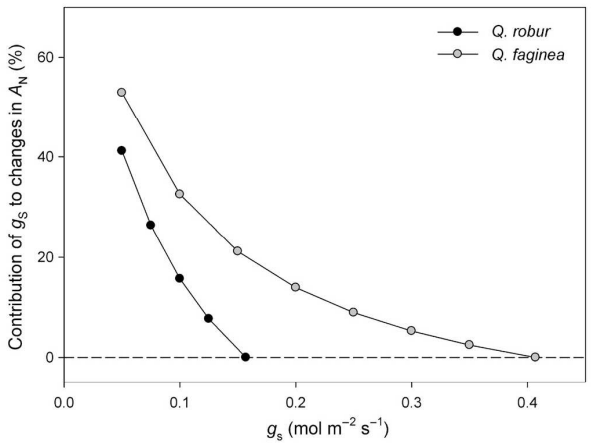

Figure 3. Contribution of stomatal conductance (g_s) to changes in net CO_2 assimilation rate (A_N) for *Q. robur* and *Q. faginea*.

Quercus robur and *Q. faginea* displayed contrasting anatomical features at the leaf and cell levels. The mesophyll thickness, f_{ias}, S_m/S, S_c/S and S_c/S_m were higher in *Q. faginea*, while T_{cyt} and T_{chl} were higher in *Q. robur*, and no differences were found in T_{cw} and L_{chl} (Table 5). The anatomical parameters were further used to estimate different components of the CO_2 transfer resistances relative to total mesophyll resistance for both species (see

Table 5. Leaf type, mesophyll thickness, f_{ias}, mesophyll surface area exposed to intercellular airspace (S_m/S), chloroplast surface area exposed to intercellular airspace (S_c/S), the ratio S_c/S_m, T_{cw}, T_{cyt}, L_{chl} and T_{chl} in *Q. robur* and *Q. faginea* leaves. Data are mean ± SE. Different letters indicate statistically significant differences ($P < 0.05$) between *Q. robur* and *Q. faginea*.

	Q. robur	*Q. faginea*
Leaf type	Hypostomatous	Hypostomatous
Mesophyll thickness (μm)	140 ± 2a	186 ± 3b
f_{ias}	0.16 ± 0.01a	0.21 ± 0.01b
S_m/S ($m^2\ m^{-2}$)	21.9 ± 1.4a	28.4 ± 2.0b
S_c/S ($m^2\ m^{-2}$)	9.2 ± 1.0a	13.4 ± 1.7b
S_c/S_m	0.42 ± 0.02a	0.48 ± 0.02b
T_{cw} (μm)	0.262 ± 0.019a	0.270 ± 0.008a
T_{cyt} (μm)	0.109 ± 0.036a	0.026 ± 0.012b
L_{chl} (μm)	4.48 ± 0.29a	4.32 ± 0.16a
T_{chl} (μm)	1.87 ± 0.07a	1.21 ± 0.03b

Materials and methods for details). On one hand, regarding the gas phase, no differences were found in r_{ias} between both species (Table 6). On the other hand, regarding the liquid phase, the results demonstrated that *Q. faginea* presented lower values of r_{liq} than *Q. robur* (Table 6), which can be attributed to the lower values of T_{cyt} and T_{chl} found in *Q. faginea* (Table 5). Consequently, the estimated value of g_m was higher in *Q. faginea* than in *Q. robur* (Table 6), in agreement with the differences found in g_m obtained by gas exchange and chlorophyll fluorescence measurements (Table 4).

In *Q. faginea*, the concentration of N, TSP and Rubisco catalytic sites per leaf area were higher than in *Q. robur* (Table 7). The decreases in the concentration of TSP and Rubisco per leaf area in *Q. robur* with respect to *Q. faginea* were of similar magnitude, so that the ratio Rubisco/TSP was similar in both species (Table 7). Again, as stated above for A_N, when the concentration of N, TSP and Rubisco was expressed per unit dry mass, no differences ($P < 0.05$) were found between *Q. robur* and *Q. faginea* (Table 7).

Table 6. CO_2 transfer resistances across the intercellular air space (r_{ias}, $s\ m^{-1}$), the liquid phase (r_{liq}, $s\ m^{-1}$) and the mesophyll conductance for CO_2 (g_m, $mol\ m^{-2}\ s^{-1}$) calculated from anatomical measurements in *Q. robur* and *Q. faginea*. Data are mean ± SE. Different letters indicate statistically significant differences ($P < 0.05$) between *Q. robur* and *Q. faginea*.

	r_{ias} ($s\ m^{-1}$)	r_{liq} ($s\ m^{-1}$)	g_m ($mol\ m^{-2}\ s^{-1}$)
Q. robur	46 ± 5a	391 ± 21a	0.091 ± 0.009a
Q. faginea	45 ± 6a	279 ± 18b	0.122 ± 0.008b

Table 7. Leaf N, TSP and Rubisco concentrations per leaf dry mass and per leaf area for *Q. robur* and *Q. faginea*. Data are mean ± SE. Different letters indicate statistically significant differences ($P < 0.05$) between *Q. robur* and *Q. faginea*.

	Q. robur	*Q. faginea*
g N/100 g	1.90 ± 0.15a	2.19 ± 0.18a
mol N m^{-2}	0.12 ± 0.02a	0.21 ± 0.03b
mg TSP g^{-1}	32.7 ± 1.4a	32.4 ± 0.4a
mg TSP m^{-2}	2922 ± 130a	4423 ± 55b
mg Rubisco/mg TSP	0.33 ± 0.01a	0.34 ± 0.01a
mg Rubisco g^{-1}	11.0 ± 0.5a	10.9 ± 0.3a
μmol Rubisco sites m^{-2}	17.6 ± 0.8a	26.7 ± 0.9b

Discussion

In this study, we have found a clear morphological and physiological segregation between *Q. robur* and *Q. faginea*, two 'roburoid oaks' occurring under contrasting climatic conditions (Table 1, Figure 1). The existence of a common ribulose-1,5-bisphosphate carboxylase/oxygenase (Rubisco) large subunit (*rbc*L) (see Figure S1 available as Supplementary Data at *Tree Physiology* Online) confirms the genetic proximity between these species, as stated in previous studies (Olalde et al. 2002, Himrane et al. 2004). Further, the identical *rbc*L sequence discards the existence of evolution trends in the 'quality' of Rubisco (i.e., related to different catalytic constants), in contrast with recent infrageneric comparative studies (Galmés et al. 2014*a*, 2014*b*). In spite of their genetic proximity, the two species constitute two very contrasting functional types, showing a coordinated response at whole-plant level that would establish a differential physiological performance in response to climate dryness. Our results agree with recent studies that demonstrate strong interspecific correlations between hydraulic and photosynthetic traits (Brodribb et al. 2005, 2007, Sack and Holbrook 2006, Flexas et al. 2013).

Among all the studied traits, the differences found in leaf size constitute one of the most outstanding divergences between both species (Table 2). Thus, *Q. faginea* diminished the transpiring area, both in terms of single leaf area and number of leaves per shoot. Both traits imply a total leaf area per shoot about six times lower in *Q. faginea* than in *Q. robur*, with a direct consequence on the whole shoot transpiration in the former. A reduction in leaf size, such as that found in *Q. faginea*, has been proposed as one of the key traits that allows other Mediterranean oaks to withstand water deficit (Baldocchi and Xu 2007, Peguero-Pina et al. 2014). A direct benefit provided by small leaves is the improvement of the ability to supply water to transpiring leaves at shoot level in *Q. faginea*, offsetting the sharp difference found in K_h between both species (about seven times) for a similar K_s (Table 3). In this way, *Q. faginea* reached LSC values very similar to those measured for *Q. robur* (Table 3). An adjustment of LSC by reducing the whole-shoot leaf area has been previously reported by Peguero-Pina et al. (2014) in a comparison among *Q. ilex* provenances from contrasting climatic conditions. Another positive aspect of reducing leaf size in *Q. faginea* is the reduction of the aerodynamic resistance of leaves, which leads to a better coupling between leaf temperature and air temperature. This reduction in the aerodynamic resistance of leaves further enhances the control of transpiration by stomata (Jarvis and McNaughton 1986).

On the contrary, the reduction in the total leaf area per shoot had a negative impact on the carbon gain of *Q. faginea* and, through the effect on LAR, on its growth ability (Poorter and Remkes 1990). In this regard, *Q. faginea* presented several physiological traits that partially counteract the negative effects of leaf area reduction in terms of carbon assimilation. For instance, when compared with *Q. robur*, *Q. faginea* showed higher values for the main photosynthetic parameters (Table 4). Among them, it must be highlighted the extremely high values of g_s in *Q. faginea*. Such high values for g_s, which have been previously reported for this species (Acherar and Rambal 1992, Mediavilla and Escudero 2003, 2004), imply a high water consumption under the atmospheric evaporative demand experienced by this species during summer. The differences found in g_s between both species agreed with the differences found in K_{leaf} and MVD (Sack and Holbrook 2006, Sack and Scoffoni 2013), confirming the existence of a coordinated response between leaf hydraulics and gas exchange (Brodribb et al. 2007).

The maximum g_s values found in *Q. faginea* can be analyzed in the context of the stomatal sensitivity (i.e., the magnitude of the reduction in g_s with increasing VPD) reported by Mediavilla and Escudero (2003) for this species. According to the empirical model given by Oren et al. (1999), an exponential decrease in g_s would be expected as VPD increases, ranging from the values obtained at VPD close to 1 kPa to an expected value close to 0.220 mol H_2O m^{-2} s^{-1} at 3 kPa (Table 4, Figure 4a), which can be considered the maximum VPD expected value in the natural habitat of this species during the hottest period of the summer (Figure 1). The higher stomatal sensitivity of *Q. faginea* when compared with *Q. robur* is coherent with the higher $g_{s,max}$ measured in the former species (Oren et al. 1999) and implies the ability to cope with the higher VPD values experienced by *Q. faginea* through the vegetative period (Figure 1). In contrast, *Q. robur* showed a relatively low $g_{s,max}$ (as previously reported by Epron and Dreyer 1993, Rust and Roloff 2002, Arend et al. 2013) and, consequently, showed a lower stomatal sensitivity, which seems to be in accordance with the lower values of VPD registered through the vegetative period—below or close to 1 kPa—in its natural habitats (Figure 1). The transpiration values (E) calculated from the values of g_s for any VPD (Figure 4b) suggest that the differential stomatal sensitivity showed by *Q. robur* and *Q. faginea* keeps quite constant the E values for both species within the range of VPD values registered in their natural habitats (Figure 1).

The high $g_{s,max}$ value for *Q. faginea* found here and in previous studies (Acherar and Rambal 1992, Mediavilla and Escudero 2003, 2004) seems to be contradictory to the capacity of this species to live in Mediterranean areas. However, the high $g_{s,max}$ and the subsequent high stomatal sensitivity (Figure 4a) in *Q. faginea* in comparison with *Q. robur* must be interpreted taking into account the analysis of the stomatal limitations to the CO_2 photosynthetic assimilation (Figure 3). Effectively, the

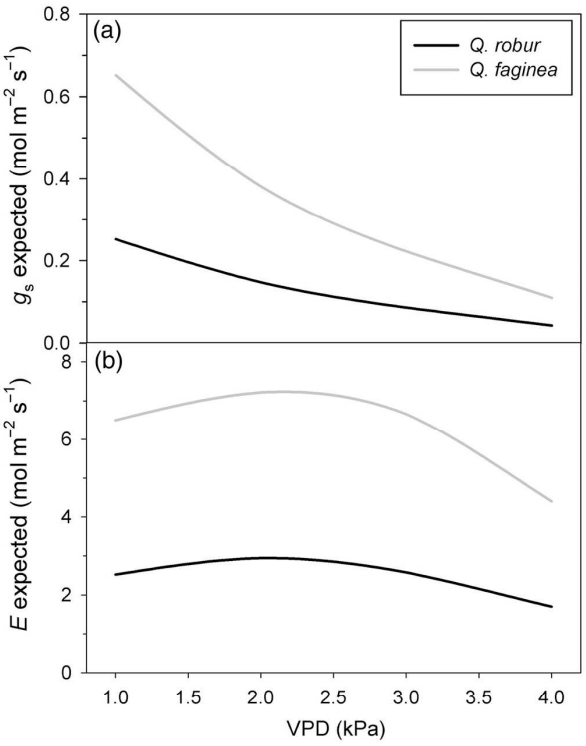

Figure 4. (a) Relationship between VPD and the expected stomatal conductance (g_s) and (b) relationship between VPD and the expected transpiration (E) for *Q. robur* and *Q. faginea* according to the empirical model given by Oren et al. (1999).

stomatal limitations to photosynthesis (A_N) in *Q. faginea* start at a g_s value of ~0.4 mol m^{-2} s^{-1}, which is expected to occur at a VPD value of ~2 kPa (Figure 4a). From this value, the contribution of g_s to the decrease in A_N (%) is progressively higher. However, at the maximum expected VPD value at midsummer (3 kPa, Figure 1), the expected contribution of g_s only diminished <20% of the maximum value of A_N at 1 kPa (Figure 3). In contrast, the curve predicting the contribution of g_s to changes in A_N (%) in *Q. robur* (Figure 3) shows a quite different shape, with a very sharp increase in the contribution of g_s to the decrease in A_N (%) once the stomatal regulation starts. In this sense, and under the climatic conditions experienced by *Q. faginea* (g_s <0.100 mol H_2O m^{-2} s^{-1} at 3 kPa), the stomatal limitations to photosynthesis in *Q. robur* will be higher than 30% (Figure 3). However, the absence of atmospheric dryness in the distribution range of *Q. robur* (Figure 1) allows this species to maintain stable photosynthetic rates along the vegetative period (Morecroft and Roberts 1999).

Contrary to *Q. robur*, the vegetative period in the distribution range of *Q. faginea* is affected by an important seasonality, expressed in terms of temperature, precipitation and VPD (Figure 1). Therefore, *Q. faginea* has to cope with a drop in the soil water content during summer that negatively affects the soil

water potential, consequently limiting the maximum values of g_s in this species (Acherar and Rambal 1992, Mediavilla and Escudero 2003, 2004). This double limitation to g_s, imposed by the stomatal sensitivity to VPD and to soil drought, may definitively limit the length of the vegetative period if the soil water reserves are depleted during the hottest and driest days of the summer. This may explain the extreme dependence of *Q. faginea* on edaphic conditions that ensure the maintenance of nonlimiting soil water potential values (Esteso-Martínez et al. 2006). In fact, different studies have evidenced the massive substitution of *Q. faginea* by the evergreen congeneric *Q. ilex* in most areas of the Iberian Peninsula as a consequence of the soil degradation associated with the human management of these areas (Corcuera et al. 2005*a*, 2005*b*).

On the other hand, the existence of a potential stress period during summer may be compensated by the prolongation of vegetative period along early- and mid-autumn, when temperature, water availability and VPD do not constrain the photosynthetic activity, as has been reported in several Mediterranean white oak species (Abadía et al. 1996, Mediavilla and Escudero 2003). Zhu et al. (2012) showed the strong dependence of vegetation phenology on latitude between 35°N and 70°N for North America, where a reduction in the length of the growing season of ~5 days per degree of latitude can be expected. The clearly southern distribution area of *Q. faginea* (from 35°N to 43°N) compared with *Q. robur* (40°N to ~60°N) (Jalas and Suominen 1976) should itself imply a longer vegetative period for the Mediterranean species, which may partially compensate for the severity of the environmental conditions in the middle of the growing season. According to this, Withington et al. (2006) found a leaf life span of 172 days (0.47 years) for *Q. robur* in central Poland at 51°N, while Mediavilla et al. (2001) reported a leaf life span of 208 days for *Q. faginea* (0.58 years) in central western Spain at 41°N.

The higher inherent photosynthetic ability of *Q. faginea* when compared with *Q. robur* was not only a consequence of its higher $V_{c,max}$ but also relies on a higher g_m, which resulted in a higher chloroplastic CO_2 concentration (C_c) (Table 4). The differences in g_m between the two species can be partially attributed to the variation in leaf anatomical traits, i.e., T_{cyt} and T_{chl} (Table 5), that decreased r_{liq} in *Q. faginea* in comparison with *Q. robur* (Table 6). It should be noted that the role of anatomical traits in determining the specific variability in g_m has been previously reported in several studies (Tosens et al. 2012*b*, Tomás et al. 2013). In the present study, the g_m modeled based on leaf anatomical properties was higher than that estimated using conventional methods in *Q. robur* and *Q. faginea* (Tables 4 and 6). The reasons for such biases are not fully understood but are often observed in other studies (Peguero-Pina et al. 2012, Tomás et al. 2013, Carriquí et al. 2015). Nevertheless, the relative difference in g_m between the two species obtained with the two methods—gas exchange/fluorescence vs anatomical—largely supports a predominant role of internal CO_2 diffusion in establishing photosynthetic differences between them.

The enhancement of all these functional traits in *Q. faginea* when compared with *Q. robur*—i.e., through the improvement of the instantaneous photosynthetic parameters—only partially counteract the negative effects of leaf area reduction in terms of carbon assimilation. Thus, taking into account the whole leaf area per shoot, *Q. robur* even shows an enhanced ability for carbon assimilation at whole-shoot level (data not shown), which results in a higher growth ability. On the other hand, the strong reduction in leaf area showed by *Q. faginea* would diminish the water losses at whole shoot level in comparison with *Q. robur* (data not shown), in spite of showing much higher g_s values (Table 4), which may be considered a key factor for withstanding the climate dryness imposed by the Mediterranean-type climates. However, in spite of the ability of *Q. faginea* to occupy most areas under Mediterranean climate (Olalde et al. 2002, Benito Garzón et al. 2008), the predictions indicate a notable reduction in its potential distribution range (Sánchez de Dios et al. 2009) as a consequence of the increment in aridity. Effectively, an increase in the length or in the intensity of summer drought will have a negative influence on the functional response of *Q. faginea* and other Mediterranean deciduous species (Gea-Izquierdo et al. 2013), as long as it would imply a shorter time period for carbon assimilation and a lower productivity (Gea-Izquierdo and Cañellas 2014). Under these conditions, evergreen oaks—such as *Q. ilex*—can obtain a benefit from their more 'conservative' leaf strategy (Wright et al. 2004) that allows the use of other periods through the year, such as the early spring or late autumn (Corcuera et al. 2005*a*).

Conclusions

Quercus faginea can be regarded as an example of adaptation of a deciduous oak to the Mediterranean-type climates, as fossil records indicate (Roiron 1983, Barrón et al. 2010). In our opinion, the reduction in transpiring area both at leaf and shoot level in *Q. faginea*, when compared with the mesic-temperate *Q. robur*, is the main trait imposed by the water deficit in Mediterranean-type climates. The reduction in LAR in *Q. faginea* should have a negative effect of carbon gain that is partially compensated with a higher A_N at the expense of a much higher maximum g_s, which has been considered one key trait for classifying this species as a 'water spender' (Mediavilla and Escudero 2004). We propose that the extremely high g_s values in *Q. faginea* counteract the reduction in g_s imposed by the stomatal sensitivity to VPD, allowing this species to maintain high A_N values through the changing conditions along the vegetative period in its natural habitat. The depletion of soil water reserves at midsummer should impose a further limitation in the vegetative activity of this species, which explain its substitution by other species (e.g., *Q. ilex*) in

degraded soils and can also explain the extreme vulnerability of this species to an increment in aridity associated with a global climatic change (Sánchez de Dios et al. 2009).

Supplementary data

Supplementary data for this article are available at *Tree Physiology* Online.

Acknowledgments

The authors are grateful to Emilio Roldán (UIB) for his help in determining leaf TSP and Rubisco content and to Arantxa Molins and Carmen Hermida (UIB) for *rbc*L sequencing.

Conflict of interest

None declared.

Funding

Financial support from Gobierno de Aragón (H38 research group) and Plan Nacional project AGL2009-07999 are acknowledged. Work of D.S.-K. is supported by a DOC INIA contract cofunded by the Spanish National Institute for Agriculture and Food Research and Technology (INIA) and the European Social Fund (ESF).

References

Abadía A, Gil E, Morales F, Montañés L, Montserrat G, Abadía J (1996) Marcescence and senescence in a submediterranean oak (*Quercus subpyrenaica* E.H. del Villar): photosynthetic characteristics and nutrient composition. Plant Cell Environ 19:685–694.

Acherar M, Rambal S (1992) Comparative water relations of four Mediterranean oak species. Vegetatio 99–100:177–184.

Arend M, Brem A, Kuster TM, Günthardt-Goerg MS (2013) Seasonal photosynthetic responses of European oaks to drought and elevated daytime temperature. Plant Biol 15:169–176.

Axelrod DI (1983) Biogeography of oaks in the Arcto-Tertiary province. Ann Mo Bot Gard 70:629–657.

Baldocchi DD, Xu L (2007) What limits evaporation from Mediterranean oak woodlands—the supply of moisture in the soil, physiological control by plants or the demand by the atmosphere? Adv Water Resour 30:2113–2122.

Barrón E, Rivas-Carballo R, Postigo-Mijarra JM, Alcalde-Olivares C, Vieira M, Castro L, Pais J, Valle-Hernández M (2010) The Cenozoic vegetation of the Iberian Peninsula: a synthesis. Rev Palaeobot Palynol 162:382–402.

Benito Garzón M, Sánchez de Dios R, Sáinz Ollero H (2007) Predictive modelling of tree species distributions on the Iberian Peninsula during the Last Glacial Maximum and Mid-Holocene. Ecography 30:120–134.

Benito Garzón M, Sánchez de Dios R, Sainz Ollero H (2008) Effects of climate change on the distribution of Iberian tree species. Appl Veg Sci 11:169–178.

Bermúdez MA, Galmés J, Moreno I, Mullineaux PM, Gotor C, Romero LC (2012) Photosynthetic adaptation to length of day is dependent on S-sulfocysteine synthase activity in the thylakoid lumen. Plant Physiol 160:274–288.

Bernacchi CJ, Portis AR, Nakano H, von Caemmerer S, Long SP (2002) Temperature response of mesophyll conductance. Implications for the determination of Rubisco enzyme kinetics and for limitations to photosynthesis in vivo. Plant Physiol 130:1992–1998.

Bradford MM (1976) A rapid and sensitive method for the quantitation of microgram quantities of protein utilizing the principle of protein-dye binding. Anal Biochem 72:248–254.

Brodribb TJ, Holbrook NM (2004) Diurnal depression of leaf hydraulic conductance in a tropical tree species. Plant Cell Environ 27:820–827.

Brodribb TJ, Holbrook NM, Zwieniecki MA, Palma B (2005) Leaf hydraulic capacity in ferns, conifers and angiosperms: impacts on photosynthetic maxima. New Phytol 165:839–846.

Brodribb TJ, Field TS, Jordan GJ (2007) Leaf maximum photosynthetic rate and venation are linked by hydraulics. Plant Physiol 144:1890–1898.

Buckley TN, Díaz-Espejo A (2015) Partitioning changes in photosynthetic rate into contributions from different variables. Plant Cell Environ 38:1200–1211.

Carriquí M, Cabrera HM, Conesa MÀ et al. (2015) Diffusional limitations explain the lower photosynthetic capacity of ferns as compared with angiosperms in a common garden study. Plant Cell Environ 38:448–460.

Chen ZD, Wang XQ, Sun HY, Han Y, Zhang ZX, Zou YP, Lu AM (1998) Systematic position of the Rhoipteleaceae: evidence from nucleotide sequences of rbcL gene. Acta Phytotaxon Sin 36:1–7.

Corcuera L, Camarero JJ, Gil-Pelegrín E (2002) Functional groups in *Quercus* species derived from the analysis of pressure-volume curves. Trees 16:465–472.

Corcuera L, Camarero JJ, Gil-Pelegrín E (2004) Effects of a severe drought on growth and wood anatomical properties of *Quercus faginea*. IAWA J 25:185–204.

Corcuera L, Morales F, Abadía A, Gil-Pelegrín E (2005*a*) Seasonal changes in photosynthesis and photoprotection in a *Quercus ilex* subsp. *ballota* woodland located in its upper altitudinal extreme in the Iberian Peninsula. Tree Physiol 25:599–608.

Corcuera L, Morales F, Abadía A, Gil-Pelegrín E (2005*b*) The effect of low temperatures on the photosynthetic apparatus of *Quercus ilex* subsp. *ballota* at its lower and upper altitudinal limits in the Iberian Peninsula and during a single freezing-thawing cycle. Trees 19:99–108.

Denk T, Grimm GW (2009) Significance of pollen characteristics for infrageneric classification and phylogeny in *Quercus* (Fagaceae). Int J Plant Sci 170:926–940.

Denk T, Grimm GW (2010) The oaks of western Eurasia: traditional classifications and evidence from two nuclear markers. Taxon 59:351–366.

Ducousso A, Bordacs S (2004) EUFORGEN Technical Guidelines for genetic conservation and use for pedunculate and sessile oaks (*Quercus robur* and *Q. petraea*). International Plant Genetic Resources Institute, Rome, Italy, 6 pp.

Epron D, Dreyer E (1993) Long-term effects of drought on photosynthesis of adult oak trees [*Quercus petraea* (Matt.) Liebl. and *Quercus robur* L.] in a natural stand. New Phytol 125:381–389.

Esteso-Martínez J, Camarero JJ, Gil-Pelegrín E (2006) Competitive effects of herbs on *Quercus faginea* seedlings inferred from vulnerability curves and spatial-pattern analyses in a Mediterranean stand (Iberian System, northeast Spain). Ecoscience 131:378–387.

Evans JR, von Caemmerer S, Setchell BA, Hudson GS (1994) The relationship between CO_2 transfer conductance and leaf anatomy in transgenic tobacco with a reduced content of Rubisco. Aust J Plant Physiol 21:475–495.

Farquhar GD, von Caemmerer S, Berry JA (1980) A biochemical model of photosynthetic CO_2 assimilation in leaves of C_3 species. Planta 149:78–90.

Flexas J, Díaz-Espejo A, Berry JA, Galmés J, Cifre J, Kaldenhoff R, Medrano H, Ribas-Carbó M (2007*a*) Analysis of leakage in IRGA's leaf chambers

of open gas exchange systems: quantification and its effects in photosynthesis parameterization. J Exp Bot 58:1533–1543.
Flexas J, Ortuño MF, Ribas-Carbó M, Díaz-Espejo A, Flórez-Sarasa ID, Medrano H (2007*b*) Mesophyll conductance to CO_2 in *Arabidopsis thaliana*. New Phytol 175:501–511.
Flexas J, Scoffoni C, Gago J, Sack L (2013) Leaf mesophyll conductance and leaf hydraulic conductance: an introduction to their measurement and coordination. J Exp Bot 64:3965–3981.
Galmés J, Andralojc PJ, Kapralov MV, Flexas J, Keys AJ, Molins A, Parry MAJ, Conesa MÀ (2014*a*) Environmentally driven evolution of Rubisco and improved photosynthesis and growth within the C_3 genus *Limonium* (Plumbaginaceae). New Phytol 203:989–999.
Galmés J, Kapralov MV, Andralojc PJ, Conesa MÀ, Keys AJ, Parry MAJ, Flexas J (2014*b*) Expanding knowledge of the Rubisco kinetics variability in plant species: environmental and evolutionary trends. Plant Cell Environ 37:1989–2001.
Gea-Izquierdo G, Cañellas I (2014) Local climate forces instability in long-term productivity of a Mediterranean oak along climatic gradients. Ecosystems 17:228–241.
Gea-Izquierdo G, Fernández-de-Uña L, Cañellas I (2013) Growth projections reveal local vulnerability of Mediterranean oaks with rising temperatures. For Ecol Manag 305:282–293.
Genty B, Briantais JM, Baker NR (1989) The relationship between the quantum yield of photosynthetic electron transport and quenching of chlorophyll fluorescence. Biochim Biophys Acta 990:87–92.
Grassi G, Magnani F (2005) Stomatal, mesophyll conductance and biochemical limitations to photosynthesis as affected by drought and leaf ontogeny in ash and oak trees. Plant Cell Environ 28:834–849.
Harley PC, Loreto F, Di Marco G, Sharkey TD (1992) Theoretical considerations when estimating the mesophyll conductance to CO_2 flux by analysis of the response of photosynthesis to CO_2. Plant Physiol 98:1429–1436.
Himrane H, Camarero JJ, Gil-Pelegrín E (2004) Morphological and ecophysiological variation of the hybrid oak *Quercus subpyrenaica* (*Q. faginea* × *Q. pubescens*). Trees 18:566–575.
Jalas J, Suominen J (eds) (1976) Atlas Florae Europaeae. Distribution of vascular plants in Europe. 3. Salicaceae to Balanophoraceae. The Committee for Mapping the Flora of Europe & Societas Biologica Fennica Vanamo, Helsinki, 128 pp. [maps 201–383].
Jarvis PG, McNaughton KG (1986) Stomatal control of transpiration: scaling up from leaf to region. Adv Ecol Res 15:1–49.
Jato V, Rodríguez-Rajo FJ, Méndez J, Aira MJ (2002) Phenological behaviour of *Quercus* in Ourense (NW Spain) and its relationship with the atmospheric pollen season. Int J Biometeorol 46:176–184.
Kikuzawa K (1995) Leaf phenology as an optimal strategy for carbon gain in plants. Can J Bot 73:158–163.
Kovar-Eder J, Kvacek Z, Zastawniak E, Givulescu R, Hably L, Mihajlovic D, Teslenko Y, Walther H (1996) Floristic trends in the vegetation of the Paratethys surrounding areas during Neogene time. In: Bernor R, Fahlbusch V, Mittmann HW (eds) The evolution of Western Eurasia Later Neogene faunas. Columbia University Press, New York, pp 399–409.
Krall JP, Edwards GE (1992) Relationship between photosystem II activity and CO_2 fixation in leaves. Physiol Plant 86:180–187.
Kremer A, Abbott AG, Carlson JE, Manos PS, Plomion C, Sisco P, Staton ME, Ueno S, Vendramin GG (2012) Genomics of Fagaceae. Tree Genet Genomes 8:583–610.
Kvacek Z, Walther H (1989) Palaeobotanical studies in Fagaceae of the European Tertiart. Plant Syst Evol 162:213–229.
Laisk AK (1977) Kinetics of photosynthesis and photorespiration in C_3-plants. Nauka, Moscow, Russia (In Russian).
Manos PS, Doyle JJ, Nixon KC (1999) Phylogeny, biogeography, and processes of molecular differentiation in *Quercus* subgenus *Quercus* (Fagaceae). Mol Phylogenet Evol 12:333–349.
Mayr S, Wieser G, Bauer H (2006) Xylem temperatures during winter in conifers at the alpine timberline. Agric For Meteorol 137:81–88.
Mediavilla S, Escudero A (2003) Stomatal responses to drought at a Mediterranean site: a comparative study of co-occurring woody species differing in leaf longevity. Tree Physiol 23:987–996.
Mediavilla S, Escudero A (2004) Stomatal responses to drought of mature trees and seedlings of two co-occurring Mediterranean oaks. For Ecol Manag 187:281–294.
Mediavilla S, Escudero A, Heilmeier H (2001) Internal leaf anatomy and photosynthetic resource-use efficiency: interspecific and intraspecific comparisons. Tree Physiol 21:251–259.
Morecroft MD, Roberts JM (1999) Photosynthesis and stomatal conductance of mature canopy Oak (*Quercus robur*) and Sycamore (*Acer pseudoplatanus*) trees throughout the growing season. Funct Ecol 13:332–342.
Niinemets Ü, Reichstein M (2003) Controls on the emission of plant volatiles through stomata: a sensitivity analysis. J Geophys Res 108:4211. doi:10.1029/2002JD002626
Ogaya R, Peñuelas J (2007) Leaf mass per area ratio in *Quercus ilex* leaves under a wide range of climatic conditions. The importance of low temperatures. Acta Oecol 31:168–173.
Olalde M, Herrán A, Espinel S, Goicoechea PG (2002) White oaks phylogeography in the Iberian Peninsula. For Ecol Manag 156:89–102.
Oren R, Sperry JS, Katul GG, Pataki DE, Ewers BE, Phillips N, Schäfer KVR (1999) Survey and synthesis of intra- and interspecific variation in stomatal sensitivity to vapour pressure deficit. Plant Cell Environ 22:1515–1526.
Patakas A, Kofidis G, Bosabalidis AM (2003) The relationships between CO_2 transfer mesophyll resistance and photosynthetic efficiency in grapevine cultivars. Sci Hortic 97:255–263.
Peguero-Pina JJ, Flexas J, Galmés J, Niinemets Ü, Sancho-Knapik D, Barredo G, Villarroya D, Gil-Pelegrín E (2012) Leaf anatomical properties in relation to differences in mesophyll conductance to CO_2 and photosynthesis in two related Mediterranean *Abies* species. Plant Cell Environ 35:2121–2129.
Peguero-Pina JJ, Sancho-Knapik D, Barrón E, Camarero JJ, Vilagrosa A, Gil-Pelegrín E (2014) Morphological and physiological divergences within *Quercus ilex* support the existence of different ecotypes depending on climatic dryness. Ann Bot 114:301–313.
Piedallu C, Gégout JC, Perez V, Lebourgeois F (2013) Soil water balance performs better than climatic water variables in tree species distribution modelling. Glob Ecol Biogeogr 22:470–482.
Poorter H, Remkes C (1990) Leaf area ratio and net assimilation rate of 24 wild species differing in relative growth rate. Oecologia 83:553–559.
Roiron P (1983) Nouvelle étude de la macroflore plio-pléistocène de Crespià (Catalogne, Espagne). Geobios 16:687–715.
Rust S, Roloff A (2002) Reduced photosynthesis in old oak (*Quercus robur*): the impact of crown and hydraulic architecture. Tree Physiol 22:597–601.
Sack L, Holbrook NM (2006) Leaf hydraulics. Annu Rev Plant Biol 57:361–381.
Sack L, Scoffoni C (2013) Leaf venation: structure, function, development, evolution, ecology and applications in the past, present and future. New Phytol 198:983–1000.
Sánchez de Dios R, Benito-Garzón M, Sainz-Ollero H (2009) Present and future extension of the Iberian submediterranean territories as determined from the distribution of marcescent oaks. Plant Ecol 204:189–205.
Scoffoni C, Rawls M, McKown A, Cochard H, Sack L (2011) Decline of leaf hydraulic conductance with dehydration: relationship to leaf size and venation architecture. Plant Physiol 156:832–843.
Suárez R, Miró M, Cerdà V, Perdomo JA, Galmés J (2011) Automated flow-based anion-exchange method for high-throughput isolation and real-time monitoring of RuBisCO in plant extracts. Talanta 84:1259–1266.

Syvertsen JP, Lloyd J, McConchie C, Kriedemann PE, Farquhar GD (1995) On the relationship between leaf anatomy and CO_2 diffusion through the mesophyll of hypostomatous leaves. Plant Cell Environ 18:149–157.

Tamura K, Peterson D, Peterson N, Stecher G, Nei M, Kumar S (2011) MEGA5: molecular evolutionary genetics analysis using maximum likelihood, evolutionary distance, and maximum parsimony methods. Mol Biol Evol 28:2731–2739.

Tholen D, Ethier G, Genty B, Pepin S, Zhu X (2012) Variable mesophyll conductance revisited: theoretical background and experimental implications. Plant Cell Environ 35:2087–2103.

Tomás M, Flexas J, Copolovici L et al. (2013) Importance of leaf anatomy in determining mesophyll diffusion conductance to CO_2 across species: quantitative limitations and scaling up by models. J Exp Bot 64:2269–2281.

Tosens T, Niinemets Ü, Vislap V, Eichelmann H, Castro Díez P (2012*a*) Developmental changes in mesophyll diffusion conductance and photosynthetic capacity under different light and water availabilities in *Populus tremula*: how structure constrains function. Plant Cell Environ 35:839–856.

Tosens T, Niinemets Ü, Westoby M, Wright IJ (2012*b*) Anatomical basis of variation in mesophyll resistance in eastern Australian sclerophylls: news of a long and winding path. J Exp Bot 63:5105–5119.

Valentini R, Epron D, De Angelis P, Matteucci G, Dreyer E (1995) In situ estimation of net CO_2 assimilation, photosynthetic electron flow and photorespiration in Turkey oak (*Q. cerris* L.) leaves: diurnal cycles under different levels of water supply. Plant Cell Environ 18:631–640.

van Ommen Kloeke AEE, Douma JC, Ordoñez JC, Reich PB, van Bodegom PM (2012) Global quantification of contrasting leaf life span strategies for deciduous and evergreen species in response to environmental conditions. Glob Ecol Biogeogr 21:224–235.

Vilagrosa A, Bellot J, Vallejo VR, Gil-Pelegrín E (2003) Cavitation, stomatal conductance, and leaf dieback in seedlings of two co-occurring Mediterranean shrubs during an intense drought. J Exp Bot 54:2015–2024.

Withington JM, Reich PB, Oleksyn J, Eissenstat DM (2006) Comparisons of structure and life span in roots and leaves among temperate trees. Ecol Monogr 76:381–397.

Wright IJ, Reich PB, Westoby M et al. (2004) The worldwide leaf economics spectrum. Nature 428:821–827.

Zhu W, Tian H, Xu X, Pan Y, Chen G, Lin W (2012) Extension of the growing season due to delayed autumn over mid and high latitudes in North America during 1982–2006. Glob Ecol Biogeogr 21:260–271.

Tree Physiology 00, 1–11
doi:10.1093/treephys/tpx057

Research paper

Coordinated modifications in mesophyll conductance, photosynthetic potentials and leaf nitrogen contribute to explain the large variation in foliage net assimilation rates across *Quercus ilex* provenances

José Javier Peguero-Pina[1,2,†], Sergio Sisó[1,†], Jaume Flexas[3], Jeroni Galmés[3], Ülo Niinemets[4], Domingo Sancho-Knapik[1,2] and Eustaquio Gil-Pelegrín[1,2,5]

[1]Unidad de Recursos Forestales, Centro de Investigación y Tecnología Agroalimentaria de Aragón, Gobierno de Aragón, Avda Montañana 930, 50059 Zaragoza, Spain; [2]Instituto Agroalimentario de Aragón-IA2 (CITA-Universidad de Zaragoza), 50013 Zaragoza, Spain; [3]Research Group on Plant Biology under Mediterranean conditions, Instituto de Investigaciones Agroambientales y de Economía del Agua (INAGEA), Departament de Biologia, Universitat de les Illes Balears, Carretera de Valldemossa, 07122 Palma de Mallorca, Spain; [4]Institute of Agricultural and Environmental Sciences, Estonian University of Life Sciences, Kreutzwaldi 1, Tartu 51014, Estonia; [5]Corresponding author (egilp@aragon.es)

Received October 25, 2016; accepted May 10, 2017; handling Editor João Pereira

Leaf dry mass per unit area (LMA) has been suggested to negatively affect the mesophyll conductance to CO_2 (g_m), the most limiting factor for photosynthesis per unit leaf area (A_N) in many evergreens. Several anatomical traits (i.e., greater leaf thickness and thicker cell walls) constraining g_m could explain the negative scaling of g_m and A_N with LMA across species. However, the Mediterranean sclerophyll *Quercus ilex* L. shows a major within-species variation in functional traits (greater LMA associated with higher nitrogen content and A_N) that might contrast the worldwide trends. The objective of this study was to elucidate the existence of variations in other leaf anatomical parameters determining g_m and/or biochemical traits improving the capacity of carboxylation ($V_{c,max}$) that could modulate the relationship of A_N with LMA across this species. The results revealed that g_m was the most limiting factor for A_N in all the studied *Q. ilex* provenances from Spain and Italy. The within-species differences in g_m can be partly attributed to the variation in several leaf anatomical traits, mainly cell-wall thickness (T_{cw}), chloroplast thickness (T_{chl}) and chloroplast exposed surface area facing intercellular air spaces (S_c/S). A positive scaling of g_m and A_N with $V_{c,max}$ was also found, associated with an increased nitrogen content per area. A strong correlation of maximum photosynthetic electron transport (J_{max}) with A_N further indicated a coordination between the carboxylase activity and the electron transport chain. In conclusion, we have confirmed the strong ecotypic variation in the photosynthetic performance of individual provenances of *Q. ilex*. Thus, the within-species increases found in A_N for *Q. ilex* with increasing foliage robustness can be explained by a synergistic effect among anatomical (at the subcellular and cellular level) and biochemical traits, which markedly improved g_m and $V_{c,max}$.

Keywords: carboxylation activity of Rubisco, CO_2 diffusion, holm oak, leaf anatomy, leaf dry mass per unit area, net CO_2 uptake, within-species variation.

Introduction

The leaf economics spectrum describes the variation in photosynthetic rates across plant species with different leaf structure and chemistry along resource availability gradients (Wright et al. 2004, 2005, Reich et al. 2007, Hallik et al. 2009). Some studies have suggested the existence of a leaf economics spectrum within single species that may resemble the trends found at global level (Bonser et al. 2010, Vasseur et al. 2012, Blonder et al. 2013).

[†]These authors contributed equally to this study.

However, it is still under discussion whether the within-species genetic (ecotypic) and environmental (plastic) variations throughout the resource availability gradients follow the trends found among different species.

Recently, Niinemets (2015) constructed an extensive database of foliage structural, chemical and photosynthetic traits covering the full species range for the Mediterranean sclerophyll *Quercus ilex* L. This study showed a major variation in leaf functional traits in *Q. ilex* and suggested that there is single-species leaf economics spectrum that might contrast the trends in the worldwide economics spectrum (Niinemets 2015). In particular, greater leaf dry mass per unit area (LMA) in *Q. ilex* was associated with higher leaf nitrogen content, and photosynthetic capacity on a leaf area basis (Niinemets 2015).

This evidence runs counter to the general consensus that LMA is a key structural trait that should negatively influence the photosynthetic performance of the plant (Wright et al. 2004, 2005) due to a higher investment in non-photosynthetic tissue and/or a lower efficiency of the photosynthetically active mesophyll (Niinemets et al. 2009*a*, Hassiotou et al. 2010). This latter effect has been explained by the reduction of mesophyll conductance to CO_2 (g_m) in leaves with greater LMA (Niinemets 1999, Flexas et al. 2008, Hassiotou et al. 2009, Niinemets et al. 2009*a*). Mesophyll conductance is often the most significant photosynthetic limitation, especially in evergreens, and its variation across species is strongly driven by a number of anatomical traits that scale with LMA (Flexas et al. 2012, 2016, Galmés et al. 2014, Niinemets and Keenan 2014, Peguero-Pina et al. 2016*a*). Specifically, the fact that net CO_2 assimilation is constrained by large LMA has been mostly related to (i) the increase in the resistance of the CO_2 diffusion in the gas-phase associated with greater leaf thickness (LT) (Niinemets et al. 2009*b*, Tosens et al. 2012*a*, Tomás et al. 2013) and (ii) the increase in the resistance of CO_2 diffusion in the leaf liquid phase associated with thicker cell walls and overall greater leaf density (Peguero-Pina et al. 2012, Tosens et al. 2012*a*, Tomás et al. 2013). As LMA is a product of LT and density (Niinemets 1999, Poorter et al. 2009), such anatomical controls could well explain the negative scaling of g_m with LMA across species (Niinemets et al. 2009*b*, Tosens et al. 2012*a*, Tomás et al. 2013).

However, there are other leaf anatomical traits (i.e., packing of mesophyll cells relative to each other and to the distance and position of stomata, chloroplast surface area exposed to intercellular air spaces and chloroplast size) that quantitatively determine the variability in g_m and photosynthetic capacity among species and that can modulate the relationships of g_m with LMA, LT and cell-wall thickness (Tomás et al. 2013, Peguero-Pina et al. 2016*b*). Such scaling relationships can even be observed within the same species under different environmental conditions (Terashima et al. 2011, Tosens et al. 2012*b*, Peguero-Pina et al. 2016*a*, 2016*c*). Several studies have indicated that leaves with thicker mesophyll have larger surface area of mesophyll cells exposed to intercellular air spaces per unit leaf area, implying a greater g_m in thicker leaves (Hanba et al. 1999, 2002, Terashima et al. 2006, Peguero-Pina et al. 2016*b*). This could be interpreted as a way of improving g_m and, consequently, photosynthesis in species with large LMA values. Given these compensatory mechanisms, Mediterranean species, on average, have similar photosynthetic capacity—despite their greater LMA—to plants from any other biome (Flexas et al. 2014). These authors hypothesized that high LMA in Mediterranean species is also responsible for the enhanced capacity of carboxylation per area ($V_{c,max}$) due to increased Rubisco content per area in thicker leaves with more cell layers.

Therefore, we hypothesize that the existence of such adaptations at anatomical and/or biochemical level improving the mesophyll CO_2 conductance and/or the capacity of carboxylation per area in *Q. ilex* would explain the within-species increases in net CO_2 assimilation with increasing foliage robustness. To the best of our knowledge, there is a lack of information on how the ecotypic variation of photosynthetic characteristics within a single species is driven by changes in ultrastructural/biochemical mesophyll traits. In order to solve this question, we compared the morphological, anatomical, chemical and photosynthetic traits of seven *Q. ilex* provenances from Spain and Italy in a common garden with the main emphasis to elucidate the ultimate causing factor(s) of the range-wide trends demonstrated by Niinemets (2015) for this species.

Materials and methods

Plant material and experimental conditions

Holm oak (*Q. ilex* subsp. *rotundifolia* and *Q. ilex* subsp. *ilex*) seeds from seven provenances located in Spain and Italy (Table 1) were

Table 1. Geographical and climatic characteristics of seed sampling locations for each *Quercus ilex* provenance. *P*, annual precipitation; *T*, mean annual temperature; MAI, Martonne aridity index. a.s.l., above sea level.

Provenance (code)	Subspecies	Country	Latitude	Longitude	Elevation (m a.s.l.)	*P* (mm)	*T* (°C)	MAI
Cazorla (1)	*rotundifolia*	Spain	38°06′N	02°33′W	1236	532	12.2	24
Extremadura (2)	*rotundifolia*	Spain	40°05′N	05°42′W	450	629	16.6	24
Soria (3)	*rotundifolia*	Spain	41°46′N	02°29′W	1074	570	10.4	28
Gerona (4)	*ilex*	Spain	42°03′N	02°46′E	177	936	14.9	38
Veneto (5)	*ilex*	Italy	45°44′N	10°48′E	617	833	10.1	41
Lazio (6)	*ilex*	Italy	41°13′N	13°03′E	29	904	15.5	36
Sardinia (7)	*ilex*	Italy	39°21′N	08°34′E	627	784	13.5	33

sown and cultivated in 2003 in 0.5 l containers inside a greenhouse under the same conditions with a mixture of 80% compost (Neuhaus Humin Substrat N6; Klasman-Deilmann GmbH, Geeste, Germany) and 20% perlite. After the first growth cycle, the seedlings were transplanted to 25 l containers filled with the same mixture of compost and perlite and cultivated outdoors at CITA de Aragón (41°39′N, 0°52′W, Zaragoza, Spain) under Mediterranean conditions (mean annual temperature 15.4 °C, total annual precipitation 298 mm). A slow-release fertilizer (15:9:12 N:P:K, Osmocote Plus, Sierra Chemical, Milpitas, CA, USA) was added to the top 10-cm layer of substrate (3 g l^{-1} growth substrate). All plants were grown under the same environmental conditions and drip-irrigated every 2 days. The measurements were carried out in ten 9-year-old plants per provenance in summer of 2012 using current-year fully developed non-water-stressed leaves (predawn water potential > −0.1 MPa, data not shown).

Long-term climatic characteristics of the sites of seed collection were obtained from the WorldClim database (http://www.worldclim.org/). Each subspecies occurs under contrasting climatic conditions (Peguero-Pina et al. 2014, Niinemets 2015). Thus, regions of *Q. ilex* subsp. *ilex* provenances sampled here had annual precipitation values (P) higher than those for *Q. ilex* subsp. *rotundifolia* (Table 1). In contrast, the mean annual temperatures (T) were very similar among all provenances (Table 1). As a consequence, the Martonne aridity index [MAI = $P/(T + 10)$] was also higher in regions of *Q. ilex* subsp. *ilex* provenances (Table 1).

Leaf gas exchange and chlorophyll fluorescence measurements

Simultaneous gas exchange and chlorophyll fluorescence measurements were conducted with an open gas exchange system (CIRAS-2, PP-Systems, Amesbury, MA, USA) fitted with an automatic universal leaf cuvette (PLC6-U, PP-Systems) and an FMS II portable pulse amplitude modulated fluorometer (Hansatech Instruments Ltd, Norfolk, UK). In all measurements, vapor pressure deficit was kept at 1.25 kPa and leaf temperature at 25 °C. The photosynthesis measurements started once the steady-state gas-exchange rate was reached at a CO_2 concentration surrounding the leaf (C_a) of 400 µmol mol^{-1}, and a saturating photosynthetic photon flux density (PPFD) of 1500 µmol m^{-2} s^{-1} (usually in 30 min after enclosure of leaf in the cuvette). Six CO_2 response curves per provenance were measured using light-adapted mature leaves under saturating PPFD of 1500 µmol m^{-2} s^{-1} by changing C_a between 50 and 1800 µmol mol^{-1} (see Peguero-Pina et al. 2016*a* for details). After each steady-state gas-exchange rate was reached, the net assimilation rate (A_N), the stomatal conductance (g_s) and the effective quantum yield of PSII (Φ_{PSII}) were estimated. The Φ_{PSII} was calculated as $(F'_M - F_S)/F'_M$, where F_S is the steady-state fluorescence and F'_M is the maximum fluorescence during a light-saturating pulse of ~8000 µmol m^{-2} s^{-1} (Genty et al. 1989). Photosynthetic electron transport rate (J_F) was then calculated according to Krall and Edwards (1992), following the methodology described in Peguero-Pina et al. (2016*a*). Leakage of CO_2 in and out of the cuvette was determined for the same range of CO_2 concentrations as described in Flexas et al. (2007*a*) and used to correct for measured leaf fluxes.

Estimation of mesophyll conductance, g_m, by gas exchange and chlorophyll fluorescence

Mesophyll conductance (g_m) was estimated according to the method of Harley et al. (1992), as follows:

$$g_m = \frac{A_N}{C_i - \frac{\Gamma^* (J_F + 8(A_N + R_L))}{J_F - 4(A_N + R_L)}}, \quad (1)$$

where A_N and the substomatal CO_2 concentration (C_i) were taken from the gas-exchange measurements at saturating light, whereas Γ^* (the chloroplastic CO_2 compensation point in the absence of mitochondrial respiration) and R_L (the respiration rate in the light) were estimated for each provenance as described in Flexas et al. (2007*b*). The obtained g_m values were used to convert A_N–C_i responses into A_N–C_c responses (where C_c is the chloroplastic CO_2 concentration) using the equation $C_c = C_i - A_N/g_m$. The maximum ribulose-1,5-bisphosphate carboxylation ($V_{c,max}$) and photosynthetic electron transport (J_{max}) capacities were calculated from the A_N–C_c curves, using the Rubisco kinetic characteristics and their temperature dependencies described by Galmés et al. (2016). The model by Farquhar et al. (1980) was fitted to the data by applying an iterative curve-fitting technique (least square difference) using the Solver tool of Microsoft Excel.

Morphological and anatomical measurements and leaf nitrogen concentration

Sections of 1 mm × 1 mm from the same leaves used for gas-exchange were cut between the main veins and processed for anatomical measurements following the methodology described in Peguero-Pina et al. (2016*b*). Semi-thin (0.8 µm) and ultrathin (90 nm) cross-sections were cut with an ultramicrotome (Reichert and Jung model Ultracut E). Semi-thin cross-sections were stained with 1% toluidine blue and viewed under a light microscope (Optika B-600TiFL, Optika Microscopes, Ponteranica, Italy). Ultrathin cross-sections were contrasted with uranyl acetate and lead citrate and viewed under a transmission electron microscope (H600, Hitachi, Tokyo, Japan). Light and electron microscopy images were analyzed with ImageJ software (http://rsb.info.nih.gov/nih-image/) to determine leaf anatomical characteristics. Light micrographs were used to measure LT, mesophyll thickness between the two epidermal layers, number of palisade layers, fraction of the mesophyll tissue occupied by the intercellular air spaces (f_{ias}), and mesophyll (S_m/S) and chloroplast (S_c/S) surface area facing intercellular air spaces per

leaf area (Evans et al. 1994, Syvertsen et al. 1995, Tomás et al. 2013). Electron micrographs were used to measure the cell-wall thickness (T_{cw}), cytoplasm thickness (T_{cyt}), chloroplast length (L_{chl}) and chloroplast thickness (T_{chl}) (Tomás et al. 2013). Each anatomical trait was measured on three different sections and four to six different fields of view.

Leaf dry mass per unit area (LMA) was measured in 30 mature leaves sampled from 10 individuals per provenance (i.e., three leaves were randomly taken from each individual). Leaf area was measured after scanning the leaves with the ImageJ software. Leaf dry mass was determined after leaves were oven dried at 70 °C for 3 days. The LMA was calculated as the ratio of foliage dry mass to foliage area. Total leaf nitrogen concentration was determined in dried leaves using an Organic Elemental Analyzer (Flash EA 112, Thermo Fisher Scientific Inc., Waltham, MA, USA).

g_m modeled on the basis of anatomical traits

Mesophyll diffusion conductance (g_m) was estimated using the measured leaf anatomical traits as a composite conductance for within-leaf gas and liquid diffusion pathways, according to the one-dimensional gas diffusion model of Niinemets and Reichstein (2003) as applied by Tosens et al. (2012*b*):

$$g_m = \frac{1}{\frac{1}{g_{ias}} + \frac{R \cdot T_k}{H \cdot g_{liq}}}, \quad (2)$$

where g_{ias} is the gas-phase conductance from substomatal cavities to outer surface of cell walls, g_{liq} is the conductance in the liquid and lipid phases from the outer surface of cell walls to chloroplasts, R is the gas constant (Pa m^3 K^{-1} mol^{-1}), T_k is the absolute temperature (K) and H is the Henry's law constant for CO_2 (Pa m^3 mol^{-1}). g_m is defined as a gas-phase conductance, and thus $H/(RT_k)$, the dimensionless form of the Henry's law constant, is needed to convert g_{liq} to corresponding gas-phase equivalent conductance (Niinemets and Reichstein 2003).

The gas-phase conductance (and the reciprocal term, r_{ias}) was calculated as desbribed in Niinemets and Reichstein (2003):

$$g_{ias} = \frac{1}{r_{ias}} = \frac{D_A \cdot f_{ias}}{\Delta L_{ias} \cdot \tau}, \quad (3)$$

where ΔL_{ias} (m) is the average gas-phase thickness, τ is the diffusion path tortuosity (1.57 m m^{-1}, Syvertsen et al. 1995), D_A is the diffusivity of the CO_2 in the air (1.51.10^{-5} m^2 s^{-1} at 25 °C) and f_{ias} is the fraction of intercellular air spaces. ΔL_{ias} was taken as the half of the mesophyll thickness. Total liquid phase conductance (g_{liq}) from the outer surface of cell walls to the carboxylation sites in the chloroplasts is the sum of serial resistance of the cell wall (r_{cw}), the plasmalemma (r_{pl}) and inside the cell ($r_{cel,tot}$) (Tomás et al. 2013):

$$g_{liq} = \frac{S_m}{(r_{cw} + r_{pl} + r_{cel,tot}) \cdot S}. \quad (4)$$

Cell-wall conductance was calculated as described in Peguero-Pina et al. (2012). We used an estimate of 0.0035 m s^{-1} for the conductance of plasma membrane (Tosens et al. 2012*b*). The conductance inside the cell was calculated considering two different pathways of CO_2 (one for cell wall parts lined with chloroplasts and the other for interchloroplastial areas, Tholen et al. 2012) as described by Tomás et al. (2013).

Quantitative limitations analyses of A_N and partial limitations of g_m

The relative controls on A_N imposed by stomatal conductance (l_s), mesophyll diffusion (l_m) and biochemical capacity (l_b) were calculated following the quantitative limitation analysis of Grassi and Magnani (2005) as applied in Tomás et al. (2013). Different fractional limitations, l_s, l_m and l_b ($l_s + l_m + l_b = 1$) were calculated as:

$$l_s = \frac{g_{tot}/g_s \cdot \partial A_N/\partial C_c}{g_{tot} + \partial A_N/\partial C_c}, \quad (5)$$

$$l_m = \frac{g_{tot}/g_m \cdot \partial A_N/\partial C_c}{g_{tot} + \partial A_N/\partial C_c}, \quad (6)$$

$$l_b = \frac{g_{tot}}{g_{tot} + \partial A_N/\partial C_c}, \quad (7)$$

where g_{tot} is the total conductance to CO_2 from ambient air to chloroplasts (sum of the inverse serial stomatal and mesophyll conductances to CO_2, g_s and g_m). $\partial A_N/\partial C_c$ was calculated as the slope of A_N–C_c response curves over a C_c range of 50–100 μmol mol^{-1}. Average estimates of the quantitative limitations of A_N were calculated for at least five different leaves for each provenance.

The determinants of g_m were separated considering the component parts of the diffusion pathway (Eqs. 1–3) as in Tomás et al. (2013). The share of g_m determined by gas-phase conductance (l_{ias}) was calculated as

$$l_{ias} = \frac{g_m}{g_{ias}}. \quad (8)$$

The share of g_m by different components of the cellular phase conductances (l_i) was estimated as

$$l_i = \frac{g_m}{g_i \frac{S_m}{S}}, \quad (9)$$

where l_i is the limitation by the cell wall, the plasmalemma and inside the cell, and g_i refers to the diffusion conductance of each corresponding diffusion pathway.

Statistical analyses

Data are expressed as means ± standard error (SE). One-way ANOVAs were carried out to identify the provenance effect on photosynthetic, morphological and anatomical traits. Traits among provenances were compared by post hoc Tukey's Honest Significant Difference test. Moreover, the Pearson pairwise correlation matrix was calculated to test for correlations among leaf traits for different provenances. Finally, to summarize the multivariate relationships among photosynthetic, morphological, anatomical, chemical and climatic parameters of holm oak provenances, we carried out a principal component analysis (PCA). According to previous analyses, we chosen the variables which: (i) accounted for a higher proportion of variance in the first two principal components of the PCA and (ii) were not redundant (uncorrelated). Then, we calculated the PCA based on a correlation matrix using the Spearman rank correlation coefficient and the selected variables. All statistical analyses were performed with SAS version 8.0 (SAS, Cary, NC, USA).

Results

Variability in photosynthetic traits among provenances

Foliage photosynthetic characteristics were statistically different ($P < 0.05$) between the studied provenances (Figure 1). Two provenances of *Q. ilex* subsp. *rotundifolia* (Extremadura and Soria) showed the highest values for A_N, g_m, $V_{c,max}$ and J_{max}, whereas two provenances of *Q. ilex* subsp. *ilex* (Lazio and Sardinia) showed the lowest ones (Figure 1). This trend was not observed for g_s since the highest and the lowest value were recorded in two provenances of *Q. ilex* subsp. *rotundifolia* (Soria and Cazorla, respectively). The relationships between A_N and g_m, A_N and $V_{c,max}$, and A_N and J_{max} were statistically significant at $P < 0.01$, whereas the relationship between A_N and g_s was statistically significant at $P < 0.05$ (Figure 2). Analysis of quantitative limitations of photosynthesis revealed that A_N was mainly limited by diffusional processes (l_s and l_m), whereas biochemical limitations (l_b) were only between 4 and 10% of total for all the studied provenances (Table 2).

Variability in leaf morphological and anatomical traits among provenances and consequences for internal CO_2 diffusion

The studied *Q. ilex* provenances displayed contrasting values of leaf and cellular anatomical traits (Table 3 and see Tables S1 and S2 available as Supplementary Data at *Tree Physiology* online). *Quercus ilex* subsp. *rotundifolia* provenances showed lower values of leaf area and higher values of LMA and LT than *Q. ilex* subsp. *ilex* provenances, especially Extremadura (1.82 ± 0.11 cm^2, 247.0 ± 9.0 $g\,m^{-2}$ and 316 ± 8 µm, respectively) and Soria (1.70 ± 0.25 cm^2, 284.9 ± 5.8 $g\,m^{-2}$ and 348 ± 10 µm, respectively) (Table 3). Regarding the cellular traits, *Q. ilex* subsp. *ilex* provenances Lazio and Sardinia had the lowest values of S_c/S (5.8 ± 0.8 and 5.6 ± 0.8, respectively) and the

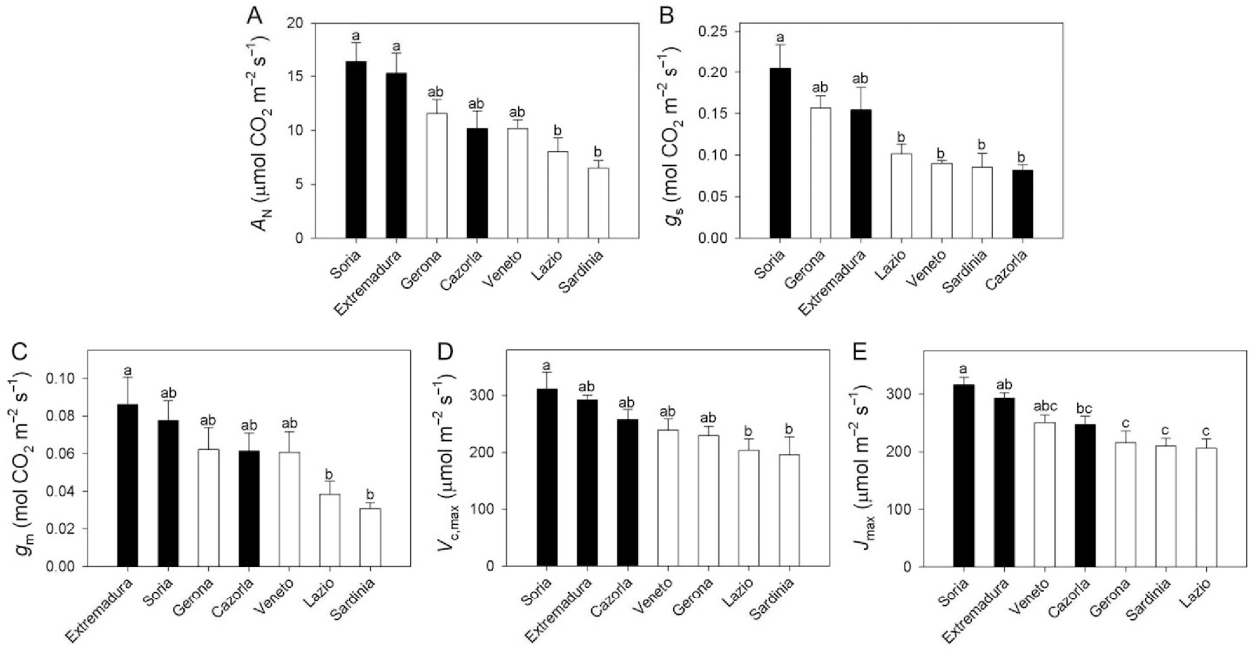

Figure 1. Average (+SE) (A) net photosynthesis rate (A_N), (B) stomatal conductance to CO_2 (g_s), (C) mesophyll conductance to CO_2 (g_m), (D) maximum velocity of carboxylation ($V_{c,max}$) and (E) maximum capacity for photosynthetic electron transport (J_{max}) for the seven studied *Quercus ilex* provenances (black bars, *Q. ilex* subsp. *rotundifolia*; white bars, *Q. ilex* subsp. *ilex*). Different letters indicate significant differences among provenances (Tukey's test, $P < 0.05$).

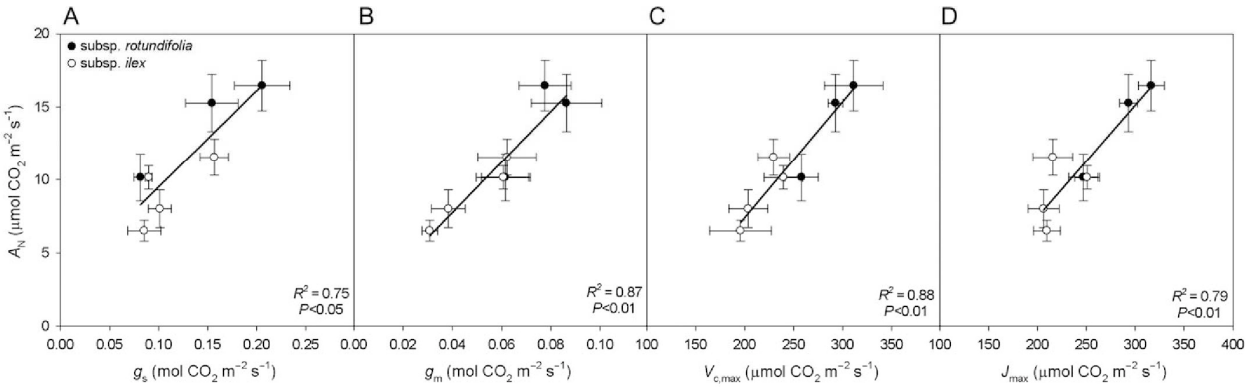

Figure 2. Relationships between average (±SE) net photosynthesis (A_N) and (A) stomatal conductance (g_s), (B) mesophyll conductance (g_m), (C) maximum velocity of carboxylation ($V_{c,max}$) and (D) maximum capacity for electron transport (J_{max}) for the seven studied *Q. ilex* provenances (subsp. *rotundifolia*: Cazorla, Extremadura and Soria; subsp. *ilex*: Gerona, Veneto, Lazio and Sardinia).

Table 2. Relative stomatal (l_s), mesophyll (l_m) and biochemical (l_b) photosynthesis limitations for the seven studied *Q. ilex* provenances (subsp. *rotundifolia*: Cazorla, Extremadura and Soria; subsp. *ilex*: Gerona, Veneto, Lazio and Sardinia). Data are mean ± SE. Different letters indicate significant differences among the provenances (Tukey's test, $P < 0.05$).

Provenance	l_s (%)	l_m (%)	l_b (%)
Cazorla	39.3 ± 1.8^{b}	53.7 ± 2.5^{a}	6.9 ± 1.0^{ab}
Extremadura	32.1 ± 2.6^{ab}	57.2 ± 3.0^{a}	10.7 ± 2.1^{b}
Soria	24.8 ± 2.5^{a}	64.9 ± 3.3^{a}	10.3 ± 0.9^{b}
Gerona	24.8 ± 3.4^{a}	65.2 ± 4.2^{a}	10.0 ± 1.1^{b}
Veneto	35.7 ± 3.8^{ab}	56.2 ± 4.7^{a}	8.1 ± 1.1^{ab}
Lazio	25.0 ± 0.9^{a}	67.8 ± 1.7^{a}	7.2 ± 1.2^{ab}
Sardinia	26.6 ± 2.4^{ab}	69.2 ± 1.9^{a}	4.2 ± 0.6^{a}

highest values of T_{cw} (0.484 ± 0.014 μm and 0.462 ± 0.010 μm, respectively), whereas *Q. ilex* subsp. *rotundifolia* provenances Extremadura and Soria showed the lowest T_{chl} values (1.04 ± 0.07 μm and 1.17 ± 0.10 μm, respectively) (Table 3).

The different components of the CO_2 transfer resistances relative to total mesophyll resistance were estimated using the leaf anatomical traits measured for each holm oak provenance. A strong positive linear relationship was found between modeled and measured g_m values ($R^2 = 0.96$, $F = 117.3$, $P < 0.01$; Figure 3). Furthermore, measured g_m was weakly associated with S_c/S ($R^2 = 0.51$, $P = 0.07$), T_{cw} ($R^2 = 0.54$, $P = 0.06$), T_{chl} ($R^2 = 0.53$, $P = 0.06$) and f_{ias} ($R^2 = 0.11$, $P > 0.1$) (data not shown). Thus, the detailed analysis of individual limitations of g_m confirms that the CO_2 diffusion in the liquid phase (mainly through the cell wall and inside the cell) is the most limiting factor for g_m in the studied provenances (Table 4).

Variability in leaf nitrogen content among provenances as a determinant for the observed differences in $V_{c,max}$

The within-species differences found among holm oak provenances in $V_{c,max}$ (Figure 1) are mainly driven by differences in leaf nitrogen content, as reflected in the linear relationship between nitrogen content and $V_{c,max}$ ($R^2 = 0.83$, $F = 24.2$, $P < 0.01$; Figure 4). Moreover, the within-species differences found in the area-based leaf nitrogen content were positively correlated with LT and LMA across the studied provenances (Figure 5).

Contrasting leaf traits between Q. ilex *subsp.* rotundifolia *and* Q. ilex *subsp.* ilex

Across the studied *Q. ilex* provenances, photosynthetic, morphological and anatomical traits were significantly correlated with each other in most cases (Table 5). The PCA based on the photosynthetic, morphological, anatomical, chemical and climatic traits of *Q. ilex* provenances indicated that the first principal component accounted for 71% and the second for 15% of the total variation (Figure 6). The scores of the holm oak provenances in the PCA biplot indicated that the variables analyzed here clearly separated *Q. ilex* subsp. *rotundifolia* and *Q. ilex* subsp. *ilex* provenances, indicating physiological and structural diversification (Figure 6).

Discussion

The within-species variation range in subcellular- and cellular-level traits in *Q. ilex* uncovered here resembles that found for traits at whole-leaf level in this species by Niinemets (2015). Thus, this evidence demonstrated in our study further underscores a major species range-wide variation in leaf functional traits in holm oak. Moreover, our work confirms the within-species increases in net CO_2 assimilation with increasing foliage robustness through the positive relationship between LMA and A_N (Table 5). In addition, we have demonstrated the existence of adaptations at anatomical and biochemical levels that are the ultimately responsible for the within-species trends found in the photosynthetic performance of *Q. ilex*.

The present study establishes a causal link between net CO_2 assimilation per unit leaf area and subcellular, cellular and

Table 3. Leaf area, leaf mass area (LMA), leaf thickness (LT), chloroplast surface area exposed to intercellular airspace (S_c/S), cell-wall thickness (T_{cw}) and chloroplast thickness (T_{chl}) for the seven studied *Q. ilex* provenances (subsp. *rotundifolia*: Cazorla, Extremadura and Soria; subsp. *ilex*: Gerona, Veneto, Lazio and Sardinia). Data are mean ± SE. Different letters indicate significant differences among the provenances (Tukey's test, $P < 0.05$).

Provenance	Leaf area (cm^2)	LMA ($g\ m^{-2}$)	LT (μm)	S_c/S ($m^2\ m^{-2}$)	T_{cw} (μm)	T_{chl} (μm)
Cazorla	2.76 ± 0.21^{a}	232.0 ± 2.3^{c}	264 ± 5^{ab}	7.1 ± 0.6^{ab}	0.372 ± 0.010^{b}	1.86 ± 0.09^{b}
Extremadura	1.82 ± 0.11^{a}	247.0 ± 9.0^{cd}	316 ± 8^{cd}	8.0 ± 0.5^{b}	0.332 ± 0.008^{b}	1.04 ± 0.07^{a}
Soria	1.70 ± 0.25^{a}	284.9 ± 5.8^{e}	348 ± 10^{d}	11.8 ± 1.0^{c}	0.362 ± 0.008^{b}	1.17 ± 0.10^{a}
Gerona	7.29 ± 0.37^{b}	212.0 ± 5.9^{b}	251 ± 11^{a}	9.0 ± 1.3^{bc}	0.301 ± 0.008^{a}	2.00 ± 0.10^{b}
Veneto	11.24 ± 0.99^{c}	215.1 ± 6.9^{b}	245 ± 6^{a}	9.4 ± 1.0^{bc}	0.293 ± 0.010^{a}	2.06 ± 0.11^{b}
Lazio	12.68 ± 0.54^{c}	172.1 ± 4.0^{a}	278 ± 14^{ab}	5.8 ± 0.8^{a}	0.484 ± 0.014^{c}	1.80 ± 0.14^{b}
Sardinia	7.35 ± 0.30^{b}	236.0 ± 6.0^{cd}	297 ± 3^{bc}	5.6 ± 0.8^{a}	0.462 ± 0.010^{c}	2.00 ± 0.11^{b}

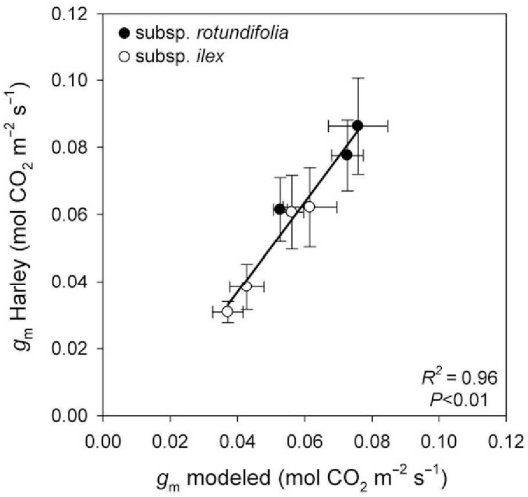

Figure 3. Correlation between average (±SE) values of mesophyll conductance (g_m) modeled using anatomical traits and g_m measured with the Harley et al. (1992) method for the seven studied *Q. ilex* provenances (subsp. *rotundifolia*: Cazorla, Extremadura and Soria; subsp. *ilex*: Gerona, Veneto, Lazio and Sardinia).

whole-leaf anatomical traits (Table 5, Figure 6). The study further highlights that the anatomical control on photosynthesis operates through mesophyll conductance (Figure 2), corroborated by the fact that g_m was the factor most strongly limiting A_N in this species (Table 2). In this regard, the strong relationship between measured and simulated g_m estimates (Figure 3) largely supports a predominant role of structural characteristics in determining the within-species differences in net CO_2 assimilation among *Q. ilex* provenances.

Comparisons of the values of g_m estimated experimentally and estimated from leaf anatomical traits have demonstrated strong correlations among both estimates across different species (Peguero-Pina et al. 2012, 2016*c*, Tosens et al. 2012*b*, Tomás et al. 2013), including several *Quercus* species (Peguero-Pina et al. 2016*a*, 2016*b*). As far as we know, this is the first study that establishes a correspondence between g_m estimated using conventional methods and modeled based on leaf anatomical properties within the same species grown in a common garden. In particular, within-species differences in g_m for *Q. ilex* can be partly attributed to the variation in several leaf anatomical traits, mainly to the changes in T_{cw}, T_{chl} and S_c/S

Table 4. Quantitative limitations of mesophyll conductance to CO_2 (g_m) due to different anatomical components of the diffusion pathway: intercellular spaces (l_{ias}), cell wall (l_{cw}), plasmalemma (l_{pl}) and inside the cell ($l_{cel,tot}$) in the seven studied *Q. ilex* provenances (subsp. *rotundifolia*: Cazorla, Extremadura and Soria; subsp. *ilex*: Gerona, Veneto, Lazio and Sardinia).

Provenance	l_{ias} (%)	l_{cw} (%)	l_{pl} (%)	$l_{cel,tot}$ (%)
Cazorla	8	55	4	33
Extremadura	15	54	4	27
Soria	42	37	3	19
Gerona	19	44	4	33
Veneto	26	40	3	31
Lazio	12	55	3	30
Sardinia	19	49	3	30

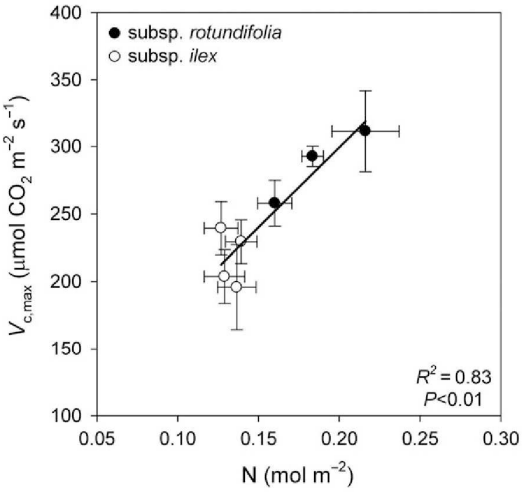

Figure 4. Relationship between area-based leaf nitrogen content (N) and maximum velocity of carboxylation ($V_{c,max}$) for the seven studied *Q. ilex* provenances (subsp. *rotundifolia*: Cazorla, Extremadura and Soria; subsp. *ilex*: Gerona, Veneto, Lazio and Sardinia). Data are means ± SE.

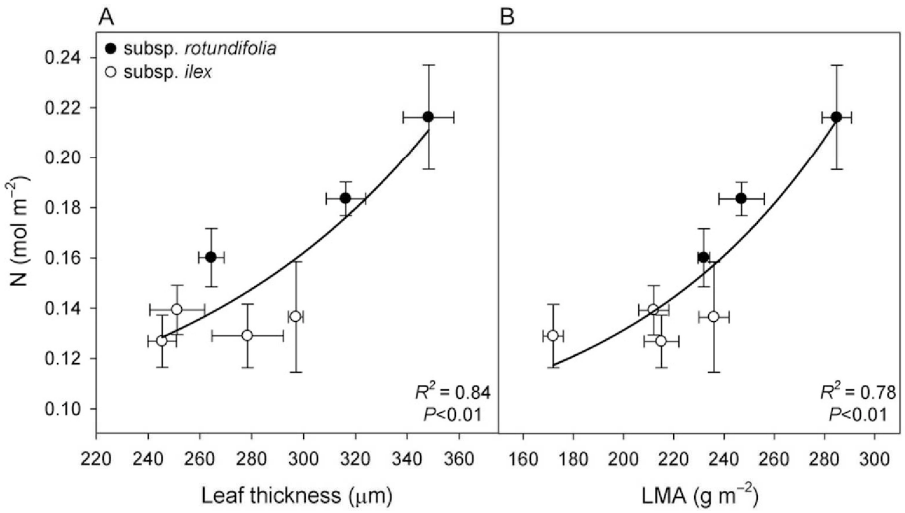

Figure 5. Exponential relationships between leaf nitrogen content per area (N) and (A) leaf thickness (LT) and (B) leaf dry mass per unit area (LMA) for the seven studied *Q. ilex* provenances (subsp. *rotundifolia*: Cazorla, Extremadura and Soria; subsp. *ilex*: Gerona, Veneto, Lazio and Sardinia). Data are means ± SE.

Table 5. Pearson pairwise correlation coefficients among leaf traits for the seven studied *Q. ilex* provenances (see Table 3 and Figures 1 and 4 for abbreviations). ***, ** and * denote that correlations are significant at $P < 0.01$, $P < 0.05$ and $P < 0.1$, respectively.

	A_N	g_m	LT	g_s	J_{max}	LMA	Nitrogen	S_c/S	T_{chl}	T_{cw}
g_m	0.947***									
LT	0.585	0.369								
g_s	0.867**	0.688*	0.648							
J_{max}	0.907***	0.860**	0.687*	0.677*						
LMA	0.691*	0.603	0.726*	0.598	0.814**					
Nitrogen	0.865**	0.737*	0.842**	0.778**	0.901***	0.861**				
S_c/S	0.800**	0.727*	0.320	0.761**	0.741*	0.618	0.625			
T_{chl}	−0.831**	−0.732*	−0.843**	−0.715*	−0.840**	−0.626	−0.874**	−0.412		
T_{cw}	−0.579	−0.736*	0.240	−0.359	−0.444	−0.302	−0.199	−0.687*	0.105	
$V_{c,max}$	0.951***	0.930***	0.604	0.715*	0.970***	0.773**	0.910***	0.746*	−0.825**	−0.520

(Table 3). These three traits are typically dominating variations in g_{liq}, although the quantitative extent of control can differ among different species (Terashima et al. 2005, 2011, Evans et al. 2009, Peguero-Pina et al. 2012, 2016*c*, Tosens et al. 2012*b*, Tomás et al. 2013). According to our data, g_m can be increased through the improvement of S_c/S, decrease of cell-wall thickness and/or chloroplast thickness (Table 5), pointing out that the combination of these factors determines to a large extent the mesophyll conductance for the studied *Q. ilex* provenances.

Besides the major importance of mesophyll diffusion limitations on net photosynthesis, there are other photosynthetic characteristics influencing A_N in *Q. ilex*. Thus, the within-species variation in photosynthetic capacity also depended on the variation in $V_{c,max}$ among the studied provenances (Figure 2), which was reflected in the positive scaling of $V_{c,max}$ with g_m (Table 5), perhaps to maximize the efficiency of the latter as the most limiting factor for photosynthesis in this species. The greater $V_{c,max}$ was associated with an increased nitrogen content per area (Figure 4), probably as a result of overall number of cell layers and greater leaf volume in thicker leaves (Niinemets 1999, Flexas et al. 2014). Indeed, increases in LT and LMA in *Q. ilex* were associated with greater leaf nitrogen content per area (Figure 5; Niinemets 2015). Therefore, this evidence suggests that the increase in foliage robustness was also responsible for the compensating greater $V_{c,max}$ among holm oak provenances, as previously suggested by Flexas et al. (2014) for Mediterranean species. A strong correlation of J_{max} with A_N (Figure 2, Table 5) further indicates a coordination between the Rubisco carboxylase activity and the generation of reducing power in the electron transport chain.

Finally, g_s was also positively correlated with A_N, although the correlation was not as strong as those found for g_m and $V_{c,max}$ and g_m and A_N (Figure 2, Table 5). The differences found in g_s could be influenced by the existence of differences in stomatal density and size (Franks and Beerling 2009). In the present

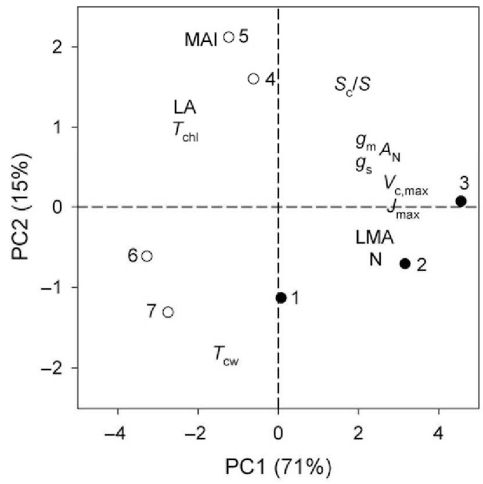

Figure 6. Relationship between the first two principal components (PC1 vs PC2) of the PCA computed using the photosynthetic, morphological, anatomical, chemical and climatic traits for the seven studied *Q. ilex* provenances: black dots, *Q. ilex* subsp. *rotundifolia*; white dots, *Q. ilex* subsp. *ilex*; provenance codes as in Table 1. Variables: net photosynthesis (A_N), stomatal conductance to CO_2 (g_s), mesophyll conductance to CO_2 (g_m), maximum velocity of carboxylation ($V_{c,max}$), maximum capacity for electron transport (J_{max}), cell-wall thickness (T_{cw}), chloroplast surface area exposed to intercellular airspace (S_c/S), chloroplast thickness (T_{chl}), leaf area (LA), leaf dry mass per unit area (LMA), area-based leaf nitrogen content (N) and Martonne aridity index (MAI).

study, large differences in stomatal density were detected between two provenances representing the higher and lower values of g_s (Soria and Lazio, data not shown), which may explain the within-species differences found in g_s.

Previous studies have underscored the great variability exhibited by *Q. ilex* across its circum-Mediterranean distribution, both in terms of morphological (Gratani 1996, Ogaya and Peñuelas 2007) and ecophysiological traits, such as xylem resistance to water stress-induced embolism (Lo Gullo and Salleo 1993, Tyree and Cochard 1996, Corcuera et al. 2004, Limousin et al. 2010). Recently, Peguero-Pina et al. (2014) concluded that the reduction in leaf area was one of the most outstanding morphological divergences between both subspecies (Table 3). The great reduction in leaf area reported in *Q. ilex* subsp. *rotundifolia* can be considered a general feature of many Mediterranean woody plants (Ackerly et al. 2002, Ackerly 2004). Moreover, Peguero-Pina et al. (2014), when comparing the hydraulic traits of *Q. ilex* subsp. *rotundifolia* and *Q. ilex* subsp. *ilex*, stated that both subspecies represent contrasting ecotypes or 'functional types' in response to climate dryness of their natural distribution ranges. The results of the present study further reinforce this hypothesis as both subspecies were clearly segregated in the functional trait space (Figure 6). Indeed, provenances of *Q. ilex* subsp. *rotundifolia* living under more arid conditions (Table 1) had increased photosynthetic capacity per unit leaf area when compared with provenances of *Q. ilex* subsp. *ilex* occurring in milder coastal areas, which might compensate for possible limitations in net CO_2 assimilation if soil water uptake is restricted during summer.

Conclusions

We conclude that g_m is the factor most strongly limiting carbon assimilation in all the studied *Q. ilex* provenances. Moreover, we have observed a strong ecotypic variation in the photosynthetic performance of individual provenances of *Q. ilex*. Thus, the higher A_N exhibited by Extremadura and Soria can be explained by a synergistic effect among anatomical and biochemical traits, which markedly improved g_m and $V_{c,max}$ in these provenances. The existence of adaptations at subcellular and cellular levels explains the within-species increases in net CO_2 assimilation per unit leaf area with increasing foliage robustness.

Supplementary Data

Supplementary Data for this article are available at *Tree Physiology* Online.

Conflict of interest

None declared.

Funding

Financial support from the Spanish National Institute for Agriculture and Food Research and Technology (INIA) (RTA2015-00054-C02-01 project) and Gobierno de Aragón (H38 research group) is acknowledged. The work of D.S.-K. is supported by a DOC INIA contract co-funded by INIA and the European Social Fund (ESF), the work of J.F. is funded by Plan National, Spain (contract CTM2014-53902-C2-1-P), and the research of Ü.N. by the Estonian Research Council (institutional grant 8-3), and the European Commission through the European Regional Development Fund (Center of Excellence EcolChange, TK 131).

References

Ackerly DD (2004) Adaptation, niche conservatism, and convergence: comparative studies of leaf evolution in the California chaparral. Am Nat 163:654–671.

Ackerly DD, Knight CA, Weiss SB, Barton K, Starmer KP (2002) Leaf size, specific leaf area and microhabitat distribution of woody plants in a California chaparral: contrasting patterns in species level and community level analyses. Oecologia 130:449–457.

Blonder B, Violle C, Enquist BJ (2013) Assessing the causes and scales of the leaf economics spectrum using venation networks in *Populus tremuloides*. J Ecol 101:981–989.

Bonser SP, Ladd B, Monro K, Hal MD, Forster MA (2010) The adaptive value of functional and life-history traits across fertility treatments in an annual plant. Ann Bot 106:979–988.

Corcuera L, Camarero JJ, Gil-Pelegrín E (2004) Effects of a severe drought on *Quercus ilex* radial growth and xylem anatomy. Trees 18: 83–92.

Evans JR, von Caemmerer S, Setchell BA, Hudson GS (1994) The relationship between CO_2 transfer conductance and leaf anatomy in transgenic tobacco with a reduced content of Rubisco. Aust J Plant Physiol 21:475–495.

Evans JR, Kaldenhoff R, Terashima I (2009) Resistances along the CO_2 diffusion pathway inside leaves. J Exp Bot 60:2235–2248.

Farquhar GD, von Caemmerer S, Berry JA (1980) A biochemical model of photosynthetic CO_2 assimilation in leaves of C_3 species. Planta 149:78–90.

Flexas J, Díaz-Espejo A, Berry JA, Galmés J, Cifre J, Kaldenhoff R, Medrano H, Ribas-Carbó M (2007*a*) Analysis of leakage in IRGA's leaf chambers of open gas exchange systems: quantification and its effects in photosynthesis parameterization. J Exp Bot 58:1533–1543.

Flexas J, Ortuño MF, Ribas-Carbó M, Díaz-Espejo A, Flórez-Sarasa ID, Medrano H (2007*b*) Mesophyll conductance to CO_2 in *Arabidopsis thaliana*. New Phytol 175:501–511.

Flexas J, Ribas-Carbó M, Díaz-Espejo A, Galmés J, Medrano H (2008) Mesophyll conductance to CO_2: current knowledge and future prospects. Plant Cell Environ 31:601–621.

Flexas J, Barbour MM, Brendel O et al. (2012) Mesophyll conductance to CO_2: an unappreciated central player in photosynthesis. Plant Sci 193-194:70–84.

Flexas J, Díaz-Espejo A, Gago J, Gallé A, Galmés J, Gulías J, Medrano H (2014) Photosynthetic limitations in Mediterranean plants: a review. Environ Exp Bot 103:12–23.

Flexas J, Díaz-Espejo A, Conesa MA et al. (2016) Mesophyll conductance to CO_2 and Rubisco as targets for improving intrinsic water use efficiency in C_3 plants. Plant Cell Environ 39:965–982.

Franks PJ, Beerling DJ (2009) Maximum leaf conductance driven by CO2 effects on stomatal size and density over geologic time. Proc Natl Acad Sci USA 106:10343–10347.

Galmés J, Andralojc PJ, Kapralov MV, Flexas J, Keys J, Molins A, Parry MAJ, Conesa MÀ (2014) Environmentally driven evolution of Rubisco and improved photosynthesis and growth within the C_3 genus *Limonium* (Plumbaginaceae). New Phytol 203:989–999.

Galmés J, Hermida-Carrera C, Laanisto L, Niinemets Ü (2016) A compendium of temperature responses of Rubisco kinetic traits: variability among and within photosynthetic groups and impacts on photosynthesis modeling. J Exp Bot 67:5067–5091.

Genty B, Briantais JM, Baker NR (1989) The relationship between the quantum yield of photosynthetic electron transport and quenching of chlorophyll fluorescence. Biochim Biophys Acta 990:87–92.

Grassi G, Magnani F (2005) Stomatal, mesophyll conductance and biochemical limitations to photosynthesis as affected by drought and leaf ontogeny in ash and oak trees. Plant Cell Environ 28:834–849.

Gratani L (1996) Leaf and shoot growth dynamics of *Quercus ilex* L. Acta Oecol 17:17–27.

Hallik L, Niinemets Ü, Wright IJ (2009) Are species shade and drought tolerance reflected in leaf-level structural and functional differentiation in Northern Hemisphere temperate woody flora? New Phytol 184:257–274.

Hanba YT, Miyazawa SI, Terashima I (1999) The influence of leaf thickness on the CO_2 transfer conductance and leaf stable carbon isotope ratio for some evergreen tree species in Japanese warm temperate forests. Funct Ecol 13:632–639.

Hanba YT, Kogami H, Terashima I (2002) The effect of growth irradiance on leaf anatomy and photosynthesis in *Acer* species differing in light demand. Plant Cell Environ 25:1021–1030.

Harley PC, Loreto F, Di Marco G, Sharkey TD (1992) Theoretical considerations when estimating the mesophyll conductance to CO_2 flux by the analysis of the response of photosynthesis to CO_2. Plant Physiol 98:1429–1436.

Hassiotou F, Ludwig M, Renton M, Veneklaas EJ, Evans JR (2009) Influence of leaf dry mass per area, CO_2 and irradiance on mesophyll conductance in sclerophylls. J Exp Bot 60:2303–2314.

Hassiotou F, Renton M, Ludwig M, Evans JR, Veneklaas EJ (2010) Photosynthesis at an extreme end of the leaf trait spectrum: how does it relate to high leaf dry mass per area and associated structural parameters? J Exp Bot 61:3015–3028.

Krall JP, Edwards GE (1992) Relationship between photosystem II activity and CO_2 fixation in leaves. Physiol Plant 86:80–187.

Limousin JM, Longepierre D, Huc R, Rambal S (2010) Change in hydraulic traits of Mediterranean *Quercus ilex* subjected to long-term throughfall exclusion. Tree Physiol 30:1026–1036.

Lo Gullo MA, Salleo S (1993) Different vulnerabilities of *Quercus ilex* L. to freeze and summer drought-induced xylem embolism: an ecological interpretation. Plant Cell Environ 16:511–519.

Niinemets Ü (1999) Research review. Components of leaf dry mass per area—thickness and density—alter leaf photosynthetic capacity in reverse directions in woody plants. New Phytol 144:35–47.

Niinemets Ü (2015) Is there a species spectrum within the world-wide leaf economics spectrum? Major variations in leaf functional traits in the Mediterranean sclerophyll *Quercus ilex*. New Phytol 205:79–96.

Niinemets Ü, Keenan TF (2014) Photosynthetic responses to stress in Mediterranean evergreens: mechanisms and models. Environ Exp Bot 103:24–41.

Niinemets Ü, Reichstein M (2003) Controls on the emission of plant volatiles through stomata: a sensitivity analysis. J Geophys Res 108:4211.

Niinemets Ü, Díaz-Espejo A, Flexas J, Galmés J, Warren CR (2009*a*) Role of mesophyll diffusion conductance in constraining potential photosynthetic productivity in the field. J Exp Bot 60:2249–2270.

Niinemets Ü, Wright IJ, Evans JR (2009*b*) Leaf mesophyll diffusion conductance in 35 Australian sclerophylls covering a broad range of foliage structural and physiological variation. J Exp Bot 60:2433–2449.

Ogaya R, Peñuelas J (2007) Leaf mass per area ratio in *Quercus ilex* leaves under a wide range of climatic conditions. The importance of low temperatures. Acta Oecol 31:168–173.

Peguero-Pina JJ, Flexas J, Galmés J, Niinemets Ü, Sancho-Knapik D, Barredo G, Villarroya D, Gil-Pelegrín E (2012) Leaf anatomical properties in relation to differences in mesophyll conductance to CO_2 and photosynthesis in two related Mediterranean *Abies* species. Plant Cell Environ 35:2121–2129.

Peguero-Pina JJ, Sancho-Knapik D, Barrón E, Camarero JJ, Vilagrosa A, Gil-Pelegrín E (2014) Morphological and physiological divergences within *Quercus ilex* support the existence of different ecotypes depending on climatic dryness. Ann Bot 114:301–313.

Peguero-Pina JJ, Sisó S, Fernández-Marín B, Flexas J, Galmés J, García-Plazaola JI, Niinemets Ü, Sancho-Knapik D, Gil-Pelegrín E (2016*a*) Leaf functional plasticity decreases the water consumption without further consequences for carbon uptake in *Quercus coccifera* L. under Mediterranean conditions. Tree Physiol 36:356–367.

Peguero-Pina JJ, Sisó S, Sancho-Knapik D, Díaz-Espejo A, Flexas J, Galmés J, Gil-Pelegrín E (2016*b*) Leaf morphological and physiological adaptations of a deciduous oak (*Quercus faginea* Lam.) to the Mediterranean climate: a comparison with a closely related temperate species (*Quercus robur* L.). Tree Physiol 36:287–299.

Peguero-Pina JJ, Sancho-Knapik D, Flexas J, Galmés J, Niinemets Ü, Gil-Pelegrín E (2016*c*) Light acclimation of photosynthesis in two closely related firs (*Abies pinsapo* Boiss. and *Abies alba* Mill.): the role of leaf anatomy and mesophyll conductance to CO_2. Tree Physiol 36: 300–310.

Poorter H, Niinemets Ü, Poorter L, Wright IJ, Villar R (2009) Tansley review. Causes and consequences of variation in leaf mass per area (LMA): a meta-analysis. New Phytol 182:565–588.

Reich PB, Wright IJ, Lusk CH (2007) Predicting leaf physiology from simple plant and climate attributes: a global Glopnet analysis. Ecology 17: 1982–1988.

Syvertsen JP, Lloyd J, McConchie C, Kriedemann PE, Farquhar GD (1995) On the relationship between leaf anatomy and CO_2 diffusion

through the mesophyll of hypostomatous leaves. Plant Cell Environ 18: 149–157.

Terashima I, Araya T, Miyazawa S-I, Sone K, Yano S (2005) Construction and maintenance of the optimal photosynthetic systems of the leaf, herbaceous plant and tree: an eco-developmental treatise. Ann Bot 95:507–519.

Terashima I, Hanba YT, Tazoe Y, Vyas P, Yano S (2006) Irradiance and phenotype: comparative eco-development of sun and shade leaves in relation to photosynthetic CO_2 diffusion. J Exp Bot 57:343–354.

Terashima I, Hanba YT, Tholen D, Niinemets Ü (2011) Leaf functional anatomy in relation to photosynthesis. Plant Physiol 155:108–116.

Tholen D, Ethier G, Genty B, Pepin S, Zhu X (2012) Variable mesophyll conductance revisited: theoretical background and experimental implications. Plant Cell Environ 35:2087–2103.

Tomás M, Flexas J, Copolovici L et al. (2013) Importance of leaf anatomy in determining mesophyll diffusion conductance to CO_2 across species: quantitative limitations and scaling up by models. J Exp Bot 64: 2269–2281.

Tosens T, Niinemets Ü, Westoby M, Wright IJ (2012*a*) Anatomical basis of variation in mesophyll resistance in eastern Australian sclerophylls: news of a long and winding path. J Exp Bot 63:5105–5119.

Tosens T, Niinemets Ü, Vislap V, Eichelmann H, Castro-Díez P (2012*b*) Developmental changes in mesophyll diffusion conductance and photosynthetic capacity under different light and water availabilities in *Populus tremula*: how structure constrains function. Plant Cell Environ 35:839–856.

Tyree MT, Cochard H (1996) Summer and winter embolism in oak: impact on water relations. Ann For Sci 53:173–180.

Vasseur F, Violle C, Enquist BJ, Granier C, Vile D (2012) A common genetic basis to the origin of the leaf economics spectrum and metabolic scaling allometry. Ecol Lett 15:1149–1157.

Wright IJ, Reich PB, Westoby M et al. (2004) The world-wide leaf economics spectrum. Nature 428:821–827.

Wright IJ, Reich PB, Cornelissen JHC et al. (2005) Modulation of leaf economic traits and trait relationships by climate. Glob Ecol Biogeogr 14: 411–421.

Tree Physiology 36, 356–367
doi:10.1093/treephys/tpv129

Research paper

Leaf functional plasticity decreases the water consumption without further consequences for carbon uptake in *Quercus coccifera* L. under Mediterranean conditions

José Javier Peguero-Pina[1,2,†], Sergio Sisó[1,†], Beatriz Fernández-Marín[3,4], Jaume Flexas[5], Jeroni Galmés[5], Jose Ignacio García-Plazaola[4], Ülo Niinemets[6], Domingo Sancho-Knapik[1,2] and Eustaquio Gil-Pelegrín[1,2,7]

[1]Unidad de Recursos Forestales, Centro de Investigación y Tecnología Agroalimentaria de Aragón, Gobierno de Aragón, Avda. Montañana 930, 50059 Zaragoza, Spain; [2]Instituto Agroalimentario de Aragón -IA2 (CITA-Universidad de Zaragoza), Zaragoza, Spain; [3]Institute of Botany and Center for Molecular Biosciences Innsbruck (CMBI), University of Innsbruck, A-6020 Innsbruck, Austria; [4]Department of Plant Biology and Ecology, University of the Basque Country (UPV/EHU), Apdo. 644, 48080 Bilbao, Spain; [5]Research Group on Plant Biology under Mediterranean conditions, Departament de Biologia, Universitat de les Illes Balears, Carretera de Valldemossa, 07071 Palma de Mallorca, Spain; [6]Institute of Agricultural and Environmental Sciences, Estonian University of Life Sciences, Kreutzwaldi 1, Tartu 51014, Estonia; [7]Corresponding author (egilp@aragon.es)

Received September 24, 2015; accepted November 14, 2015; published online December 24, 2015; handling Editor João Pereira

The accumulation of epicuticular waxes over stomata in *Quercus coccifera* L. contributes to a severe reduction in maximum stomatal conductance ($g_{s,max}$) under Mediterranean (MED) conditions. However, this phenomenon was not observed in this species under temperate (TEM) conditions, which could lead to differences in the ability to assimilate CO_2 between the sites. We hypothesise that the overall importance of such a reduction in $g_{s,max}$ on photosynthesis is modulated by other factors affecting carbon gain, mainly mesophyll conductance to CO_2 (g_m), through a plastic response to changes in environmental conditions (i.e., vapour pressure deficit, VPD, and mean daily quantum flux density, Q_{int}). The results reveal that leaves grown at the TEM site did not show an increased ability for net CO_2 assimilation (A_N), mainly due to an equal g_m at both sites. This fact is explained by a trade-off between an increased conductance of the gas phase (g_{ias}) and a reduced conductance of the liquid phase (g_{liq}) at the TEM site compared with the MED site. In spite of the reduction in $g_{s,max}$ at the MED site, transpiration (E) did not diminish during midsummer to the levels of the TEM site due to a higher VPD found at the MED site, yielding a higher water use efficiency (A_N/E) at the TEM site. Moreover, photosynthetic nitrogen use efficiency was also higher at the TEM site, indicating these leaves can reach similar values of A_N with lower nitrogen investment that those at the MED site. These results suggest that *Q. coccifera* does not always use the main resources (water and nutrients) at leaf level as efficiently as possible. Moreover, the different patterns of resource use (in particular N), together with the functional plasticity, cannot overcome the morpho-functional constraints that limit photosynthetic activity, even under potentially favourable conditions.

Keywords: epicuticular waxes, Mediterranean climate, mesophyll conductance, photosynthesis, PNUE, stomatal conductance, WUE.

Introduction

Kermes oak (*Quercus coccifera* L.) is a sclerophyllous species that is considered one of the main components of the shrublands in the most arid areas of the Iberian Peninsula (Castro-Díez and Navarro 2007, Peguero-Pina et al. 2008). This species is able to withstand long and intense drought periods during summer, the driest season in the Mediterranean region (Vilagrosa 2002, Vilagrosa et al. 2003, Peguero-Pina et al. 2008). This

[†]These authors contributed equally to this study.

high drought tolerance is associated with its ability to tolerate very low water potentials without signs of irreversible damage in either the apoplast or the symplast (Vilagrosa et al. 2010) and by the remarkable plasticity of its photo-protective systems in response to environmental challenges (García-Plazaola et al. 2003, 2008). *Quercus coccifera* has been considered a water-saving plant (Valladares et al. 2005) due to its capacity to regulate water loss and thereby withstand prolonged dry periods (Sakcali and Ozturk 2004, Ozturk et al. 2010). In addition, its constitutive drought tolerance is manifested in lower values of maximum stomatal conductance ($g_{s,max}$) than those reported for other co-occurring species that are also considered to be genuine representative of the Mediterranean woody flora (Peguero-Pina et al. 2009, Vilagrosa et al. 2010).

Roth-Nebelsick et al. (2013) found that this low $g_{s,max}$ can be partly explained by particular morphological features of the stomata in this species. Specifically, they reported a *c.* sixfold reduction in stomatal pore area in mature leaves of *Q. coccifera* growing under Mediterranean conditions due to the accumulation of epicuticular waxes overarching the cuticular rims of the stomatal pore. Such reduction of stomatal pore area, which has a major influence on $g_{s,max}$ (Franks and Beerling 2009, Kaiser 2009, Dow et al. 2014), caused a strong reduction in transpiration under high vapour pressure deficit (VPD) conditions registered during the Mediterranean summer (Roth-Nebelsick et al. 2013).

Although *Q. coccifera* is well adapted to Mediterranean conditions, it covers a large climatic space similar to congeneric *Quercus ilex* L. (e.g., Peguero-Pina et al. 2014, Niinemets 2015), exceptionally even reaching the Atlantic coast of the Iberian Peninsula on south-facing limestone slopes under oceanic temperate climate conditions (Castro-Díez et al. 1997, Castro-Díez and Navarro 2007). The occurrence of *Q. coccifera* in these contrasting habitats is in part explained by its capacity to plastically respond to environmental variations at leaf and crown level (Rubio de Casas et al. 2007). Under these temperate conditions, with summer VPD values much lower than those registered under typical Mediterranean conditions, Roth-Nebelsick et al. (2013) reported a smaller degree of stomatal closure by cuticular wax cover, with stomatal pore area being *c.* 4 times higher than that found under Mediterranean conditions. This phenomenon was interpreted as a plastic response of $g_{s,max}$ in *Q. coccifera* to changes in environmental conditions during plant growth, i.e., air temperature and relative humidity, with further consequences for net CO_2 assimilation (Roth-Nebelsick et al. 2013).

Species response to site climatic drivers is affected by both genetic and phenotypic (i.e., plastic) components of variation that cannot be separated in field studies (Niinemets 2015). In fact, several common garden studies have demonstrated important genetic sources of variation among Mediterranean evergreen oak ecotypes (Balaguer et al. 2001, Valladares et al. 2002*a*, Gimeno et al. 2009, Ramírez-Valiente et al. 2010). However, there is currently little information on adaptability of stomatal traits in *Q. coccifera* as driven by genetic and plastic sources of variation. Furthermore, provided that plastic components of variation dominate stomatal differentiation, the important question is when and how rapidly cuticular wax crypts can develop. There is evidence that cuticle thickness and wax deposition increase through leaf development (Pallardy and Kozlowski 1980, Hauke and Schreiber 1998), but to our knowledge there is little data on development of cuticular crypts around stomata.

Though it is well known that stomatal conductance plays a key role in determining maximum rates of carbon assimilation, other factors such as mesophyll conductance to CO_2 (g_m) can constrain photosynthesis and, under certain conditions, be the most significant photosynthetic limitation (Flexas et al. 2012, 2014), especially in evergreen species with inherently low g_m (Niinemets et al. 2009, 2011). Recently, several studies have quantified the importance of several leaf anatomical traits (including leaf thickness, packing of mesophyll cells relative to the distance and position of stomata, chloroplast exposed surface area facing intercellular air spaces, thickness of mesophyll cell walls and chloroplast size) in determining the variability in g_m and photosynthetic capacity among species (Tomás et al. 2013) or even within the same species growing under contrasting environmental conditions (Terashima et al. 2011, Peguero-Pina et al. 2015).

We hypothesise that the overall importance of cryptic stomata as a determinant of $g_{s,max}$ on foliage photosynthetic performance depends on how other foliage photosynthetic traits, including foliage photosynthetic capacity and g_m, respond to environment, i.e., the extent to which plasticity in the amount of wax covering stomatal pores and g_m and photosynthetic capacity of *Q. coccifera* are linked under contrasting environmental conditions. In order to test this hypothesis, the specific objectives of this study were: (i) to determine if the existence of differences in stomatal conductance has further consequences for net CO_2 assimilation and other gas exchange parameters between *Q. coccifera* growing under contrasting environmental conditions, (ii) to determine if the modification of $g_{s,max}$ shown by Roth-Nebelsick et al. (2013) in *Q. coccifera* is mainly due to environmental effects (plastic component of variation) regardless of the genetic background, and (iii) to analyse the influences of site environmental conditions on several morphological and anatomical leaf traits of *Q. coccifera* that could modify g_m and plant photosynthetic performance.

Materials and methods

Plant material and experimental conditions

In this study we used individuals from the same open-pollinated family in order to reduce the within-species genetic variability (Himrane et al. 2004). Seeds of *Q. coccifera* L. were collected from the same mother tree in a natural population of the Sistema

Ibérico Meridional provenance of Spain. The seeds were sown in 2009 and cultivated in 0.5 l containers inside a greenhouse under the same conditions with a mixture of 80% compost (Neuhaus Humin Substrat N6; Klasman-Deilmann GmbH, Geeste, Germany) and 20% perlite. After the first growth cycle, seedlings were transplanted to 25 l containers filled with the same mixture of compost and perlite and cultivated outdoors at CITA de Aragón (41°39′N, 0°52′W, Zaragoza, Spain) under Mediterranean (MED) conditions (see Figure S1 available as Supplementary Data at *Tree Physiology* Online, mean annual temperature 15.4 °C, total annual precipitation 298 mm). Nutrients were supplied as slow-liberation fertilizer (Osmocote Plus, Sierra Chemical, Milpitas, CA, USA). The fertilizer (3 g l^{-1} growth substrate) was applied to the top 10-cm layer of substrate. At the end of 2011, half of these seedlings were randomly selected and moved to the Jardín Botánico de Iturrarán (43°13′N, 02°01′W, 70 m a.s.l., Gipuzkoa, Spain), which features temperate (TEM) conditions (see Figure S1 available as Supplementary Data at *Tree Physiology* Online, mean annual temperature 14.5 °C, total annual precipitation 1631 mm). Measurements were performed during the summer of 2012 on the current-year fully developed leaves of 4-year-old seedlings of *Q. coccifera* at both the MED and the TEM site.

Air temperature (T, °C) and relative humidity (RH, %) were measured at both sites using three Hobo Pro temp/RH data loggers (Onset Computer, Bourne, MA, USA) located at 1.30 m above the soil surface. Measurements were recorded every 30 min during the growing season (April to September) of 2012. Vapour pressure deficit (VPD, kPa) was calculated for both sites from mean values of T and RH according to Rundel and Jarrell (1989). Mean daily quantum flux density (Q_{int}, mol m^{-2} day^{-1}) was calculated for both sites from the mean values of incident global solar radiation (Cescatti and Zorer 2003) obtained from the nearby meteorological stations for both sites. At the MED site, Q_{int} and VPD were consistently higher than at the TEM site ($P < 0.05$) (Figure 1). Moreover, maximum diurnal vapour pressure deficit (VPD_{max}, kPa) was also higher at the MED site ($P < 0.05$), reaching values up to ~4 kPa during summer (Figure 1).

Stomatal pore area

The size of the orifice of the cuticular cover above stomata and the stomatal pore area of *Q. coccifera* leaves grown at the MED and TEM sites were measured on 20 fully mature leaves collected from four plants (five leaves from each plant) per site. To obtain the dimensions of the stomatal pore, which is usually occluded by the cuticular cover, it was necessary to remove epicuticular waxes by immersion of leaf samples twice for 30 s into chloroform at room temperature (Jetter et al. 2000). After this treatment, samples were viewed with scanning electron microscopy (VP-SEM S-3400N, Hitachi, Japan, low vacuum range 6–270 Pa) and stomatal characteristics were measured from micrographs with ImageJ software (http://rsb.info.nih.gov/nih-image/).

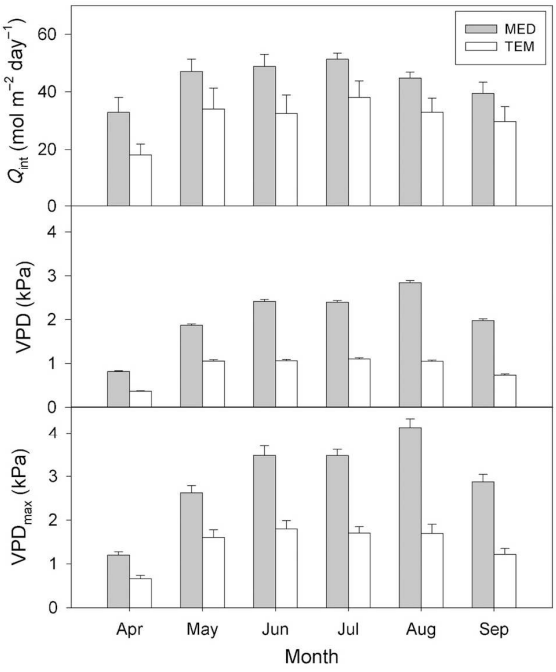

Figure 1. Mean daily quantum flux density (Q_{int}, mol m^{-2} day^{-1}), mean diurnal (from dawn to sunset) vapour pressure deficit (VPD, kPa) and maximum diurnal (from dawn to sunset) vapour pressure deficit (VPD_{max}, kPa) for the Mediterranean (MED) and temperate (TEM) sites during the growing season of 2012 (from April to September). Data are mean ± SE. All the values were statistically different ($P < 0.05$) between sites.

Analysis of changes in leaf area, leaf dry mass per area and stomatal pore area during the growing season at the MED site

At the MED site, changes in leaf area, leaf dry mass per unit area (LMA) and cuticular cover above stomata were periodically measured from 7 May 2012 (Day 1, 1 week after bud burst). Twenty leaves were collected from four plants (five leaves from each plant) at each sampling date. Leaf area was measured from scanned leaf images using ImageJ software. Leaves were then oven-dried at 70 °C for 72 h, and their dry mass was estimated. LMA was calculated as the ratio of foliage dry mass to foliage area, and was used as an estimator of sclerophylly (Castro-Díez et al. 1997, Corcuera et al. 2002, Niinemets 2015). Another set of 20 leaves was used to quantify changes in stomatal pore area due to cuticular cover. Stomatal characteristics were measured with ImageJ software from micrographs obtained with a scanning electron microscope (VP-SEM S-3400N, Hitachi, Japan, low vacuum range 6–270 Pa).

Leaf gas exchange and chlorophyll fluorescence measurements

Leaf gas exchange parameters were measured simultaneously with measurements of chlorophyll fluorescence using an open gas exchange system (CIRAS-2, PP-Systems, Amesbury, MA,

USA) fitted with an automatic universal leaf cuvette (PLC6-U, PP-Systems) with an FMS II portable pulse amplitude modulated fluorometer (Hansatech Instruments Ltd, King's Lynn, UK). Six CO_2 response curves were measured at both the MED and the TEM site using light-adapted mature leaves. The photosynthesis measurements started at a CO_2 concentration surrounding the shoot (C_a) of 400 µmol mol^{-1}, and a saturating photosynthetic photon flux density (PPFD) of 1500 µmol m^{-2} s^{-1}. Leaf temperature and VPD were maintained at 25 °C and 1.25 kPa, respectively, during all the measurements. Once the steady state gas-exchange rate was reached under these conditions (usually in 30 min after clamping the leaf), net assimilation rate (A_N), stomatal conductance (g_s) and effective quantum yield of PSII (Φ_{PSII}) were estimated. Thereafter, C_a was decreased stepwise down to 50 µmol mol^{-1}. Upon completion of measurements at low C_a, C_a was increased again to 400 µmol mol^{-1} to restore the original value of A_N. C_a was further increased stepwise to 1800 µmol mol^{-1} and all the steady-state photosynthetic characteristics were recorded at each C_a. Leakage of CO_2 in and out of the cuvette was determined for the same range of CO_2 concentrations with a photosynthetically inactive leaf enclosed (obtained by heating the leaf until no variable chlorophyll fluorescence was observed), and used to correct measured leaf fluxes (Flexas et al. 2007*a*).

For Φ_{PSII}, steady-state fluorescence (F_S) and maximum fluorescence during a light-saturating pulse of ~8000 µmol m^{-2} s^{-1} (F_M') were estimated, and Φ_{PSII} was calculated as $(F_M' - F_S)/F_M'$ (Genty et al. 1989). Photosynthetic electron transport rate (J_{flu}) was then calculated according to Krall and Edwards (1992), multiplying Φ_{PSII} by PPFD and by α (a term which includes the product of leaf absorbance and the partitioning of absorbed quanta between photosystems I and II); α was previously determined as the slope of the relationship between Φ_{PSII} and Φ_{CO_2} (i.e., quantum efficiency of CO_2 fixation) obtained by varying light intensity under non-photorespiratory conditions in an atmosphere containing <1% O_2 (Valentini et al. 1995). Five photosynthesis vs PPFD response curves at both the MED and the TEM site were measured to determine α.

Estimation of mesophyll conductance by gas exchange and chlorophyll fluorescence

Mesophyll conductance (g_m) was estimated according to the method of Harley et al. (1992), as follows:

$$g_m = \frac{A_N}{C_i - \dfrac{\Gamma^*(J_F + 8(A_N + R_L))}{J_F - 4(A_N + R_L)}} \quad (1)$$

where A_N and substomatal CO_2 concentration (C_i) were taken from gas exchange measurements at saturating light, whereas Γ^* (chloroplastic CO_2 compensation point in the absence of mitochondrial respiration) and R_L (respiration rate in the light) were estimated for both sites following the methodology described in Flexas et al. (2007*b*). The values of g_m obtained were used to convert A_N–C_i into A_N–C_c curves (where C_c is chloroplastic CO_2 concentration) using the equation $C_c = C_i - A_N/g_m$. Maximum carboxylation and photosynthetic electron transport capacities ($V_{c,max}$ and J_{max}, respectively) were calculated from the A_N–C_c curves, using the Rubisco kinetic constants and their temperature dependence described by Bernacchi et al. (2002). The Farquhar model was fitted to the data by applying iterative curve-fitting (minimum least-square difference) using the Solver tool of Microsoft Excel.

Morphological and anatomical measurements

After gas-exchange measurements, sections of 1 × 1 mm were cut between the main veins for anatomical measurements from the same leaves used for gas exchange. Leaf material was quickly fixed under vacuum with *p*-formaldehyde (2%) and glutaraldehyde (4%) in 0.1 M phosphate buffer (pH = 7.2) and post-fixed 1 h in 1% osmium tetroxide. Samples were dehydrated in (i) a graded ethanol series and (ii) propylene oxide and subsequently embedded in Embed-812 embedding medium (EMS, Hatfield, PA, USA). Semi-thin (0.8 µm) and ultrathin (90 nm) cross-sections were cut with an ultramicrotome (Reichert–Jung model Ultracut E). Semi-thin cross-sections were stained with 1% toluidine blue and viewed under a light microscope (Optika B-600TiFL, Optika Microscopes, Ponteranica, Italy). Ultrathin cross-sections were contrasted with uranyl acetate and lead citrate and viewed under a transmission electron microscope (H600, Hitachi, Japan). ImageJ software was further used to measure leaf anatomical characteristics from the micrographs. Light microscopy images were used to determine leaf thickness, mesophyll thickness between the two epidermal layers, number of palisade layers, fraction of the mesophyll tissue occupied by intercellular air spaces (f_{ias}), and mesophyll (S_m/S) and chloroplast (S_c/S) surface area facing intercellular air spaces per leaf area (Evans et al. 1994, Syvertsen et al. 1995, Tomás et al. 2013). All parameters were analysed in at least four different fields of view and in three different sections. Electron microscopy images were used to determine cell wall thickness (T_{cw}), cytoplasm thickness (T_{cyt}), chloroplast length (L_{chl}) and chloroplast thickness (T_{chl}) (Tomás et al. 2013). Three different sections and four to six different fields of view were used for measurements of each anatomical characteristic.

Leaf dry mass per area (LMA) was measured in 30 mature leaves sampled from 10 individuals per site (i.e., three leaves were randomly taken from each individual) as described above.

Mesophyll conductance modelled on the basis of anatomical characteristics

Leaf anatomical characteristics were used to estimate g_m as a composite conductance for within-leaf gas and liquid components, according to the one-dimensional gas diffusion model of

Niinemets and Reichstein (2003) as applied by Tosens et al. (2012):

$$g_m = \frac{1}{\frac{1}{g_{ias}} + \frac{R \cdot T_k}{H \cdot g_{liq}}} \quad (2)$$

where g_{ias} is the gas phase conductance inside the leaf from substomatal cavities to outer surface of cell walls, g_{liq} is the conductance in liquid and lipid phases from outer surface of cell walls to chloroplasts, R is the gas constant (Pa m^3 K^{-1} mol^{-1}), T_k is the absolute temperature (K), and H is the Henry's law constant for CO_2 (Pa m^3 mol^{-1}); g_m is defined as a gas-phase conductance, and thus $H/(RT_k)$, the dimensionless form of the Henry's law constant, is needed to convert g_{liq} to the corresponding gas-phase equivalent conductance (Niinemets and Reichstein 2003).

The intercellular gas-phase conductance (and the reciprocal term, r_{ias}) was obtained according to Niinemets and Reichstein (2003) as:

$$g_{ias} = \frac{1}{r_{ias}} = \frac{D_A \cdot f_{ias}}{\Delta L_{ias} \cdot \tau} \quad (3)$$

where ΔL_{ias} (m) is the average gas-phase thickness, τ is the diffusion path tortuosity (1.57 m m^{-1}, Syvertsen et al. 1995), D_A is the diffusivity of the CO_2 in the air ($1.51 \cdot 10^{-5}$ m^2 s^{-1} at 25 °C) and f_{ias} is the fraction of intercellular air spaces. ΔL_{ias} was taken as half the mesophyll thickness. Total liquid phase conductance (g_{liq}) from the outer surface of cell walls to the carboxylation sites in chloroplasts is the sum of serial conductances in the cell wall, plasmalemma and inside the cell (Tomás et al. 2013):

$$g_{liq} = \frac{S_m}{(r_{cw} + r_{pl} + r_{cel,tot}) \cdot S} \quad (4)$$

The conductance of the cell wall was calculated as previously described in Peguero-Pina et al. (2012). For the conductance of plasma membrane we used an estimate of 0.0035 m s^{-1} as previously suggested (Tosens et al. 2012). The conductance inside the cell was calculated following the methodology described in Tomás et al. (2013), considering two different pathways of CO_2 inside the cell: one for cell wall parts lined with chloroplasts and the other for interchloroplastial areas (Tholen et al. 2012).

Analysis of quantitative limitations of A_N

To separate the relative controls on A_N resulting from limited stomatal conductance (l_s), mesophyll diffusion (l_m) and limited photosynthetic capacity (l_b), we used the quantitative limitation analysis of Grassi and Magnani (2005) as applied in Tomás et al. (2013). Different fractional limitations, l_s, l_m and l_b ($l_s + l_m + l_b = 1$) were calculated as:

$$l_s = \frac{g_{tot}/g_s \cdot \partial A_N/\partial C_c}{g_{tot} + \partial A_N/\partial C_c} \quad (5)$$

$$l_m = \frac{g_{tot}/g_m \cdot \partial A_N/\partial C_c}{g_{tot} + \partial A_N/\partial C_c} \quad (6)$$

$$l_b = \frac{g_{tot}}{g_{tot} + \partial A_N/\partial C_c} \quad (7)$$

where g_s is the stomatal conductance to CO_2, g_m is the mesophyll conductance according to Harley et al. (1992, Eq. (1)), and g_{tot} is the total conductance to CO_2 from ambient air to chloroplasts (sum of the inverse CO_2 serial conductances g_s and g_m). The value of $\partial A_N/\partial C_c$ was calculated as the slope of A_N–C_c response curves over a C_c range of 50–100 µmol mol^{-1}. Quantitative limitations of photosynthesis were estimated for at least five different leaves of *Q. coccifera* at both the MED and the TEM site, and average estimates of the component photosynthetic limitations were calculated.

Leaf N, photosynthetic pigments and tocopherol analysis

Total leaf N concentration was determined in dried leaves from the MED and TEM sites using an Organic Elemental Analyzer (Flash EA 112, Thermo Fisher Scientific Inc., Waltham, MA, USA). Photosynthetic nitrogen use efficiency (PNUE) was calculated as the ratio between A_N and N concentration per leaf area.

For pigment extraction six replicates per site of four leaf discs (6 mm ø) were frozen in liquid N_2 and stored at −80 °C until use. Frozen samples were homogenised with a Tissue Tearor homogeniser (Model 395, Dremel, Mexico) in 1 ml of pure acetone solution buffered with $CaCO_3$. The extracts were centrifuged at 16,100*g* for 20 min, and supernatants were filtered through 0.2-µm PTFE filters (Teknokroma, Barcelona, Spain). The pigments were separated by HPLC on a reversed-phase C18 column (Waters Spherisorb ODS1, 4.6 × 250 mm, Milford, MA, USA) and detected with a photodiode array detector, following the method of García-Plazaola and Becerril (1999, 2001). Tocopherol detection and quantification were performed with a Waters 474 Scanning Fluorescence Detector (SRD) operating in series with a photodiode array detector following García-Plazaola and Becerril (1999, 2001). The relative de-epoxidation state of the violaxanthin-cycle pigments was estimated by the ratio $(A + Z)/(V + A + Z)$, abbreviated AZ/VAZ.

Statistical analyses and plasticity index

Data are expressed as mean ± standard error (SE). Student's *t*-test was used to compare the trait values between *Q. coccifera* leaves from the MED and TEM sites. One-way ANOVA was performed to compare the temporal changes in leaf area, LMA and stomatal pore area at different stages during the growing season at the MED site. Multiple comparisons were carried out among different stages for these variables using Tukey's post hoc honestly significant difference test. Furthermore, the plasticity index (PI) was calculated as the ratio between the range of variation for a parameter and its maximum value described (Valladares

et al. 2002*b*, García-Plazaola et al. 2008). This index has the advantage that changes in variables expressed in different units can be compared. All statistical analyses were carried out using SAS version 8.0 (SAS Institute, Cary, NC, USA).

Results

Site differences in stomatal characteristics

The aperture of the cuticular cup of *Q. coccifera* leaves from the MED site was significantly lower ($P < 0.05$) than that from the TEM site (Table 1). However, no significant differences ($P > 0.05$) were found among stomatal dimensions when epicuticular waxes were removed (Table 1). The distribution frequency of effective pore area in both sites revealed that, before wax removal, >40% of stomata at the MED site were smaller than 15 μm^2 (Figure 2). By contrast, >40% of stomata were >45 μm^2 for *Q. coccifera* leaves grown at the TEM site (Figure 2).

Temporal changes in foliage characteristics at the MED site

The cuticular wax deposition around stomatal pores found at the MED site was the consequence of a gradual process—in parallel with the increase in leaf area and LMA—since the onset of the growing season (Figure 3). The evolution of the different parameters indicates that leaf area reached the maximum value at Day 21 (*c.* 28 May), LMA at Day 29 (*c.* 5 June) and stomatal pore area at Day 42 (*c.* 18 June).

Site effects on foliage photosynthetic traits

Foliage photosynthetic measurements demonstrated that at 400 μmol CO_2 mol^{-1} air and saturating light, g_s was much higher at the TEM site (0.243 mol CO_2 m^{-2} s^{-1}) than at the MED site (0.143 mol CO_2 m^{-2} s^{-1}) (Table 2). Despite this, A_N was very similar at both sites, and therefore, intrinsic water use efficiency (iWUE = A_N/g_s) was lower at the TEM site (Table 2). The mesophyll conductance to CO_2 (g_m) and the substomatal CO_2 concentration (C_i) did not show statistically significant differences between the sites, whereas the chloroplastic CO_2 concentration (C_c) was higher at the MED site (Table 2). Parameterisation of the Farquhar et al. (1980) model of photosynthesis yielded statistically significant higher values for V_{c,max_Cc} and J_{max_Cc} at the TEM site, although the ratio J_{max_Cc}:V_{c,max_Cc} did not show differences between sites (Table 2). The electron transport rate estimated by chlorophyll fluorescence (J_{flu}) was also higher at the TEM site (Table 2).

Table 1. Area of the vent of the cuticular cups (stomatal pore area with waxes) and stomatal pore area without waxes of *Q. coccifera* leaves from the Mediterranean (MED) and temperate (TEM) sites. Data are mean ± SE. Different letters indicate statistically significant differences ($P < 0.05$) between sites.

Characteristic	Stomatal pore area (μm^2)	
	MED	TEM
With waxes	22 ± 2 b	54 ± 4 a
Without waxes	64 ± 2 a	61 ± 2 a

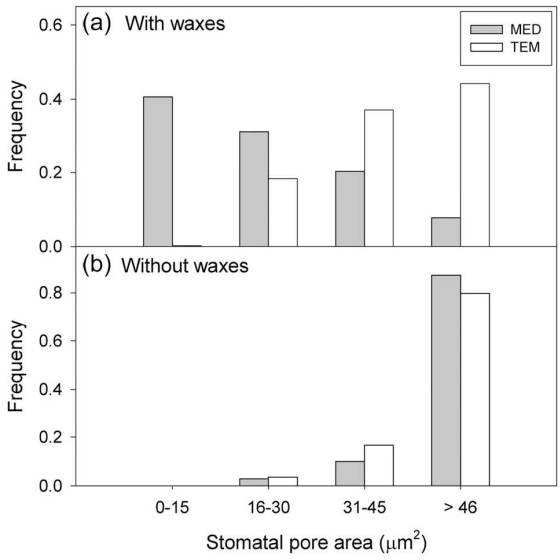

Figure 2. Frequency distribution of stomatal pore area (μm^2) for *Q. coccifera* leaves from the Mediterranean (MED) and temperate (TEM) sites with (a) and without (b) epicuticular waxes.

Differences in leaf morphological and anatomical characteristics between sites and implications for mesophyll conductance

Leaf thickness, LMA, total mesophyll thickness, spongy and palisade mesophyll thickness, number of palisade layers, S_m/S and S_c/S were higher at the MED site, whereas f_{ias} was higher at the TEM site (Table 3). However, no differences were found in S_c/S_m, T_{cw}, T_{cyt}, L_{chl} and T_{chl} between sites (Table 3).

The anatomical characteristics were further used to estimate different components of the CO_2 transfer conductances relative to total mesophyll conductance at both sites (see Materials and methods for details), resulting in a good correspondence between the estimates of g_m from anatomy (Eqs (2–4)) and from gas exchange and chlorophyll fluorescence measurements (Eq. (1), Table 2). In the case of the gas phase, the results demonstrated that *Q. coccifera* leaves grown at the TEM site showed higher values of g_{ias} than those at the MED site (Table 4), which can be attributed to a higher f_{ias} and a lower mesophyll thickness found at the TEM site (Table 3). Regarding the liquid phase, *Q. coccifera* leaves grown at the MED site showed higher values of g_{liq} than at the TEM site (Table 4), which can be attributed to a higher S_m/S value found at the MED site (Table 3). Consequently, the effects of g_{ias} and g_{liq} on g_m were opposite, explaining the absence of differences in the estimated value of g_m between sites (Table 4).

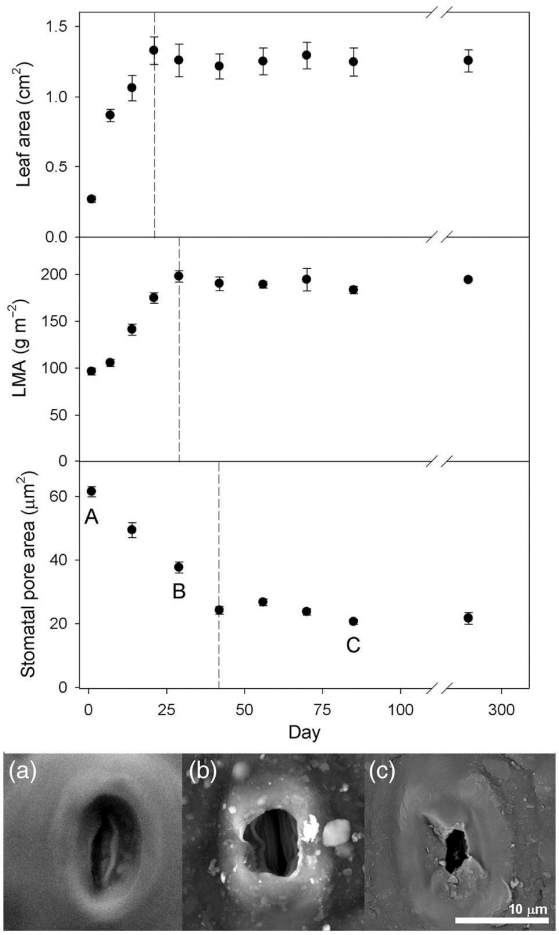

Figure 3. Evolution of the leaf area (cm^2), leaf mass area (LMA, g m^{-2}) and stomatal pore area (μm^2) for *Q. coccifera* leaves from the Mediterranean site (MED) since 7 May 2012 (Day 1, 1 week after bud bursting). Data are mean ± SE. Dashed lines indicate the end of the evolution of each measured parameter. Scanning electron micrographs correspond to different stages (a–c) of the evolution of the stomatal pore area due to cuticular wax covering during the growing season of 2012 at the MED site.

Site effects on foliage chemistry

The concentration of leaf N was higher at the MED site, in terms of both dry mass and leaf area (Table 5). However, because A_N values were similar between sites, TEM site plants showed higher photosynthetic nitrogen-use efficiency (PNUE) than MED site plants (Table 5). Pigment composition differed largely between leaves from the TEM and MED sites (Table 6). Thus, despite the higher LMA and thickness at the MED site, chlorophyll *a* content per unit of leaf area was higher at the TEM site. Chlorophyll *a*/*b* together with all the carotenoid to chlorophyll ratios also differed significantly, being higher for all parameters, except for the neoxanthin/chlorophyll ratio, at the MED site. According to the higher contents of protective carotenoids (violaxanthin-cycle total pool, lutein and β-carotene) at the MED site,

Table 2. Mean values for the photosynthetic parameters of *Q. coccifera* leaves from the Mediterranean (MED) and temperate (TEM) sites. Data are mean ± SE. Different letters indicate statistically significant differences ($P < 0.05$) between sites. A_N, net photosynthesis; g_s, stomatal conductance; iWUE, intrinsic water use efficiency; g_m, mesophyll conductance to CO_2; C_i, substomatal CO_2 concentration; C_c, chloroplastic CO_2 concentration; V_{c,max_Cc} and J_{max_Cc}, maximum velocity of Rubisco carboxylation and maximum capacity for electron transport; J_{flu}, electron transport rate estimated by chlorophyll fluorescence.

Parameter	MED	TEM
A_N (μmol CO_2 m^{-2} s^{-1})	10.2 ± 0.7 a	12.4 ± 1.3 a
g_s (mol CO_2 m^{-2} s^{-1})	0.143 ± 0.013 b	0.243 ± 0.011 a
iWUE (μmol CO_2 mol^{-1} H_2O)	46.8 ± 4.9 a	31.6 ± 2.5 b
g_m (mol CO_2 m^{-2} s^{-1})	0.050 ± 0.006 a	0.050 ± 0.007 a
C_i (μmmol CO_2 mol^{-1} air)	304 ± 5 b	312 ± 5 a
C_c (μmmol CO_2 mol^{-1} air)	120 ± 5 a	74 ± 3 b
V_{c,max_Cc} (μmol m^{-2} s^{-1})	178 ± 11 b	258 ± 12 a
J_{max_Cc} (μmol m^{-2} s^{-1})	228 ± 21 b	327 ± 17 a
J_{flu} (μmol m^{-2} s^{-1})	216 ± 12 b	363 ± 25 a
J_{max_Cc}:V_{c,max_Cc}	1.27 ± 0.06 a	1.33 ± 0.07 a

Table 3. Leaf mass area (LMA), leaf thickness, total mesophyll thickness, spongy and palisade mesophyll thickness, number of palisade layers, fraction of the mesophyll tissue occupied by the intercellular air spaces (f_{ias}), mesophyll surface area exposed to intercellular airspace (S_m/S), chloroplast surface area exposed to intercellular airspace (S_c/S), the ratio S_c/S_m, cell wall thickness (T_{cw}), cytoplasm thickness (T_{cyt}), chloroplast length (L_{chl}) and chloroplast thickness (T_{chl}) in *Q. coccifera* leaves from the Mediterranean (MED) and temperate (TEM) sites. Data are mean ± SE. Different letters indicate statistically significant differences ($P < 0.05$) between sites.

Parameter	MED	TEM
LMA (g m^{-2})	189.3 ± 6.5 a	138.8 ± 6.3 b
Leaf thickness (μm)	315 ± 8 a	231 ± 3 b
Total mesophyll thickness (μm)	278 ± 17 a	195 ± 6 b
Spongy mesophyll thickness (μm)	143 ± 5 a	113 ± 3 b
Palisade mesophyll thickness (μm)	135 ± 4 a	83 ± 3 b
Number of palisade layers	3	2
f_{ias}	0.08 ± 0.01 b	0.14 ± 0.02 a
S_m/S (m^2 m^{-2})	17.3 ± 2.6 a	13.3 ± 1.5 b
S_c/S (m^2 m^{-2})	9.9 ± 1.6 a	6.1 ± 0.9 b
S_c/S_m	0.57 ± 0.02 a	0.47 ± 0.08 a
T_{cw} (μm)	0.454 ± 0.026 a	0.446 ± 0.016 a
T_{cyt} (μm)	0.063 ± 0.026 a	0.087 ± 0.028 a
L_{chl} (μm)	5.13 ± 0.23 a	5.10 ± 0.17 a
T_{chl} (μm)	2.43 ± 0.13 a	2.27 ± 0.09 a

Table 4. CO_2 transfer conductances across the intercellular air space (g_{ias}, m s^{-1}), the liquid phase (g_{liq}, m s^{-1}), and the mesophyll conductance for CO_2 (g_m, mol m^{-2} s^{-1}) calculated from anatomical measurements in *Q. coccifera* leaves from the Mediterranean (MED) and temperate (TEM) sites. Data are mean ± SE. Different letters indicate statistically significant differences ($P < 0.05$) between sites.

Parameter	MED	TEM
g_{ias} (m s^{-1})	0.0056 ± 0.0007 b	0.0137 ± 0.0010 a
g_{liq} (m s^{-1})	0.0020 ± 0.0002 a	0.0015 ± 0.0001 b
g_m (mol m^{-2} s^{-1})	0.057 ± 0.009 a	0.055 ± 0.008 a

Table 5. Leaf N content per dry mass and per area and photosynthetic nitrogen use efficiency (PNUE) for *Q. coccifera* leaves from the Mediterranean (MED) and temperate (TEM) sites. Data are mean ± SE. Different letters indicate statistically significant differences ($P < 0.05$) between sites.

Parameter	MED	TEM
N content per dry mass (%)	1.37 ± 0.05 a	1.21 ± 0.04 b
N content per area (mol m^{-2})	0.18 ± 0.02 a	0.12 ± 0.01 b
PNUE (μmol mol^{-1} s^{-1})	55.3 ± 4.0 b	103.3 ± 10.9 a

Table 6. Photosynthetic pigment and tocopherol contents for *Q. coccifera* leaves expressed per leaf area or per total chlorophyll content from the Mediterranean (MED) and temperate (TEM) sites. Data are mean ± SE. Different letters indicate statistically significant differences ($P < 0.05$) between sites. Chl, chlorophyll; Neo, neoxanthin; Lut, lutein; β-Car, β-carotene; α-Toc, α-tocopherol; VAZ, violaxanthin-cycle total pool; AZ/VAZ, de-epoxidation state of the violaxanthin-cycle pigments.

Parameter	MED	TEM
Chl *a* (μmol m^{-2})	318.2 ± 20.6 a	393.1 ± 52.0 a
Chl *b* (μmol m^{-2})	86.6 ± 6.8 a	113.4 ± 13.8 a
Chl *a*/*b*	3.7 ± 0.1 a	3.4 ± 0.1 b
Neo/Chl (mmol mol^{-1})	37.7 ± 0.6 b	40.2 ± 0.7 a
Lut/Chl (mmol mol^{-1})	126.8 ± 2.8 a	106.6 ± 2.2 b
VAZ/Chl (mmol mol^{-1})	88.1 ± 5.3 a	64.5 ± 2.4 b
AZ/VAZ	0.384 ± 0.048 a	0.123 ± 0.008 b
β-Car/Chl (mmol mol^{-1})	111.2 ± 0.9 a	103.4 ± 1.5 b
α-Toc/Chl (mmol mol^{-1})	1132.0 ± 71.3 a	525.5 ± 57.2 b

the α-tocopherol to chlorophyll ratio and the de-epoxidation index of the xanthophyll cycle (AZ/VAZ) were also two- to threefold higher at the MED site.

Discussion

Mediterranean climate constitutes a highly stressful environment for plants that has triggered a number of unique structural and physiological adaptations (Corcuera et al. 2002, Flexas et al. 2014, Niinemets and Keenan 2014). While such adaptation is highly beneficial in improving water use efficiency, constitutive expression of many of these traits, such as cryptic stomata, would reduce carbon gain when water becomes more available. The present study has demonstrated the existence of a plastic response in functional attributes of *Q. coccifera* leaves (see Table S1 available as Supplementary Data at *Tree Physiology* Online) to changes in environmental conditions (i.e., Q_{int} and VPD) during growth, which agrees with previous studies on phenotypic responses of *Q. coccifera* saplings (Balaguer et al. 2001, Valladares et al. 2002*a*, 2005). The climatic conditions that demarcate the TEM and MED sites, both in terms of Q_{int} and VPD (Figure 1), can be considered as the extremes of the Atlantic–Mediterranean gradient along which *Q. coccifera* is distributed (Castro-Díez et al. 1997).

The individual encryption of stomata by epicuticular waxes in *Q. coccifera* leaves grown at the MED site strongly reduced the area of the vent of the cuticular cup when compared with the TEM site (Table 1 and Figure 2). It should be noted that the process of stomatal wax covering at the MED site finished in late spring (Figure 3), while VPD values started to reach the maximum values registered during summer (Figure 1). Interestingly, both sites only differed in the degree of encryption, being identical in the dimensions of stomatal pore area after wax removal (Table 1 and Figure 2), as previously showed by Roth-Nebelsick et al. (2013) for this species. In this regard, the epicuticular wax deposition found at the MED site implied a sharp decrease in g_s (*c.* 0.6 times) with respect to the TEM site (Table 2), which constitutes an effective mechanism for reducing water losses while keeping stomata open.

In spite of this, maximum water losses by transpiration (E) during midsummer would be *c.* 2 times higher here than at the TEM site (data not shown), due to the higher VPD found at the MED site (Figure 1). This fact reveals that this xeromorphic trait in *Q. coccifera* can only partially mitigate the extreme water vapour gradient between the mesophyll and the surrounding atmosphere found at the MED site. Consequently, water use efficiency (WUE)—expressed as the ratio between A_N and E—is expected to be *c.* 2 times higher at the TEM site, but iWUE is instead larger at the MED site, as commonly found in plants of dry habitats (Field et al. 1983). These facts indicate that water losses per unit of carbon uptake for *Q. coccifera* living at the most arid extreme of its climatic gradient (the MED site) cannot be diminished to the level of the TEM site, even with such a large reduction in stomatal pore size by epicuticular wax deposition. In order to achieve WUE values similar to the TEM site, g_s at the MED site should be ~0.1 mol H_2O m^{-2} s^{-1}, which would imply a reduction in A_N of *c.* threefold, as reported by Peguero-Pina et al. (2009) for this species growing under Mediterranean conditions.

Contrary to that suggested by Roth-Nebelsick et al. (2013) from modelled data, the absence of such extra resistance in stomata of *Q. coccifera* leaves grown at the TEM site did not imply an increased ability to take up carbon (Table 2). Therefore, the existence of adjustments in other traits influencing net CO_2 assimilation should be considered. One of the key traits that determine the maximum photosynthetic rate is g_m, which often is the most significant limitation on photosynthesis, especially in evergreens (Flexas et al. 2012, Galmés et al. 2014, Niinemets and Keenan 2014). In this way, the analysis of the quantitative limitations of photosynthesis revealed that A_N in *Q. coccifera* was mainly limited by g_m both at the MED (65%) and at the TEM site (76%) (data not shown). Moreover, contrary to g_s, g_m in *Q. coccifera* did not exhibit a plastic response to changes in growth environmental conditions (Table 2). Therefore, the lack of a plastic response in the most limiting factor to net CO_2 assimilation in *Q. coccifera*—i.e., mesophyll conductance—may be one of the causes that explains the lack of differences in A_N between the sites.

Besides the sharp increase in g_s, several anatomical leaf traits in *Q. coccifera* also showed a plastic response to changes in

growth environmental conditions, especially mesophyll thickness, f_{ias}, S_m/S and S_c/S (Table 3 and Figure 4). Recently, several studies have quantitatively determined the importance of these leaf anatomical traits in determining the variability in g_m and photosynthetic capacity among species (see Tomás et al. 2013 and references therein). According to the one-dimensional gas diffusion model used to estimate g_m from leaf anatomical characteristics (Niinemets and Reichstein 2003, Tosens et al. 2012), the higher g_{ias} (due to higher f_{ias} and lower mesophyll thickness) counteracted the lower g_{liq} (due to lower S_m/S) in *Q. coccifera* leaves grown at the TEM site when compared with the MED site (Table 4). Consequently, this trade-off resulted in the same estimated value of g_m for both sites (Table 4) which, as stated above, may be one of the causal factors explaining the lack of differences in net CO_2 assimilation. On the other hand, no differences were found in ultrastructural anatomical traits influencing g_m, such as cell wall and chloroplast thickness (Table 3). Recently, Peguero-Pina et al. (2015) have found changes in these anatomical traits in *Abies pinsapo* in response to changes in light environment that strongly determined changes in g_m. However, it should be noted that the light gradients found by Peguero-Pina et al. (2015) were much higher than the differences in Q_{int} found between the MED and TEM sites of *Q. coccifera*.

The changes in morphological and anatomical leaf traits found in the present study agree with those previously found in other studies in response to growth irradiance in this (Balaguer et al. 2001, Valladares et al. 2002*a*) and other species (Oguchi et al. 2003, Terashima et al. 2011). These previous studies also found changes at biochemical level in response to changes in growth irradiance that point in the same direction as those found in the present study (Table 5). In this regard, the lower N at the TEM site could constitute an additional limiting factor for net CO_2 assimilation. On the other hand, the chlorophyll *a*/*b* ratio was lower at the TEM site (Table 6), suggesting a larger antenna size (Esteban et al. 2015). This conclusion was also supported by the higher content of neoxanthin, a carotenoid that is mostly bound to the outer trimeric antenna proteins (Morosinotto and Bassi 2012). These observations are indicative of a larger allocation of N to light harvesting proteins in the less stressful TEM site.

The combination of lower g_s and higher growth irradiance at the MED site can be potentially harmful for the maintenance of photosynthetic function. In fact, comparison of pigment composition between both sites showed that at the MED site the structure of photosynthetic apparatus had a greater capacity for dissipating the excess of light energy than at the TEM site, being characterised by a higher content of protective carotenoids (β-carotene, lutein and violaxanthin-cycle total pool) (Esteban et al. 2015). Furthermore, this plastic photo-protective response was maximised for the content of lipophilic antioxidants (α-tocopherol) and AZ/VAZ. The exceptional relevance of these lipophilic photo-protective mechanisms has been observed in this and other Mediterranean evergreens in response to climatic

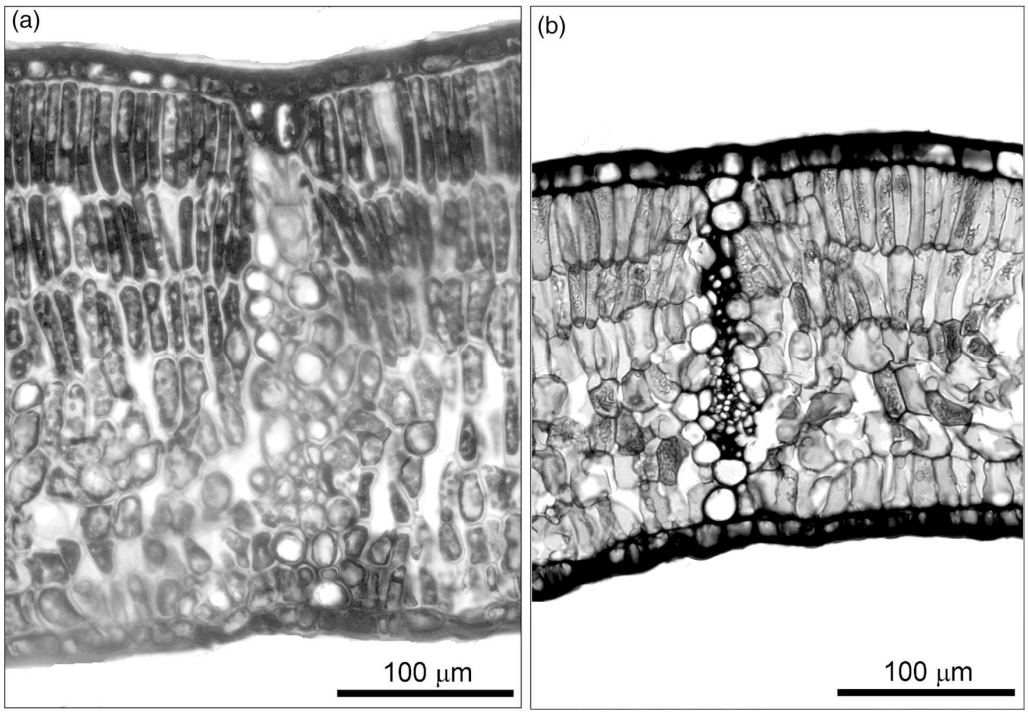

Figure 4. Transverse section of the mesophyll of *Q. coccifera* from the Mediterranean (MED; a) and temperate (TEM; b) sites.

extremes (García-Plazaola et al. 2003, 2008, Camarero et al. 2012).

In agreement with pigment data, photosynthesis on a mass basis was clearly higher at the TEM site (0.089 µmol CO_2 g^{-1} s^{-1}) than at MED site (0.054 µmol CO_2 g^{-1} s^{-1}). This is a direct consequence of the reduction in LMA found at the TEM site (Table 3) and is in line with predictions of leaf economics spectrum (Wright et al. 2004). Previously, such a within-species shift within the economics spectrum has been developed for congeneric *Q. ilex* across its bioclimatic range (Niinemets 2015). Moreover, PNUE was also higher at the TEM site (Table 5), indicating that leaves developed under the environmental conditions of the TEM site can reach similar values of A_N with lower nitrogen investment that those leaves grown at the most arid extreme of its climatic gradient (MED). In this regard, it can be discussed how long the higher nitrogen content on an area basis associated with a higher thickness at the MED site has a direct counterpart in terms of A_N. So-called 'resource substitution' postulates the existence of a trade-off between stomatal conductance and foliar N that has been linked to changes in photosynthetic rate (Buckley and Roberts 2006, Taylor and Eamus 2008). According to this, similar A_N values might be reached at the expense of a higher N investment, compensating for the lower g_s at the MED site, as leaf nitrogen concentration is often correlated with leaf photosynthetic rates (see Meziane and Shipley 2001 and references therein). On the other hand, as stated above, the same values of A_N for different g_s in both sites may be the consequence of a similar g_m, which can be explained by the higher S_m/S associated with the higher mesophyll thickness found at the MED site. Previous studies have already related the increase in leaf thickness in *Q. coccifera* to xeric habitats (Balaguer et al. 2001, Valladares et al. 2002*a*). Another factor directly related to leaf construction cost is the higher amount of epicuticular wax production associated with stomatal covering at the MED site (Villar and Merino 2001), which has been associated with a conservative leaf economics spectrum strategy (Mason and Donovan 2015).

Conclusions

From an ecological perspective, *Q. coccifera* has been considered the main component of the climax vegetation under climatic conditions that correspond to the MED site, while its presence is assumed to be merely marginal in areas under climates similar to that defining the TEM site (Castro-Díez et al. 1997). This seems to be contradictory to the better physiological performance in terms of WUE, PNUE and photosynthesis on a mass basis of *Q. coccifera* found at the TEM site. A lower investment in N and dry matter for a given leaf area at the TEM site would constitute an advantage in terms of leaf construction costs (Merino et al. 1982) A possible explanation for this apparent paradox is that *Q. coccifera* can compete successfully in stressful environments such as the MED site due to its ability to withstand long and intense drought periods (i) without signs of irreversible damage in either the apoplast or the symplast (Vilagrosa et al. 2010), (ii) through a high resistance to drought-induced cavitation (Vilagrosa et al. 2003), and (iii) through the exceptional capacity for activation of drought-mediated photo-protective mechanisms (García-Plazaola et al. 2008, Peguero-Pina et al. 2009). The results found in the present study suggest that *Q. coccifera*, a Mediterranean evergreen oak species, does not always use the main resources (water and nutrients) at leaf level as efficiently as possible. In this, it would be interesting to consider the existence of this adaptation process at the whole-plant level, which is a matter that deserves further investigation.

Overall, in the case study reported here, the different patterns of resource use (in particular N) together with functional plasticity are not able to overcome the morpho-functional constraints that limit photosynthetic activity, even under potentially favourable conditions. This limitation in the expression of phenotypic plasticity probably represents an example of genetic canalisation (Valladares et al. 2002*a*), a process frequent in unstable and unpredictable environments such as the Mediterranean ecosystems.

Supplementary data

Supplementary data for this article are available at *Tree Physiology* Online.

Acknowledgments

The authors are grateful to José Almandoz and the people of Jardín Botánico de Iturrarán for their help in the maintenance of plant material.

Conflict of interest

None declared.

Funding

Financial support is acknowledged from Gobierno de Aragón (H38 research group) and by the Spanish Ministry of Economy and Competitiveness (MINECO) (Research grant BFU 2010-15021 co-funded by the ERDF-FEDER). The work of D.S.-K. is supported by a DOC INIA contract co-funded by the Spanish National Institute for Agriculture and Food Research and Technology (INIA) and the European Social Fund (ESF). Financial support to B.F.-M. is acknowledged from the Research Vicerrectorate (UPV/EHU) and the EU (Marie Curie Action FP7-PEOPLE-2012-IEF 328370 'MELISSA'). J.F. acknowledges support from Plan Nacional, Spain (project CTM2014-53902-C2-1-P).

References

Balaguer L, Martínez-Ferri E, Valladares F, Pérez-Corona ME, Baquedano FJ, Castillo FJ, Manrique E (2001) Population divergence in the plasticity of the response of *Quercus coccifera* to the light environment. Funct Ecol 15:124–135.

Bernacchi CJ, Portis AR, Nakano H, von Caemmerer S, Long SP (2002) Temperature response of mesophyll conductance. Implications for the determination of Rubisco enzyme kinetics and for limitations to photosynthesis in vivo. Plant Physiol 130:1992–1998.

Buckley TN, Roberts DW (2006) How should leaf area, sapwood area and stomatal conductance vary with tree height to maximize growth? Tree Physiol 26:145–157.

Camarero JJ, Olano JM, Arroyo SJ, Fernández-Marín B, Becerril JM, García-Plazaola JI (2012) Photoprotection mechanisms in *Quercus ilex* under contrasting climatic conditions. Flora 207:557–564.

Castro-Díez P, Navarro J (2007) Water relations of seedlings of three *Quercus* species: variations across and within species grown in contrasting light and water regimes. Tree Physiol 27:1011–1018.

Castro-Díez P, Villar-Salvador P, Pérez-Rontomé C, Maestro-Martínez M, Montserrat-Martí G (1997) Leaf morphology and leaf chemical composition in three *Quercus* (Fagaceae) species along a rainfall gradient in NE Spain. Trees 11:127–134.

Cescatti A, Zorer R (2003) Structural acclimation and radiation regime of silver fir (*Abies alba* Mill.) shoots along a light gradient. Plant Cell Environ 26:429–442.

Corcuera L, Camarero JJ, Gil-Pelegrín E (2002) Functional groups in *Quercus* species derived from the analysis of pressure–volume curves. Trees 16:465–472.

Dow GJ, Bergmann DC, Berry JA (2014) An integrated model of stomatal development and leaf physiology. New Phytol 201: 1218–1226.

Esteban R, Barrutia O, Artetxe U, Fernández-Marín B, Hernández A, García-Plazaola JI (2015) Internal and external factors affecting photosynthetic pigment composition in plants: a meta-analytical approach. New Phytol 206:268–280.

Evans JR, von Caemmerer S, Setchell BA, Hudson GS (1994) The relationship between CO_2 transfer conductance and leaf anatomy in transgenic tobacco with a reduced content of Rubisco. Aust J Plant Physiol 21:475–495.

Farquhar GD, von Caemmerer S, Berry JA (1980) A biochemical model of photosynthetic CO_2 assimilation in leaves of C_3 species. Planta 149:78–90.

Field C, Merino J, Mooney HA (1983) Compromises between water-use efficiency and nitrogen-use efficiency in five species of California evergreens. Oecologia 60:384–389.

Flexas J, Díaz-Espejo A, Berry JA, Galmés J, Cifre J, Kaldenhoff R, Medrano H, Ribas-Carbó M (2007*a*) Analysis of leakage in IRGA's leaf chambers of open gas exchange systems: quantification and its effects in photosynthesis parameterization. J Exp Bot 58:1533–1543.

Flexas J, Ortuño MF, Ribas-Carbó M, Díaz-Espejo A, Flórez-Sarasa ID, Medrano H (2007*b*) Mesophyll conductance to CO_2 in *Arabidopsis thaliana*. New Phytol 175:501–511.

Flexas J, Barbour MM, Brendel O et al. (2012) Mesophyll diffusion conductance to CO_2: an unappreciated central player in photosynthesis. Plant Sci 193–194:70–84.

Flexas J, Díaz-Espejo A, Gago J, Gallé A, Galmés J, Gulías J, Medrano H (2014) Photosynthetic limitations in Mediterranean plants: a review. Environ Exp Bot 103:12–23.

Franks PJ, Beerling DJ (2009) Maximum leaf conductance driven by CO_2 effects on stomatal size and density over geologic time. Proc Natl Acad Sci USA 106:10343–10347.

Galmés J, Andralojc PJ, Kapralov MV, Flexas J, Keys AJ, Molins A, Parry MAJ, Conesa MÀ (2014) Environmentally driven evolution of Rubisco and improved photosynthesis and growth within the C_3 genus *Limonium* (Plumbaginaceae). New Phytol 203:989–999.

García-Plazaola JI, Becerril JM (1999) A rapid high-performance liquid chromatography method to measure lipophilic antioxidants in stressed plants: simultaneous determination of carotenoids and tocopherols. Phytochem Anal 10:307–313.

García-Plazaola JI, Becerril JM (2001) Seasonal changes in photosynthetic pigments and antioxidants in beech (*Fagus sylvatica*) in a Mediterranean climate: implications for tree decline diagnosis. Aust J Plant Physiol 28:225–232.

García-Plazaola JI, Olano JM, Hernández A, Becerril JM (2003) Photoprotection in evergreen Mediterranean plants during sudden periods of intense cold weather. Trees 17:285–291.

García-Plazaola JI, Esteban R, Hormaetxe K, Fernández-Marín B, Becerril JM (2008) Photoprotective responses of Mediterranean and Atlantic trees to the extreme heat-wave of summer 2003 in Southwestern Europe. Trees 22:385–392.

Genty B, Briantais JM, Baker NR (1989) The relationship between the quantum yield of photosynthetic electron transport and quenching of chlorophyll fluorescence. Biochim Biophys Acta 990:87–92.

Gimeno TE, Pias B, Lemos-Filho JP, Valladares F (2009) Plasticity and stress tolerance override local adaptation in the responses of Mediterranean holm oak seedlings to drought and cold. Tree Physiol 29:87–98.

Grassi G, Magnani F (2005) Stomatal, mesophyll conductance and biochemical limitations to photosynthesis as affected by drought and leaf ontogeny in ash and oak trees. Plant Cell Environ 28:834–849.

Harley PC, Loreto F, Di Marco G, Sharkey TD (1992) Theoretical considerations when estimating the mesophyll conductance to CO_2 flux by analysis of the response of photosynthesis to CO_2. Plant Physiol 98:1429–1436.

Hauke V, Schreiber L (1998) Ontogenetic and seasonal development of wax composition and cuticular transpiration of ivy (*Hedera helix* L.) sun and shade leaves. Planta 207:67–75.

Himrane H, Camarero JJ, Gil-Pelegrín E (2004) Morphological and ecophysiological variation of the hybrid oak *Quercus subpyrenaica* (*Q. faginea* × *Q. pubescens*). Trees 18:566–575.

Jetter R, Schäffer S, Riederer M (2000) Leaf cuticular waxes are arranged in chemically and mechanically distinct layers: evidence from *Prunus laurocerasus* L. Plant Cell Environ 23:619–628.

Kaiser H (2009) The relation between stomatal aperture and gas exchange under consideration of pore geometry and diffusional resistance in the mesophyll. Plant Cell Environ 32:1091–1098.

Krall JP, Edwards GE (1992) Relationship between photosystem II activity and CO_2 fixation in leaves. Physiol Plant 86:180–187.

Mason CM, Donovan LA (2015) Does investment in leaf defenses drive changes in leaf economic strategy? A focus on whole-plant ontogeny. Oecologia 177:1053–1066.

Merino J, Field C, Mooney HA (1982) Construction and maintenance costs of Mediterranean-climate evergreen and deciduous leaves. I. Growth and CO_2 exchange analysis. Oecologia 53:208–213.

Meziane D, Shipley B (2001) Direct and indirect relationships between specific leaf area, leaf nitrogen and leaf gas exchange. Effects of irradiance and nutrient supply. Ann Bot 88:915–927.

Morosinotto T, Bassi R (2012) Assembly of light harvesting pigment-protein complexes in photosynthetic eukaryotes. In: Eaton-Rye JJ, Tripathy BC, Sharkey TD (eds) Photosynthesis: plastid biology, energy conversion and carbon assimilation. Advances in Photosynthesis and Respiration 34. Springer, Dordrecht, pp 113–126.

Niinemets Ü (2015) Is there a species spectrum within the world-wide leaf economics spectrum? Major variations in leaf functional traits in the Mediterranean sclerophyll *Quercus ilex*. New Phytol 205:79–96.

Niinemets Ü, Keenan T (2014) Photosynthetic responses to stress in Mediterranean evergreens: mechanisms and models. Environ Exp Bot 103:24–41.

Niinemets Ü, Reichstein M (2003) Controls on the emission of plant volatiles through stomata: a sensitivity analysis. J Geophys Res 108:4211. doi:10.1029/2002JD002626.

Niinemets Ü, Díaz-Espejo A, Flexas J, Galmés J, Warren CR (2009) Role of mesophyll diffusion conductance in constraining potential photosynthetic productivity in the field. J Exp Bot 60:2249–2270.

Niinemets Ü, Flexas J, Peñuelas J (2011) Evergreens favored by higher responsiveness to increased CO_2. Trends Ecol Evol 26:136–142.

Oguchi R, Hikosaka K, Hirose T (2003) Does the photosynthetic light-acclimation need change in leaf anatomy? Plant Cell Environ 26:505–512.

Ozturk M, Dogan Y, Sakcali MS, Doulis A, Karam F (2010) Ecophysiological responses of some maquis (*Ceratonia siliqua* L., *Olea oleaster* Hoffm. & Link, *Pistacia lentiscus* and *Quercus coccifera* L.) plant species to drought in the east Mediterranean ecosystem. J Environ Biol 31:233–45.

Pallardy SG, Kozlowski TT (1980) Cuticle development in the stomatal region of *Populus* clones. New Phytol 85:363–368.

Peguero-Pina JJ, Morales F, Flexas J, Gil-Pelegrín E, Moya I (2008) Photochemistry, remotely sensed physiological reflectance index and de-epoxidation state of the xanthophyll cycle in *Quercus coccifera* under intense drought. Oecologia 156:1–11.

Peguero-Pina JJ, Sancho-Knapik D, Morales F, Flexas J, Gil-Pelegrín E (2009) Differential photosynthetic performance and photoprotection mechanisms of three Mediterranean evergreen oaks under severe drought stress. Funct Plant Biol 36:453–462.

Peguero-Pina JJ, Flexas J, Galmés J, Niinemets Ü, Sancho-Knapik D, Barredo G, Villarroya D, Gil-Pelegrín E (2012) Leaf anatomical properties in relation to differences in mesophyll conductance to CO_2 and photosynthesis in two related Mediterranean *Abies* species. Plant Cell Environ 35:2121–2129.

Peguero-Pina JJ, Sancho-Knapik D, Barrón E, Camarero JJ, Vilagrosa A, Gil-Pelegrín E (2014) Morphological and physiological divergences within *Quercus ilex* support the existence of different ecotypes depending on climatic dryness. Ann Bot 114:301–313.

Peguero-Pina JJ, Sancho-Knapik D, Flexas J, Galmés J, Niinemets Ü, Gil-Pelegrín E (2016) Light acclimation of photosynthesis in two closely related firs (*Abies pinsapo* Boiss. and *Abies alba* Mill.): the role of leaf anatomy and mesophyll conductance to CO_2. Tree Physiol 36:300–310.

Ramírez-Valiente JA, Sánchez-Gómez D, Aranda I, Valladares F (2010) Phenotypic plasticity and local adaptation in leaf ecophysiological traits of 13 contrasting cork oak populations under different water availabilities. Tree Physiol 30:618–627.

Roth-Nebelsick A, Fernández V, Peguero-Pina JJ, Sancho-Knapik D, Gil-Pelegrín E (2013) Stomatal encryption by epicuticular waxes as a plastic trait modifying gas exchange in a Mediterranean evergreen species (*Quercus coccifera* L.). Plant Cell Environ 36:579–589.

Rubio de Casas R, Vargas P, Pérez-Corona E, Manrique E, Quintana JR, García-Verdugo C, Balaguer L (2007) Field patterns of leaf plasticity in adults of the long-lived evergreen *Quercus coccifera*. Ann Bot 100:325–334.

Rundel PW, Jarrell WM (1989) Water in the environment. In: Pearcy RW, Ehleringer J, Mooney HA, Rundel PW (eds) Plant physiological ecology: field methods and instrumentation. Chapman and Hall, London, pp 29–56.

Sakcali MS, Ozturk M (2004) Eco-physiological behaviour of some Mediterranean plants as suitable candidates for reclamation of degraded areas. J Arid Environ 57:141–153.

Syvertsen JP, Lloyd J, McConchie C, Kriedemann PE, Farquhar GD (1995) On the relationship between leaf anatomy and CO_2 diffusion through the mesophyll of hypostomatous leaves. Plant Cell Environ 18:149–157.

Taylor D, Eamus D (2008) Coordinating leaf functional traits with branch hydraulic conductivity: resource substitution and implications for carbon gain. Tree Physiol 28:1169–1177.

Terashima I, Hanba YT, Tholen D, Niinemets U (2011) Leaf functional anatomy in relation to photosynthesis. Plant Physiol 155:108–116.

Tholen D, Ethier G, Genty B, Pepin S, Zhu XG (2012) Variable mesophyll conductance revisited: theoretical background and experimental implications. Plant Cell Environ 35:2087–2103.

Tomás M, Flexas J, Copolovici L et al. (2013) Importance of leaf anatomy in determining mesophyll diffusion conductance to CO_2 across species: quantitative limitations and scaling up by models. J Exp Bot 64:2269–2281.

Tosens T, Niinemets Ü, Vislap V, Eichelmann H, Castro-Díez P (2012) Developmental changes in mesophyll diffusion conductance and photosynthetic capacity under different light and water availabilities in *Populus tremula*: how structure constrains function. Plant Cell Environ 35:839–856.

Valentini R, Epron D, De Angelis P, Matteucci G, Dreyer E (1995) *In situ* estimation of net CO_2 assimilation, photosynthetic electron flow and photorespiration in Turkey oak (*Q. cerris* L.) leaves: diurnal cycles under different levels of water supply. Plant Cell Environ 18:631–640.

Valladares F, Balaguer L, Martínez-Ferri E, Pérez-Corona E, Manrique E (2002*a*) Plasticity, instability and canalization: is the phenotypic variation in seedlings of sclerophyll oaks consistent with the environmental unpredictability of Mediterranean ecosystems? New Phytol 156:457–467.

Valladares F, Chico JM, Aranda I, Balaguer L, Dizengremel P, Manrique E, Dreyer E (2002*b*) The greater seedling high-light tolerance of *Quercus robur* over *Fagus sylvatica* is linked to a greater physiological plasticity. Trees 16:395–403.

Valladares F, Dobarro I, Sánchez-Gómez D, Pearcy RW (2005) Photoinhibition and drought in Mediterranean woody saplings: scaling effects and interactions in sun and shade phenotypes. J Exp Bot 56:483–494.

Vilagrosa A (2002) Estrategias de resistencia al déficit hídrico en *Pistacia lentiscus* L. y *Quercus coccifera* L. Implicaciones en la repoblación forestal. PhD thesis. University of Alicante, Spain.

Vilagrosa A, Bellot J, Vallejo VR, Gil-Pelegrín E (2003) Cavitation, stomatal conductance, and leaf dieback in seedlings of two co-occurring Mediterranean shrubs during an intense drought. J Exp Bot 54:2015–2024.

Vilagrosa A, Morales F, Abadía A, Bellot J, Cochard H, Gil-Pelegrín E (2010) Are symplast tolerance to intense drought conditions and xylem vulnerability to cavitation coordinated? An integrated analysis of photosynthetic, hydraulic and leaf level processes in two Mediterranean drought-resistant species. Environ Exp Bot 69:233–242.

Villar R, Merino J (2001) Comparison of leaf construction costs in woody species with differing leaf life-spans in contrasting ecosystems. New Phytol 151:213–226.

Wright IJ, Reich PB, Westoby M et al. (2004) The worldwide leaf economics spectrum. Nature 428:821–827.

3. RESUMEN

3.1. OBJETIVOS DE LA INVESTIGACIÓN

Con base en lo expuesto en la introducción, el objetivo general de la presente tesis doctoral es estudiar una serie de factores morfológicos y anatómicos que regulan el intercambio de gases en especies mediterráneas del género *Quercus*. Por consiguiente, los objetivos específicos de la investigación son los que se enumeran a continuación:

1. Realizar un estudio comparado de los parámetros anatómicos, morfológicos y fotosintéticos en 7 especies perennifolias mediterráneas de *Quercus* de Europa (*Q. coccifera*, *Q. ilex* subp. *rotundifolia*, *Q. ilex* subsp. *ilex* y *Q. suber*) y Norteamérica (*Q. agrifolia*, *Q. chrysolepis* y *Q. wislizeni*) y en 2 especies caducifolias de *Quercus* de Europa (*Q. robur* y *Q. faginea*) para determinar la existencia de mecanismos compensatorios anatómicos y/o bioquímicos en las especies perennifolias.

2. Realizar un estudio comparado de los parámetros anatómicos, morfológicos y fotosintéticos en 4 procedencias de Q. *ilex subsp. ilex* (Gerona, Veneto, Lazio y Sardinia) y 3 de *Q. ilex subsp. rotundifol*ia (Cazorla, Extremadura y Soria) para determinar el grado de variabilidad intra-específica de estos parámetros.

3. Realizar un estudio comparado de los parámetros anatómicos, morfológicos y fotosintéticos en *Q. coccifera* creciendo bajo condiciones mediterráneas (Zaragoza) y oceánicas (Gipuzkoa) para determinar el grado de plasticidad fenotípica de estos parámetros en una especie mediterránea perennifolia de *Quercus*.

3.2. APORTACIONES DEL DOCTORANDO

Las contribuciones del doctorando en los trabajos para el estudio de factores morfológicos y anatómicos que regulan el intercambio de gases en especies mediterráneas del género *Quercus* se establecen en lo siguiente:

Diseño y planificación de cada uno de los trabajos que componen la presente tesis doctoral.

- Medidas simultáneas de intercambio de gases y fluorescencia de clorofila utilizando un sistema portátil de medida de intercambio de gases.
- Cálculo de la conductancia del mesófilo (g_m) a partir de las medidas simultáneas de intercambio de gases y fluorescencia, siguiendo la metodología descrita por Harley et al. (1992)
- Toma de medidas morfológicas y anatómicas en secciones foliares de 1 mm x 1 mm obtenidas de las mismas hojas empleadas para las medidas de intercambio de gases.
- Modelización de la conductancia del mesófilo con base en parámetros anatómicos.

Además, el doctorando ha aportado la importante tarea de servir de nexo de unión entre los diferentes grupos implicados en este trabajo (Unidad de Recursos Forestales, Centro de Investigación y Tecnología Agroalimentaria del gobierno de Aragón, Instituto Agroalimentario de Aragón, Departamento de Biología, Universidad de las islas Baleares, Departamento de Sistemas Físicos, Químicos y Naturales, Universidad Pablo Olavide, Instituto de Ciencias Agrícolas y Ambientales, Universidad de Ciencias de la Vida de Estonia, Instituto de Recursos Naturales y Agrobiología de Sevilla, Instituto de Botánica y Centro de Biociencias Moleculares de Innsbruck, Departamento de Biología Vegetal y Ecología, Universidad del País Vasco). Fruto del estudio de las diferentes temáticas implicadas y de su contacto directo con los grupos que las desarrollan, el doctorando ha aportado una perspectiva interdisciplinar entre las diferentes áreas y una comprensión de conceptos en los tres grupos, permitiendo el diseño óptimo y el seguimiento de los experimentos; la interpretación y discusión de los resultados y la posterior publicación de los mismos.

3.3. METODOLOGÍA UTILIZADA

1. Se realizaron medidas simultáneas de intercambio de gases y fluorescencia de clorofila utilizando un sistema portátil de medida de intercambio de gases (CIRAS-2, PP-Systems, Amesbury, MA, USA) acoplado a una cuveta automática universal (PLC6-U, PP-Systems, Amesbury, MA, USA) y a un fluorímetro portátil FMS II (Hansatech Instruments Ltd., Norfolk, UK). Se realizaron 6 curvas de respuesta a CO_2 por especie en hojas completamente desarrolladas a 1500 µmol m^{-2} s^{-1}, empezando a una concentración de

CO_2 de 400 ppm. La temperatura foliar se mantuvo a 25°C y 1.25 kPa, respectivamente, durante todas las medidas. Una vez alcanzado el estado estacionario en el intercambio de gases se registraron los parámetros de asimilación neta de CO_2 (A_N), conductancia estomática (gs), concentración subestomática de CO_2 (Ci) y eficiencia del fotosistema II (Φ_{PSII}). Entonces se disminuyó paulatinamente la concentración de CO2 hasta 50 ppm. Una vez completadas las medidas en el rango de concentraciones bajas, se incrementó el CO_2 hasta 400 ppm y a partir de ahí hasta 1800 ppm. Todos los parámetros fotosintéticos se registraron para cada una de las concentraciones de CO2. La eficiencia del fotosistema II (Φ_{PSII}) se calculó de acuerdo con la metodología descrita por Genty et al. (1989) y la tasa de transporte electrónico de acuerdo con la metodología descrita por Krall & Edwards (1992).

2. Se calculó la conductancia del mesófilo (g_m) a partir de las medidas simultáneas de intercambio de gases y fluorescencia, siguiendo la metodología descrita por Harley et al. (1992), a partir de esta ecuación:

$$g_m = \frac{A_N}{\frac{C_i - \Gamma^*(J_F + 8(A_N + R_L))}{J_F - 4(A_N + R_L)}} \qquad \text{Eq.1}$$

donde A_N y la concentración subestomática de CO_2 (C_i) fueron tomadas de las medidas de intercambio de gases a luz saturante, mientras que Γ* (el punto de compensación de CO_2 cloroplástico en ausencia de respiración mitocondrial) y R_L (la tasa respiratoria en condiciones de iluminación) se estimaron para cada especie siguiendo el método descrito por Flexas et al. (2007b). Los valores de g_m se utilizaron para convertir las curvas A_N-C_i en curvas A_N-C_c (siendo C_c la concentración de CO_2 en el cloroplasto) utilizando la ecuación $C_c = C_i - A_N / g_m$. La velocidad máxima de carboxilación de la enzima Rubisco ($V_{c,\,max}$) y la capacidad máxima de transporte electrónico (J_{max}) se calcularon a partir de las curvas AN-C_c, utilizando las constantes cinéticas de Rubisco y su dependencia de la temperatura estimadas por Bernacchi et al. (2002). El modelo de Farquhar et al. (1980) fue ajustado a estos datos aplicando ajustes de curva iterativos (diferencia mínima de mínimos cuadrados) usando la herramienta Solver de Microsoft Excel.

3. Se realizaron medidas morfológicas y anatómicas en secciones foliares de 1 mm x 1 mm obtenidas de las mismas hojas empleadas para las medidas de intercambio de gases. El material vegetal fue fijado en vacío con p-formaldehido (2%) y glutaraldehido (4%) en tampón fosfato 0.1 M (pH =7.2) y post-fijado en O_sO_4 (1%). Posteriormente las muestras se deshidrataron en etanol, oxido de propileno y se incluyeron en Embed-812 (EMS,

Hatfield, PA, USA). Se realizaron cortes semifinos (0.8 μm) y ultrafinos (90 nm) con un ultramicrotomo (Reichert & Jung model Ultracut E). Los cortes semifinos se tiñeron con azul de toluidina (1%) para su posterior observación en microscopio óptico (Optika B-600TiFL, Optika Microscopes, Italia). Los cortes ultrafinos se contrastaron con acetato de uranilo para su posterior observación en microscopio electrónico de transmisión (H600, Hitachi, Japón). Los parámetros anatómicos se midieron en las micrografías obtenidas utilizando el software Image-J (http://rsb.info.nih.gov/nih-image/). Las imágenes de microscopio óptico se usaron para determinar el espesor foliar, espesor de mesófilo, fracción de mesófilo ocupado por espacios aéreos (Syvertsen et al., 1995; Tomás et al., 2013). Las superficies de mesófilo (S_m/S) y cloroplasto (S_c/S) expuesta a espacios aéreos intercelulares se calcularon con imágenes de microscopio óptico y electrónico siguiendo la metodología descrita por Syvertsen et al. (1995). Para el cálculo de la superficie del mesófilo se utilizó la siguiente ecuación:

$$S_{\text{mes}}/S = \frac{L_{\text{mes}}}{W}\gamma \qquad \text{Eq.2}$$

donde W es el espesor foliar, y L_{mes} es la longitud total de mesófilo expuesta a espacios aéreos intercelulares. El factor de corrección de curvatura (c), que depende de la forma de las células (Evans et al., 1994), se midió y calculó para el mesófilo en empalizada y esponjoso de cada especie según Thain (1983) midiendo la anchura y altura de las células y calculando el valor medio de la relación anchura / altura.

Para el cálculo de S_c/S se utilizó la siguiente ecuación:

$$S_c/S = \frac{L_c}{L_{\text{mes}}} S_{\text{mes}}/S \qquad \text{Eq.3}$$

donde L_c es la longitud total de superficie de cloroplasto expuesta a espacios aéreos intercelulares.

El grosor de la pared celular, grosor de citoplasma y tamaño de cloroplastos (longitud y anchura) se midieron con imágenes de microscopio electrónico. Todos los parámetros se midieron en 4-6 campos de visión de 3 secciones diferentes por especie.

4.Se realizó la modelización de la conductancia del mesófilo (g_m) con base en parámetros anatómicos utilizando el modelo de difusión de gases unidimensional de Niinemets & Reichstein (2003) tal y como se describe y aplica por Tosens et al. (2012b), según la siguiente ecuación:

$$g_m = \frac{1}{\frac{1}{g_{ias}} + \frac{R \cdot T_k}{H \cdot g_{liq}}} \qquad \text{Eq.4}$$

donde g_{ias} es la conductancia de la fase gaseosa desde la cavidad subestomática a la superficie externa de la pared celular, g_{liq} es la conductancia de la fase liquida desde la pared celular hasta el cloroplasto, R es la constante de los gases (Pa m^3 K^{-1} mol^{-1}), Tk es la temperatura absoluta (K) y H es la constante de la ley de Henry para el CO_2 (Pa m^3 mol^{-1}). gm se define como una conductancia en fase gaseosa, y por lo tanto deberemos convertir g_{liq} a conductancia equivalente en fase gaseosa (Niinemets y Reichstein, 2003). La conductancia de la fase gaseosa g_{ias} (y su término recíproco como resistencia, r_{ias}) se obtuvo de acuerdo con Niinemets y Reichstein (2003) como:

$$g_{ias} = \frac{1}{r_{ias}} = \frac{D_A \cdot f_{ias}}{\Delta L_{ias} \cdot \tau} \qquad \text{Eq.5}$$

donde el ΔL_{ias} (m) es el espesor medio de la fase gaseosa, s es la tortuosidad del camino (1.57 m m^{-1}, Syvertsen et al., 1995), D_A es la difusividad del CO_2 en el aire (1.51 x 10^{-5} m^2 s^{-1} a 25 °C) y f_{ias} es la fracción de los espacios aéreos intercelulares. ΔL_{ias} fue estimado como la media del espesor del mesófilo. La conductancia total en la fase líquida (g_{liq}), desde la superficie exterior de las paredes celulares hasta los sitios de carboxilación en los cloroplastos, es el sumatorio de las resistencias en serie de la pared celular (r_{cw}), el plasmalema (r_{pl}) y el interior de la célula ($r_{cel,\,tot}$) (Tomas et al., 2013), y se calculó según la siguiente fórmula:

$$g_{liq} = \frac{S_m}{(r_{cw} + r_{pl} + r_{cel,tot}) \cdot S} \qquad \text{Eq.6}$$

La conductancia de la pared celular se calculó siguiendo la metodología descrita por Peguero-Pina et al. (2012). Para la conductancia del plasmalema se utilizó un valor estimado de 0,0035 m s-1, según Tosens et al. (2012b). La conductancia dentro de la célula se calculó siguiendo la metodología descrita por Tomás et al. (2013), considerando dos vías diferentes para la entrada del CO_2 dentro de la célula: una para aquéllas partes

de la pared celular alineadas con los cloroplastos y otra para las áreas entre cloroplastos (Tholen et al. 2012).

3.4. CONCLUSIONES FINALES

- A pesar de las similitudes morfológicas existentes entre las diversas especies de robles mediterráneos perennifolios objeto de estudio, se observan diferencias importantes y significativas en el comportamiento funcional de cada una de ellas individualmente. Entre todos los parámetros analizados es la conductancia del mesófilo (g_m) el factor más determinante para explicar las diferencias encontradas en los valores de asimilación neta de CO_2 (A_N). Las diferencias encontradas en g_m no vienen determinadas por la pared celular sino por otros componentes anatómicos que también ejercen un control sobre g_m. Así, las especies con mayor A_N mostraron mayores valores de superficie de cloroplastos expuesta a espacios aéreos intercelulares (S_c/S), lo que implica un aumento de los valores de g_m sin cambios significativos en la conductancia estomática y, por tanto, en las pérdidas de agua.
Otro aspecto a destacar es que esta adaptación anatómica a nivel celular permite a robles de hoja perenne alcanzar valores de A_N comparables a los obtenidos en robles de hoja caduca del mismo género a pesar de presentar unos valores más altos de índice de esclerofilia (LMA).

- La reducción del área transpirante de *Q. faginea*, característica que se considera clave para la adaptación de esta especie a climas mediterráneos, se ve parcialmente compensada en términos de ganancia de carbono por un incremento de A_N a expensas de un gran incremento en los valores máximos de g_s. Por otro lado, los valores g_s extremadamente altos de *Q. faginea* contrarrestan la posible reducción en g_s impuesta por la sensibilidad estomática al VPD, lo que permite a esta especie mantener valores altos de A_N bajo condiciones cambiantes a lo largo del período vegetativo en su hábitat natural. Este hecho hace que esta especie sea clasificada como una “consumidora de agua” (Mediavilla y Escudero 2004), lo que podría explicar que no compita bien con *Q. ilex* en zonas con suelos degradados con menores reservas de agua. Así mismo, este comportamiento pone a *Q. faginea* en una posición de vulnerabilidad en un hipotético escenario de incremento en la aridez asociada con un cambio climático global (Sánchez de dios et al. 2009).

- El factor más limitante para la asimilación de carbono es g_m para todas las procedencias de *Q. ilex* estudiadas. A pesar de esta característica común, se ha observado una gran variación ecotípica en la actividad fotosintética entre las diferentes procedencias estudiadas de esta especie. La explicación a este fenómeno reside en el hecho de que las procedencias con valores más altos de A_N (Extremadura y Soria) poseen rasgos anatómicos (grosor de la pared celular, grosor del cloroplasto y superficie de cloroplastos expuesta a espacios aéreos intercelulares) y bioquímicos (concentración de nitrógeno por área foliar) que mejoran notablemente y de manera coordinada g_m y la velocidad de carboxilación de la Rubisco ($V_{c,max}$), respectivamente. También se evidencia una fuerte correlación entre $V_{c,max}$ y la tasa de transporte electrónico máximo (J_{max}), lo que indica una coordinación entre la actividad carboxilativa y el funcionamiento de la cadena de transporte electrónico. La existencia de estas adaptaciones a nivel subcelular y celular explica los aumentos en la asimilación de CO_2 por unidad de área foliar dentro de la especie.

- Por último, la inversión en nitrógeno y materia seca por área foliar que realiza *Q. coccifera* bajo condiciones poco estresantes (clima templado) es menor que cuando vive en un clima mediterráneo con aridez estival, lo que puede constituir una ventaja en términos de coste de construcción de la hoja. Sin embargo, a pesar de que los valores de conductancia estomática son mucho mayores bajo clima templado, este hecho no redunda en unas mayores tasas de fotosíntesis, ya que la conductancia del mesófilo es la misma en ambos lugares. Por lo tanto, la eficiencia en el uso del nitrógeno (A_N/N) es mayor en el clima templado, mientras que la eficiencia en el uso del agua (A_N/g_s) es mayor en el clima mediterráneo. Es decir, esta especie no siempre utiliza los principales recursos (agua y nutrientes) a nivel de la hoja tan eficientemente como podría. En general, los diferentes patrones de uso de recursos (en particular N) junto con su plasticidad funcional no pueden superar las restricciones morfo-funcionales que limitan posibles incrementos de la conductancia del mesófilo, lo que limita la actividad fotosintética incluso bajo condiciones potencialmente favorables.

4. BIBLIOGRAFÍA

Abadía A, Gil E, Morales F, Montañés L, Montserrat G, Abadía J (1996) Marcescence and senescence in a submediterranean oak (*Quercus subpyrenaica* E.H. del Villar): photosynthetic characteristics and nutrient composition. Plant, Cell Environ 19:685–694

Ackerly DD (2009) Evolution, origin and age of lineages in the Californian and Mediterranean floras. J Biogeogr 36:1221–1233

Atjay GL, Ketner P, Duvigneaud P (1979) Terrestrial primary production and phytomass. In: Bolin B, Degens ET, Kempe S, Ketner P (eds) The global carbon cycle, SCOPE Report 13. Wiley, UK, pp 129–181

Axelrod DI (1973) History of the Mediterranean ecosystem in California. In: Di Castri F, Mooney HA (eds) Mediterranean type ecosystems. Origin and structure. Springer, Berlin, pp 225–277

Axelrod DI (1975) Evolution and biogeography of Madrean-Tethyan sclerophyll vegetation. *Ann Mo Bo*t Gar 62:280–334

Axelrod DI (1977) Outline history of California vegetation. In: Barbour MG, Major J (eds) Terrestrial vegetation of California. John Wiley, New York, pp 139–193

Axelrod DI (1989) Age and origin of Chaparral. The California Chaparral: paradigms *revisited (ed. SC Keeley)* Natural History Museum of Los Angeles County, Los Angeles, pp 7–19

Baldocchi DD, Ma S, Rambal S, Misson L, Ourcival JM, Limousin JM, Papale D (2010) On the differential advantages of evergreenness and deciduousness in Mediterranean oak woodlands: a flux perspective. Ecol Appl 20:1583–1597

Barbero M, Loisel R, Quèzel P (1992) Biogeography, ecology and history of Mediterranean Quercus ilex ecosystems. Vegetatio 99–100:19–34

Barbour MG (1988) Californian upland forests and woodlands. In: Barbour MG, Billings WD (eds) North American terrestrial vegetation. Cambridge University Press, Cambridge, pp 131–164

Bernacchi CJ, Portis AR, Nakano H, von Caemmerer S, Long SP. 2002. Temperature response of mesophyll conductance. Implications for the determination of Rubisco enzyme kinetics and for limitations to photosynthesis in vivo. Plant Physiology 130: 1992-1998.

Blondel J, Aronson J (1995) Biodiversity and ecosystem function in the Mediterranean Basin: human and nonhuman determinants. In: Davis GW, Richardson DM (eds) Mediterranean-type ecosystems: the function of biodiversity. Springer, Berlin, pp 43–119

Blumler MA (1991) Winter-deciduous versus evergreen habit in Mediterranean regions: a model. USDA Forest Service Gen Tech Rep PSW-126

Blumler MA (2005) Three conflated definitions of Mediterranean climates. Middle States Geographer 38:52–60

Bryson RA, Hare FK (1974) Climates of North America. World Survey of Climatology, vol 11. Elsevier Scientific Publishing Co., Amsterdam

Breckle SW (2002) Walter's vegetation of the earth. The ecological systems of the geo-biosphere. 4th edn. Springer, Berlin

Blumler MA (1991) Winter-deciduous versus evergreen habit in Mediterranean regions: a model. USDA Forest Service Gen Tech Rep PSW-126

Büntgen U, Tegel W, Nicolussi K, McCormick M, Frank D, Trouet V, Kaplan JO, Franz Herzig F, Heussner KU, Wanner H, Luterbacher J, Esper J (2011) 2500 years of European climate variability and human susceptibility. Science 33:578–582

Castro-Díez P, Pedro Villar-Salvador P, Pérez-Rontomé C, Maestro-Martínez M Montserrat-Martí G (1997) Leaf morphology and leaf chemical composition in three *Quercus* (Fagaceae) species along a rainfall gradient in NE Spain. Trees 11:127–134

Castro-Díez P, Montserrat-Martí G (1998) Phenological pattern of fifteen Mediterranean phanaerophytes from *Quercus ilex* communities of NE-Spain. Plant Ecol 139:103–112

Cano FJ, Sánchez-Gómez D, Rodríguez-Calcerrada J, Warren CR, Gil L, Aranda I. 2013. Effects of drought on mesophyll conductance and photosynthetic limitations at different tree canopy layers. Plant Cell & Environment 36: 1961-1980.

Chabot BF, Hicks DJ (1982) The ecology of leaf life spans. Annu Rev Ecol Syst 13:229–259

Corcuera L, Camarero JJ, Gil-Pelegrín E (2004a) Effects of a severe drought on *Quercus ilex* radial growth and xylem anatomy. Trees 18:83–92

Corcuera L, Morales F, Abadía A, Gil-Pelegrín E (2005a) The effect of low temperatures on the photosynthetic apparatus of *Quercus ilex subsp. ballota* at its lower and upper altitudinal limits in the Iberian peninsula and during a single freezing-thawing cycle. Trees 19:99–108

Corcuera L, Morales F, Abadía A, Gil-Pelegrín E (2005b) Seasonal changes in photosynthesis and photoprotection in a *Quercus ilex subsp. ballota* woodland located in its upper altitudinal extreme in the Iberian Peninsula. Tree Physiol 25:599–608

Corcuera L, Camarero JJ, Gil-Pelegrín E. 2002. Functional groups in *Quercus* species derived from the analysis of pressure-volume curves. Trees – Structure and Function 16: 465-472.

Cody ML, Mooney HA (1978) Convergence versus nonconvergence in Mediterranean-Climate ecosystems. Annu Rev Ecol Syst 9:265–321

Cuadrat JM, Saz MA, Vicente-Serrano S, González-Hidalgo JC (2007) Water resources and precipitation trends in Aragon (Spain). Int J Water Resour D 23:107–124

Damesin C, Rambal S (1995) Field study of leaf photosynthetic performance by a Mediterranean deciduous oak tree (*Quercus pubescens*) during a severe summer drought. New Phytol 131:159–167

Damesin C, Rambal S, Joffre R (1998) Co-occurrence of trees with different leaf habit: a functional approach on Mediterranean oaks. Acta Oecol 19:195–204

Deitch MJ, Sapundjieff MJ, Feirer ST (2017) Characterizing precipitation variability and trends in the world's Mediterranean-Climate areas. Water 9:259.

del Río S, Penas A (2006) Potential distribution of semi-deciduous forests in Castile and Leon (Spain) in relation to climatic variations. Plant Ecol 185:269–282

Denk T, Grimm GW (2009) Significance of pollen characteristics for infrageneric classification and phyllogeny in *Quercus* (Fagaceae). Int J Plant Sci 170(7):926–940

Di Paola A, Paquette A, Trabucco A, Mereu S, Valentini R, Paparella F (2017) Coexistence trend contingent to Mediterranean oaks with different leaf habits. Ecol Evol 7:3006–3015

Dufour-Dror JM, Ertas (2004) A Bioclimatic perspectives in the distribution of *Quercus ithaburensis* Decne. Subspecies in Turkey and in the Levant. J Biogeogr 31:461–474

Esteso-Martínez J, Camarero JJ, Gil-Pelegrín E (2006) Competitive effects of herbs on *Quercus faginea* seedlings inferred from vulnerability curves and spatial-pattern analyses in a Mediterranean stand (Iberian System, northeastern Spain). Ecoscience 13(3):378–387

Epron D, Dreyer E, Aussenac G. 1993. A comparison of photosynthetic responses to water stress in seedlings from 3 oak species: *Quercus petraea (Matt.) Liebl., Q. rubra L. and Q. cerris L*. Annales des Sciences Forestières 50(suppl. 1): 48-60.

Epron D, Dreyer E, Breda N. 1992. Photosynthesis of oak trees [*Quercus petraea* (Matt.) Liebl.] during drought under field conditions: diurnal course of net CO2 assimilation and photochemical efficiency of photosystem II. Plant, Cell and Environment 15: 809-820.

Evans JR, von Caemmerer S, Setchell BA, Hudson GS. 1994. The relationship between CO2 transfer conductance and leaf anatomy in transgenic tobacco with a reduced content of Rubisco. Australian Journal of Plant Physiology 21: 475–495.

Faria T, Silvério D, Breia E, Cabral R, Abadia A, Abadia J, Pereira JS, Chaves MM (1998) Differences in the response of carbon assimilation to summer stress (water deficits, high light and temperature) in four Mediterranean tree species. Physiol Plant 102:419–428

Farquhar GD, von Caemmerer S, Berry JA. 1980. A biochemical model of photosynthetic CO2 assimilation in leaves of C3 species. Planta 149: 78-90.

Fick SE, Hijmans RJ (2017). WorldClim 2: new 1-km spatial resolution climate surfaces for global land areas. Int J Climatol doi:10.1002/joc.5086

Flexas J, Ribas-Carbó M, Díaz-Espejo A, Galmés J, Medrano H (2008) Mesophyll conductance to CO2: current knowledge and future prospects. Plant Cell Environ 31:602–621

Flexas J, Barbour MM, Brendel O, Cabrera HM, Carriquí M, Díaz-Espejo A, Douthe C, Dreyer E, Ferrio JP, Gago J, et al. 2012. Mesophyll diffusion conductance to CO2: an unappreciated central player in photosynthesis. Plant Science 193-194: 70-84.

Flexas J, D_ıaz-Espejo A, Berry JA, Galm_es J, Cifre J, Kaldenhoff R, Medrano H, Ribas-Carb_o M. 2007a. Analysis of leakage in IRGA's leaf chambers of open gas exchange systems: quantification and its effects in photosynthesis parameterization. Journal of Experimental Botany 58: 1533–1543.

Flexas J, Díaz-Espejo A, Gago J, Gallé A, Galmés J, Gulías J, Medrano H. 2014. Photosynthetic limitations in Mediterranean plants: a review. Environmental and Experimental Botany 103: 12-23.

Flexas J, Ortu~no MF, Ribas-Carb_o M,D_ıaz-Espejo A, Fl_orez-Sarasa ID, Medrano H. 2007b. Mesophyll conductance to CO2 in *Arabidopsis thaliana.* New Phytologist 175: 501–511.

Follieri M, Magri D, Sadori L (1988) 250,000-year pollen record from Valle di Castigliore (Roma). Pollen Spores 30:329–356

Galmés J, Andralojc PJ, Kapralov MV, Flexas J, Keys J, Molins A, Parry MAJ, Conesa MÀ. 2014. Environmentally driven evolution of Rubisco and improved photosynthesis and growth within the C3 genus *Limonium* (Plumbaginaceae). New Phytologist 203: 989-999.

García-Plazaola JI, Artetxe U, Duñabeitia MK, Becerril JM (1999) Role of photoprotective systems of Holm-Oak (*Quercus ilex*) in the adaptation to winter conditions. J Physiol 155:25–630

Gasith A, Resh VH (1999) Streams in Mediterranean climate regions: abiotic influences and biotic responses to predictable seasonal events. Annu Rev Ecol Syst 30:51–81

Genty B, Briantais JM, Baker NR. 1989. The relationship between the quantum yield of photosynthetic electron transport and quenching of chlorophyll fluorescence. Biochimica et Biophysica Acta 990: 87-92.

Gil-Pelegrín E, Saz MA, Cuadrat JM, Peguero-Pina JJ, Sancho-Knapik D (2017) Oaks under mediterranean-type climates: functional response to summer aridity. In: Gil-Pelegrín E, Peguero-Pina JJ, Sancho-Knapik D (eds.) Oaks Physiological Ecology. Exploring the Functional Diversity of Genus *Quercus L*. Springer International Publishing AG, Cham, Switzerland. (pp. 137–193). doi:10.1007/978-3-319-69099-5_5

Givnish TJ (2002) Adaptive significance of evergreen versus deciduous leaves: solving the triple paradox. Silva Fenn 36:703–743

González-Rebollar JL, García-Álvarez A, Ibáñez JJ (1995) A mathematical model for predicting the impact of climate changes on mediterranean plant landscapes. In: Zewer S, van Rompaey RSAR, Kok MTJ, Berk MM (eds) Climate change research: evaluation and policy implications. Elsevier, Amsterdam, pp 757–762

González-Zurdo P, Escudero A, Babiano J, García-Ciudad A, Mediavilla S (2016) Costs of leaf reinforcement in response to winter cold in evergreen species. Tree Physiol 36:273–286

Griffin JR (1971) Oak regeneration in the upper Carmel Valley, California. Ecology 52:862–868

Griffin JR (1973) Xylem sap tension in three woodland oaks of central California. Ecology 54:152–159

Griffin JR (1977) Oak woodland. In: Barbour MG, Major J (eds) Terrestrial vegetation of California. Wiley, New York, pp 383–415

Hanba YT, Kogami H, Terashima I. 2002. The effect of growth irradiance on leaf anatomy and photosynthesis in *Acer* species differing in light demand. Plant Cell & Environment 25: 1021-1030.

Hanba YT, Miyazawa SI, Terashima I. 1999. The influence of leaf thickness on the CO_2 transfer conductance and leaf stable carbon isotope ratio for some evergreen tree species in Japanese warm temperate forests. Functional Ecology 13: 632-639.

Harley PC, Loreto F, Di Marco G, Sharkey TD. 1992. Theoretical considerations when estimating the mesophyll conductance to CO2 flux by the analysis of the response of photosynthesis to CO_2. Plant Physiology 98: 1429-1436.

Hassiotou F, Ludwig M, Renton M, Veneklaas EJ, Evans JR. 2009. Influence of leaf dry mass per area, CO2 and irradiance on mesophyll conductance in sclerophylls. Journal of Experimental Botany 60: 2303–2314.

Hassiotou F, Renton M, Ludwig M, Evans JR, Veneklaas EJ (2010) Photosynthesis at an extreme end of the leaf trait spectrum: how does it relate to high leaf dry mass per area and associated structural parameters? J Exp Bot 61:3015–3028

Herrera CM (1992) Historical effects and sorting processes as explanations for contemporary ecological patterns: character syndromes in Mediterranean Woody plants. Am Nat 140:421–446

Himrane H, Camarero JJ, Gil-Pelegrín E (2004) Morphological and ecophysiological variation of the hybrid oak *Quercus subpyrenaica* (*Q. faginea* _ *Q. pubescens*). Trees 18:566–575

Kikuzawa K (1991) A cost-benefit analysis of leaf habit and leaf longevity of trees and their geographical pattern. Am Nat 138:1250–1263

Köppen W (1936) Das geographische system der klimate. In: Köppen W, Geiger R (eds) Handbuch der Klimatologie 3. Gebrueder Borntraeger, Berlin.

Kovar-Eder J (2003) Vegetation dynamics in Europe during the Neogene. In: Reumer JWF, Wessels W (eds) Distribution and migration of tertiary mamals in Eurasia. A volume in honour of Hans de Bruijn. Deinsea 10:373–392

Krall JP, Edwards GE. 1992. Relationship between photosystem II activity and CO_2 fixation in leaves. Physiologia Plantarum 86: 80-187.

Kremer A, Abbott AG, Carlson JE, Manos PS, Plomion C, Sisco P, Staton ME, Ueno S, Vendramin GG. 2012. Genomics of Fagaceae. Tree Genetics and Genomes 8:583-610.

Lasanta T, Nadal-Romero E, Errea P, Arnáez J (2016) The effect of landscape conservation measures in changing landscape patterns: a case study in mediterranean mountains. Land Degrad Dev 27(2):373–386

Limousin JM, Misson L, Lavoir AV, Martin NK, Rambal S (2010a) Do photosynthetic limitations of evergreen *Quercus ilex* leaves change with long-term increased drought severity? Plant, Cell Environ 33:863–875

Lionello, P, Malanotte-Rizzoli, P, Boscolo, R, et al (2006) The Mediterranean climate: an overview of the main characteristics and issues. In: Lionello P, Malanotte-Rizzoli P, R Boscolo R (eds). Mediterranean Climate Variability. Elsevier, Amsterdam, p 1–26

Mai DH (1991) Palaeofloristic changes in Europe and the confirmation of the arctotertiary-palaeotropical geoflora concept. Rev Palaeobot Palyno 68:29–36

Manes F, Vitale M, Donato E, Giannini M, Puppi G (2006) Different ability of three Mediterranean oak species to tolerate progressive water stress. Photosynthetica 44(3):387–393

Manos PS, Doyle JJ, Nixon KC. 1999. Phylogeny, biogeography and processes of molecular differentiation in *Quercus* subgenus *Quercus* (Fagaceae). Molecular Phylogenetics and Evolution 12:333-349.

Mediavilla S, Escudero A (2003) Stomatal responses to drought at a Mediterranean site: a comparative study of co-occurring woody species differing in leaf longevity. Tree Physiol 23:987–996

Mediavilla S, Escudero A (2004) Stomatal responses to drought of mature trees and seedlings of two co-occurring Mediterranean oaks. For Ecol Manag 187:281–294

Millar CI (2012) Geologic, climatic, and vegetation history of California. In: Baldwin BG, Goldman DH, Keil DJ, Patterson R, Rosatti TJ, Wilken DH (eds) The Jepson Manual: Vascular Plants of California, 2nd edn. University of California Press, pp 49–67

Montserrat-Martí G, Camarero JJ, Palacio S, Pérez-Rontomé C, Milla R, Albuixech J, Maestro M b(2009) Summer-drought constrains the phenology and growth of two co-existing Mediterranean oaks with contrasting leaf habit: implications for their persistence and reproduction. Trees 23:787–799

Moreno G, Gallardo JF, Vicente MA (2011) How mediterranean deciduous trees cope with long summer drought? The case of *Quercus pyrenaica* forests in western Spain. In: Bredemeier M, Cohen S, Godbold DL, Lode E, Pichler V, Schleppi P (eds) Forest management and the water cycle. An ecosystem-based approach. Ecological Studies 212, Springer, Dordrecht, pp 181–207

Mooney HA, Dunn EL (1970) Convergent evolution of Mediterranean-climate evergreen sclerophyll shrubs. Evolution 24:292–303

Mitrakos KA (1980) A theory for Mediterranean plant life. Acta Oecol 1:245–252

Nardini A, Lo Gullo MA, Salleo S (1999) Competitive strategies for water availability in two Mediterranean *Quercus* species. Plant, Cell Environ 22:109–116

Niinemets U (2001) Global-scale climatic controls of leaf dry mass per area, density, and thickness in trees and shrubs. Ecology 82:453–469

Niinemets Ü, Díaz-Espejo A, Flexas J, Galmés J, Warren CR (2009) Role of mesophyll diffusion conductance in constraining potential photosynthetic productivity in the field. J Exp Bot 60:2249–2270

Niinemets Ü, Díaz-Espejo A, Flexas J, Galmés J, Warren CR (2009a) Role of mesophyll diffusion conductance in constraining potential photosynthetic productivity in the field. J Exp Bot 60:2249–2270

Niinemets Ü, Wright IJ, Evans JR (2009b) Leaf mesophyll diffusion conductance in 35 Australian sclerophylls covering a broad range of foliage structural and physiological variation. J Exp Bot 60:2433–2449

Niinemets Ü, Keenan TF. 2014. Photosynthetic responses to stress in Mediterranean evergreens: mechanisms and models. Environmental and Experimental Botany 103: 24-41.

Niinemets Ü (2015) Is there a species spectrum within the world-wide leaf economics spectrum? Major variations in leaf functional traits in the Mediterranean sclerophyll Quercus ilex. New Phytol 205:79–96

Niinemets Ü, Reichstein M. 2003. Controls on the emission of plant volatiles through stomata: a sensitivity analysis. Journal of Geophysical Research 108: 4211.

Nixon KC (2002) The oak (*Quercus)* biodiversity of California and adjacent regions. USDA Forest Service Gen Tech Rep. PSW-GTR-184

Noce S, Collalti A, Valentini R, Santini M (2016) Hot spot maps of forest presence in the Mediterranean Basin. iForest 9:766

Ogaya R, Peñuelas J (2003) Phenological patterns of *Quercus ilex*, *Phillyrea latifolia*, and *Arbutus unedo* growing under a field experimental drought. Écoscience 11:263–270

Pasho E, Camarero JJ, de Luis M, Vicente-Serrano SM (2011) Impacts of drought at different time scales on forest growth across a wide climatic gradient in north-eastern Spain. Agr Forest Meteorol 151:1800–1811

Peel MC, Finlayson BL, McMahon TA (2007) Updated world map of the Köppen-Geiger climate classification. Hydrol Earth Syst Sci Discuss 4:439–473

Peguero-Pina JJ, Flexas J, Galmés J, Niinemets Ü, Sancho-Knapik D, Barredo G, Villarroya D, Gil-Pelegrín E. 2012. Leaf anatomical properties in relation to differences in mesophyll conductance to CO_2 and photosynthesis in two related Mediterranean *Abies* species. Plant Cell & Environment 35: 2121-2129.

Peguero-Pina JJ, Sancho-Knapik D, Barrón E, Camarero JJ, Vilagrosa A, Gil-Pelegrín E (2014) Morphological and physiological divergences within *Quercus ilex* support the existence of different ecotypes depending on climatic dryness. Ann Bot 114:301–313

Peguero-Pina JJ, Sancho-Knapik D, Martín P, Saz MA, Gea-Izquierdo G, Cañellas I, Gil-Pelegrín E (2015) Evidence of vulnerability segmentation in a deciduous Mediterranean oak (*Quercus subpyrenaica* E. H. del Villar). Trees 29:1917–1927

Peguero-Pina JJ, Sancho-Knapik D, Morales F, Flexas J, Gil-Pelegrín E. 2009. Differential photosynthetic performance and photoprotection mechanisms of three Mediterranean evergreen oaks under severe drought stress. Functional Plant Biology 36: 453-462.

Peguero-Pina JJ, Sisó S, Sancho-Knapik D, Díaz-Espejo Flexas J, Galmés J, Gil-Pelegrín E (2016a) Leaf morphological and physiological adaptations of a deciduous oak (*Quercus faginea Lam*.) to the Mediterranean climate: a comparison with a closely related temperate species (*Quercus robur L*.). Tree Physiol 36:287–299

Piel C (2002) Diffusion du CO_2 dans le mésophylle des plantes à métabolisme C3. Ph.D. thesis, Université Paris XI Orsay, Paris, France

Poudyal K, Jha PK, Zobel DB, Thapa CB (2004) Patterns of leaf conductance and water potential of five Himalayan tree species. Tree Physiol 24:689–699

Poyatos R, Llorens P, Piñol J, Rubio C (2008) Response of Scots pine (*Pinus sylvestris L*.) and pubescent oak (*Quercus pubescens* Willd.) to soil and atmospheric water deficits under Mediterranean mountain climate. Ann For Sci 65:306

Radoglou K (1996) Environmental control of CO_2 assimilation rates and stomatal conductance in five oak species growing under field conditions in Greece. Ann Sci Forest 53:269–278

Reale O, Dirmeyer P (2000) Modeling the effects of vegetation on Mediterranean climate during the Roman classical period—Part I: climate history and model sensitivity. Global Planet 25:163–184

Reille M, Pons A (1992) The ecological significance of sclerophyllous oak forests in the western part of the Mediterranean Basin: a note on pollen analytical data. Vegetatio 99–100:13–17

Riera-Mora S, Esteban-Amat A (1994) Vegetation history and human activity during the last 6000 years on the central Catalan coast (north-eastern Iberian Peninsula). Veg His Archaebot 3:7–23

Rivas-Martínez S, Rivas-Sáenz S, Penas-Merino A (2011) Worldwide bioclimatic classification system. Global geobotany 1:1–634

Roupsard O, Gross P, Dreyer E (1996) Limitation of photosynthetic activity by CO_2 availability in the chloroplasts of oak leaves from different species and during drought. Ann Sci For 53:243– 254

Salleo S, Pitt F, Nardini A, Hamzé M, Jomaa I (2002) Differential drought resistance of two Mediterranean oaks growing in the Bekaa Valley (Lebanon). Plant Biosyst 136:91–99

Sánchez de Dios R, Benito-Garzón M, Sainz-Ollero H (2009) Present and future extension of the Iberian submediterranean territories as determined from the distribution of marcescent oaks. Plant Ecol 204:189–205

Scarascia-Mugnozza G, Oswald H, Piussi P, Radoglou K (2000) Forests of the Mediterranean region: gaps in knowledge and research needs. Forest Ecol Manag 132:97–109

Schimper AFW (1903) Plant-geography on a physiological basis. Clarendon Press, Oxford

Shmida A (1981) Mediterranean vegetation in California and Israel: similarities and differences. Israel J Bot 30:105–123.

Shmida A, Whittaker RH (1984) Convergence and non-convergence of Mediterranean type communities in the old and the new world. In: Margaris NS, Arianoustou-Farragitaki M, Oechel WC (eds) Being alive on land. Dr W. Junk, The Hague, pp 5–11

Siam AMJ, Radoglou KM, Noitsakis B, Smiris P (2009) Differences in ecophysiological responses to summer drought between seedlings of three deciduous oak species. Forest Ecol Manag 258:35–42

Singh SP, Zobel DB, Garkoti SC, Tewari A, Negi CMS (2006) Patterns in water relations of central Himalayan trees. Trop Ecol 47:159–182

Slaton MR, Smith WK. 2002. Mesophyll architecture and cell exposure to intercellular air space in alpine, desert, and forest species. International Journal of Plant Sciences 163: 937-948.

Syvertsen JP, Lloyd J, McConchie C, Kriedemann PE, Farquhar GD. 1995. On the relationship between leaf anatomy and CO_2 diffusion through the mesophyll of hypostomatous leaves. Plant Cell & Environment 18: 149-157.

Steinbrecher R, Contran N, Gugerli F, Schnitzler JP, Zimmer I, Menard T, Günthardt-Goerg MS. 2013. Inter- and intra-specific variability in isoprene production and photosynthesis of Central European oak species. Plant Biology 15(suppl. 1): 148-156.

Suc JP (1984) Origin and evolution of the Mediterranean vegetation and climate in Europe. Nature 307:429–432

Terashima I, Hanba YT, Tazoe Y, Vyas P, Yano S. 2006. Irradiance and phenotype: comparative eco-development of sun and shade leaves in relation to photosynthetic CO_2 diffusion. Journal of Experimental Botany 57: 343-354.

Terashima I, Hanba YT, Tholen D, Niinemets Ü. 2011. Leaf functional anatomy in relation to photosynthesis. Plant Physiology 155: 108-116.

Thain JF. 1983. Curvature correlation factors in the measurements of cell surface areas in plant tissues. Journal of Experimental Botany 34: 87–94.

Tholen D, Ethier G, Genty B, Pepin S, Zhu X. 2012. Variable mesophyll conductance revisited: theoretical background and experimental implications. Plant, Cell & Environment 35: 2087–2103.

Tognetti R, Longobucco A, Raschi A (1998) Vulnerability of xylem to embolism in relation to plant hydraulic resistance in *Quercus pubescens* and *Quercus ilex* co-occurring in a Mediterranean coppice stand in central Italy. New Phytol 139:347–448

Tomás M, Flexas J, Copolovici L, Galmés J, Hallik L, Medrano H, Ribas-Carbó M, Tosens T, Vislap V, Niinemets Ü. 2013. Importance of leaf anatomy in determining mesophyll diffusion conductance to CO_2 across species: quantitative limitations and scaling up by models. Journal of Experimental Botany 64: 2269-2281.

Tosens T, Niinemets Ü, Vislap V, Eichelmann H, Castro-Díez P. 2012b. Developmental changes in mesophyll diffusion conductance and photosynthetic capacity under different light and water availabilities in *Populus tremula*: how structure constrains function. Plant Cell & Environment 35: 839-856.

Tosens T, Niinemets Ü, Westoby M, Wright IJ. 2012a. Anatomical basis of variation in mesophyll resistance in eastern Australian sclerophylls: news of a long and winding path. Journal of Experimental Botany 63: 5105-5119.

Turnbull MH, Whitehead D, Tissue DT, Schuster WSF, Brown KJ, Engel VC, Griffin KL. 2002. Photosynthetic characteristics in canopies of *Quercus rubra*, *Quercus prinus* and *Acer rubrum* differ in response to soil water availability. Oecologia 130: 515-524.

Urbieta IR, Zavala MA, Marañón T (2008) Human and non-human determinants of forest composition in Southern Spain: evidence of shifts towards cork oak dominance as a result of management over the ast century. J Biogeogr 35:1688–1700

Valentini R, Epron D, De Angelis P, Matteucci G, Dreyer E. 1995. In situ estimation of net CO_2 assimilation, photosynthetic electron flow and photorespiration in Turkey oak (*Quercus cerris L*.) leaves: diurnal cycles under different levels of water supply. Plant Cell & Environment 18: 631-640.

Valiente-Banuet A, Rumebe AV, Verdú M, Callaway RM (2006) Modern quaternary plant lineages promote diversity through facilitation of ancient tertiary lineages. PNAS 103:16812–16817

Vankat JL (1982) A gradient perspective on the vegetation of Sequoia National Park, California. Madrorño 29:200–214

Vaz M, Pereira JS, Gazarini LC, David TS, David JS, Rodrigues A, Maroco J, Chaves MM (2010) Drought-induced photosynthetic inhibition and autumn recovery in two Mediterranean oak species (*Quercus ilex* and *Quercus suber*). Tree Physiol 30:946–956

Verdú M, Dávila P, García-Fayos P, Flores-Hernández N, Valiente-Banuet A (2003) 'Convergent' traits of Mediterranean woody plants belong to pre-Mediterranean lineages. Biol J Linn Soc 78:415–427

Vilagrosa A, Cortina J, Gil-Pelegrín E, Bellot J (2003a) Suitability of drought-preconditioning techniques in Mediterranean climate. Restor Ecol 11:208–216

Vilagrosa A, Morales F, Abadía A, Bellot J, Cochard H, Gil-Pelegrin E (2010) Are symplast tolerance to intense drought conditions and xylem vulnerability to cavitation coordinated? An integrated analysis of photosynthetic, hydraulic and leaf level processes in two Mediterranean drought-resistant species. Environ Exp Bot 69:233–242

Wallen CC (1970) Climates of Central and Southern Europe. World survey of climatology

Volume 6. Elsevier Scientific Publishing Co, Amsterdam

Walter H (1985) Vegetation of the Earth and ecological systems of the geo-biosphere, 3rd edn. Springer, Berlin, p 318

Xu L, Baldocchi DD (2003) Seasonal trends in photosynthetic parameters and stomatal conductance of blue oak (*Quercus douglasii*) under prolonged summer drought and high temperature. Tree Physiol 23:865–877

Zhang SB, Zhou ZK, Hu H, Xu K, Yan N, Li SY (2005) Photosynthetic performances of *Quercus pannosa* vary with altitude in the Hengduan Mountains, Southwest China. Forest Ecol Manag 212:291–30

APÉNDICE I: Factor de impacto y área temática de las revistas

New Phytologist: Factor de Impacto 7.33, Área Temática “Plant Sciences”.
Tree Physiology: Factor de Impacto 3.65, Área Temática “Forestry”.